INFORMATION TO USERS

This manuscript has been reproduced from the microfilm master. UMI films the text directly from the original or copy submitted. Thus, some thesis and dissertation copies are in typewriter face, while others may be from any type of computer printer.

The quality of this reproduction is dependent upon the quality of the copy submitted. Broken or indistinct print, colored or poor quality illustrations and photographs, print bleedthrough, substandard margins, and improper alignment can adversely affect reproduction.

In the unlikely event that the author did not send UMI a complete manuscript and there are missing pages, these will be noted. Also, if unauthorized copyright material had to be removed, a note will indicate the deletion.

Oversize materials (e.g., maps, drawings, charts) are reproduced by sectioning the original, beginning at the upper left-hand corner and continuing from left to right in equal sections with small overlaps.

Photographs included in the original manuscript have been reproduced xerographically in this copy. Higher quality 6" x 9" black and white photographic prints are available for any photographs or illustrations appearing in this copy for an additional charge. Contact UMI directly to order.

ProQuest Information and Learning
300 North Zeeb Road, Ann Arbor, MI 48106-1346 USA
800-521-0600

UMI®

DISSERTATION

PARAQUAT GENOTOXICITY IN MAMMALIAN CELLS: THE ROLE OF DNA REPAIR IN INDUCED MUTATION

Submitted by

Sandra J. Gunselman

Cell & Molecular Biology Program

In partial fulfillment of the requirements

For the degree of Doctor of Philosophy

Colorado State University

Fall, 2001

Colorado State University

August 10, 2001

We hereby recommend that the dissertation prepared under our supervision by Sandra J. Gunselman entitled, *"Paraquat Genotoxicity in Mammalian Cells: the Role of DNA Repair in Induced Mutation"* be accepted as fulfilling in part requirements for the degree of Doctor of Philosophy.

Signatures of Graduate Advisory Committee:

Charles A. Waldren, Ph.D., Chairman — Date 8/22/01

Thomas J. Slaga, Ph.D., Member — Date 8/17/01

Henry S. Gardner, Dr.PH., Member — Date 8/9/01

Susan M. LaRue, DVM, Ph.D., Member — Date 8/17/01

Michael H. Fox, Program Head, Cell and Molecular Biology — Date 8/23/01

Abstract of Dissertation

PARAQUAT GENOTOXICITY IN MAMMALIAN CELLS: THE ROLE OF DNA REPAIR IN INDUCED MUTATION

Paraquat (1,1'-dimethyl-4, 4'-bipyridinium, PQ) is an herbicide, which poses serious human health concerns where it is in widespread use. It is the leading cause of accidental death in some parts of the world including Taiwan and Thailand. The United States Environmental Protection Agency (EPA) has classified PQ as a toxin and weak carcinogen. PQ is redox-cycled in cells producing reactive oxygen species (ROS) and causing lipid peroxidation, gene inactivation and DNA damage. PQ has been reported to cause chromosomal aberrations in cells however, until recently, it has been considered non-mutagenic.

The genotoxicity of PQ was studied using the human x Chinese hamster ovary (CHO) cell line, A_LH. These cells contain a single copy of human chromosome 11 and express the surface cell antigen CD59. New variants of A_LH were also created which expressed the *E. coli* fpg gene. This gene encodes for the base excision repair protein, formamidopyrimidine glycosylase (FPG), and by transfecting it into the A_LH cell line, cells with increased DNA repair capacity were produced. Mutations induced by PQ were measured in both cell types at the CD59 locus.

FPG activity was measured in A_LH and fpg transformant cells and compared with survival and induced mutation data following PQ exposure. Protein extracts from a number of the fpg transformants were found to more efficiently excise 8oxoG, the major

damage caused by oxidation in the cell, than A_LH cells. One of the transformants that displayed effective excision was found to have increased survival when compared to A_LH cells and induced mutation was virtually eliminated - clear evidence that PQ causes mutagenic DNA damage in mammalian cells.

Results of this study demonstrate, for the first time, that PQ is an effective mutagen in mammalian cells and that its mutagenicity is abrogated by the activity of the bacterial fpg gene. These results offer important insight into the role DNA repair plays in preventing mutagenic changes caused by oxidizing reagents. Cells possessing an impaired or non-functioning repair enzyme system would likely build up mutagenic changes in their genome, increasing genomic instability and placing them at heightened risk for oxidatively-induced disease.

Sandra Jean Gunselman
Cell & Molecular Biology
Colorado State University
Fort Collins, CO 80523
Fall, 2001

Dedication:

To my father, Dr. Marshall Gunselman, who always believed in me.

Acknowledgments

This study was supported by the United States Center for Environmental Health Research (USACEHR) through contracts DAMD-17-98-D-0016 and DAMD17-93-C-3006, NIH grant CA36447, the AMC Cancer Research Center and NIH National Research Service Award grant T32 ES07321.

The contents of this paper do not necessarily reflect the views of the Department of the Army unless so designated by other official documentation.

Table of Contents

Chapter I

Introduction

A. General Introduction

The ability to repair DNA damage has been a key factor in the survival of living systems throughout time. Damage occurs on a continual basis as a result of normal intracellular metabolism and environmental exposures to UV light, ionizing radiation and chemical compounds in the environment. Both of these sources produce reactive oxygen species (ROS), which are normally dealt with by various antioxidant enzymes.[1] The imbalance between the production of ROS and its removal by cellular enzymes leads to what is referred to as oxidative stress. Early evidence of the importance of various enzymes dealing with oxidative stress was provided by the discovery of superoxide dismutase (SOD).[2] SOD catalyzes the conversion of superoxide radical ($\bullet O_2^-$) to hydrogen peroxide (H_2O_2). H_2O_2 is subsequently neutralized to water (H_2O) by glutathione and catalase, two intracellular "antioxidants" that work to counteract any deleterious effects of H_2O_2. If H_2O_2 is not scavenged, the potential remains for triggering a number of events especially damaging to deoxyribonucleic acid (DNA). For example, H_2O_2 causes the oxidation of cysteine, which in turn can modulate protein phosphorylation.[3] H_2O_2 can also lead to the production of even more harmful ROS,

including the hydroxyl radical (•OH) through the iron-catalyzed Fenton Reaction.[4,5]. •OH binds indiscriminately to molecules, causing oxidation of proteins, lipids, nucleic acids and DNA structure. The biological implications of unchecked oxidation are enormous and have been the focus of a large volume of scientific research.[6-14]. Some ROS serve useful purposes as in cytotoxicity against pathogenic organisms.[15] The immune-mediated stimulation of NADPH-oxidase in leukocytes, monocytes, neutrophils and macrophages produces a burst of $\bullet^{-}O_2$, nitric oxide (•NO), and peroxynitrite ($ONOO^{-}$).[15] Evidence is also beginning to accumulate which implicates ROS-mediated recombination events with immune class-switching events and aging. [16]

This study examines the genotoxic properties of, Paraquat (PQ), a chemical known to produce ROS during the biotransformation process. Specifically, studies were undertaken to determine if PQ produced mutations in mammalian cells and if so, could those mutations be prevented by increasing DNA repair.

The production of free radicals

ROS are produced through three basic pathways: 1) normal cellular metabolism (i.e., phagocytosis and mitochondrial respiration), 2) enzymatic oxidation and 3) biotransformation processing of intracellular chemicals and xenobiotics from environmental exposures to chemicals, ionizing and UV radiation. Cellular respiration involves the reduction of molecular oxygen (O_2) to water. O_2 is reduced in a four-step process in the electron transport chain. Each step produces a partially reduced reactive intermediate known as a free radical. It has been estimated that as much as 5% of the ROS produced in the electron transport chain escapes and attacks cellular components. [17]

Electron Transport Chain	Reaction	Free Radical Produced
Step 1:	$O_2 \rightarrow e^- \rightarrow \bullet O_2^-$	(superoxide anion)
Step 2:	$\bullet O_2^- + e^- \rightarrow H_2O_2$	(hydrogen peroxide)
Step 3:	$H_2O_2 + e^- \rightarrow H_2O + \bullet OH$	(hydroxyl radical)
Step 4:	$\bullet OH + e^- \rightarrow H_2O$	

A second source of intracellular ROS production is from the oxidation of certain enzymes. For example, diamine oxidase, tryptophan dioxygenase, xanthine oxidase, cytochrome P-450 and the NADPH-cycle generate $\bullet O_2^-$ [18]; and glucose oxidase and guanyl cyclase produce H_2O_2.[19]

Thirdly, ROS can result from the metabolism of xenobiotics. Xenobiotics are man-made or natural chemical compounds such as medicinal drugs, pesticides and pollutants. Once absorbed these chemicals undergo biotransformation into water-soluble form that can be excreted. During this process ROS are produced. [20-22].

Of particular significance to this study is the redox cycling of the compound PQ (Figure 1). PQ actively produces ROS by the reduction of $PQ^{2+} \rightarrow PQ^{+}$ in the presence of nicotinamide adenine dinucleotide phosphate (NADPH) and NADPH cytochrome reductase supplied by microsomes.[21] PQ oxidation is coupled with the reduction of molecular oxygen to $\bullet O_2^-$, a free radical species.

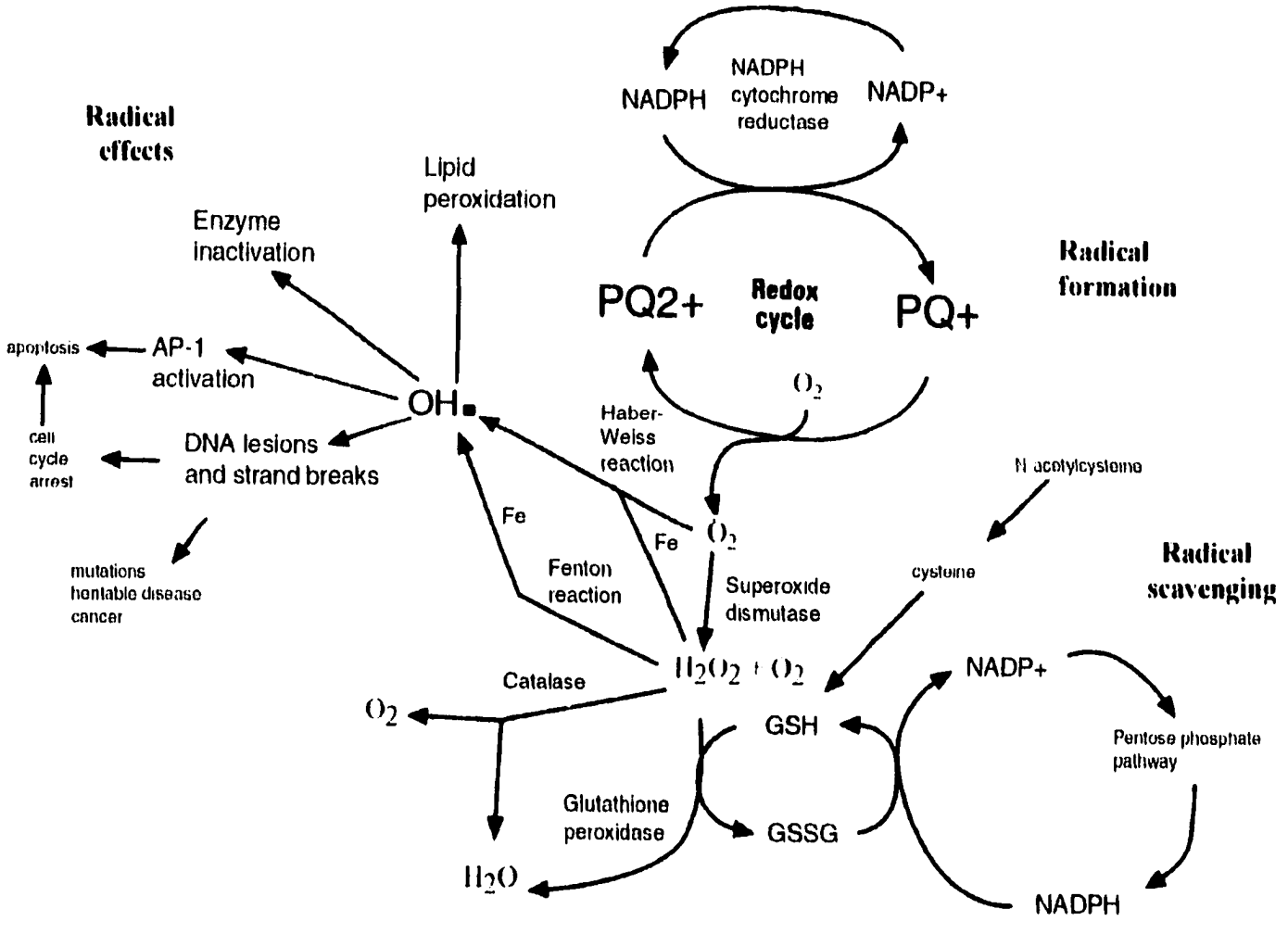

Figure 1. Schematic of Paraquat Metabolism

Effects of oxidative damage to DNA

Over one hundred different types of DNA damage have been classified via gas chromatography-mass spectrometry (GC-MS) and high pressure liquid chromatography (HPLC),[23,24] including oxidized purines and pyrimidines as well as fragmentation of the deoxyribose structure. Some of the products of oxidation are stable and can be broken down into by-products or returned to the original base.[25] Others remain as modifications of the DNA structure and go on to effect cell cycle regulation, protein function (or non-function) and gene expression .[26]

There are many biological implications of DNA alterations. For example, 2,6-diamino-4-hydroxy-5-N-methylformamidopyrimidine (7-methyl guanine with an open imidazole ring) has been shown to inhibit DNA polymerase I.[27] The known mutagenic form of damaged DNA, 8-hydroxyguanine (8oxoG)[9,28], forms 8oxoG:A during replication leading to a GC:TA transversion[29] [30] both *in vivo* and *in vitro.* [31,32]. Numerous studies have examined the mutagenic properties of 8oxoG [9] and 8-hydroxyadenine [33] and other studies have been able to correlate amounts of 8oxoG in tissues to cancer status.[12,34]

Another type of DNA damage caused by oxidation is the opening of the imidazole ring to form the formamidopyrimidine (Fapy) structure. *In vitro* studies have shown that Fapy lesions block DNA polymerases[30] and mRNA transcription.[35] *In vivo* studies of ring-opened modifications of DNA have been much more difficult to study given the lack of a method to incorporate the Fapy lesion into DNA or an oligonucleotide. Therefore, genotoxicity studies of Fapy lesions[36,37] and repair of Fapy[38-40] have been conducted using an *N*-methylated analog of Fapy known as me-Fapy. How relevant these studies are to actual events *in vivo* with regards to Fapy lesions is not understood at this time but,

what is clear is that unlike 8oxoG lesions which require a specific base to be paired with it for FPG recognition, Fapy lesions are identified for excision and repair based solely on their structure.[41]

In addition, Paul Doestch has conducted a number of studies on the consequences of DNA adduct formation on RNA, including 8oxoG, uracil, and O-6-methylguanine.[26,42]. It was found that these types of DNA damage did not block RNA polymerases during elongation but instead allow the insertion of mutagenic bases into the genome during transcription. Therefore, not only can DNA damage cause mutation and threaten genome integrity but RNA transcripts can also be affected. The transcription of damaged RNA can lead to the production of mutant proteins with the potential of affecting initiation of replication, cell division and genetic disease.

The accumulation of oxidative DNA damage has been linked to aging[43], ischemia[44], cancer[45], neural cell death[46], autoimmune disease[47], cell cycle arrest and apoptosis.[48] Oxidative DNA damage has been estimated to occur at the level of 10^4 lesions per cell per day in humans.[49] These lesions include hydrolytic depurination, hydrolytic deamination of cytosine and 5-methylcytosine bases, covalent adduct with DNA and oxidation of bases and damage to the phosphodiesterdeoxyribose backbone.[50-52]

Cellular mechanisms that counteract effects of ROS

Cells possess a number of defense mechanisms to counteract free radical damage (Figure 1). These mechanisms include SOD, which acts to prevent DNA nicking and blocks the Fenton Reaction[4]; catalase, which converts H_2O_2 to O_2 and H_2O; glutathione (GSH), which scavenges radicals by cycling between un-oxidized and oxidized forms;[53]

alpha tocopherol, Vitamins A, E, and C, which acts as antioxidants; the immune system and apoptosis. In addition, cellular enzymes can be induced which can stop cell cycle progression to allow time for DNA repair to occur[54](Figure 2) so far as to counteract changes to nucleic acids that may lead to mutation or gene activation/inactivation.[26] It is important to note that redox cycling of a chemical such as PQ can generate a large quantity of free radicals from a single molecule meaning that even minute quantities of a xenobiotic can have significant biological effect.

Damaged DNA can be processed through several types of repair systems including base excision repair (BER), nucleotide excision repair (NER), translesional synthesis (TLS), postreplication recovery (PRR) and recombination. Once thought to be highly specific, evidence is mounting[55] that these repair pathways have overlapping binding specificities and work in a cooperative network to maintain genome stability. Good reviews of DNA repair systems and their cooperative effort in maintaining genome integrity include those by Friedberg[54], Norbury and Hickson[56], Krokan[1],[57] and Hoeijmahers.[58]

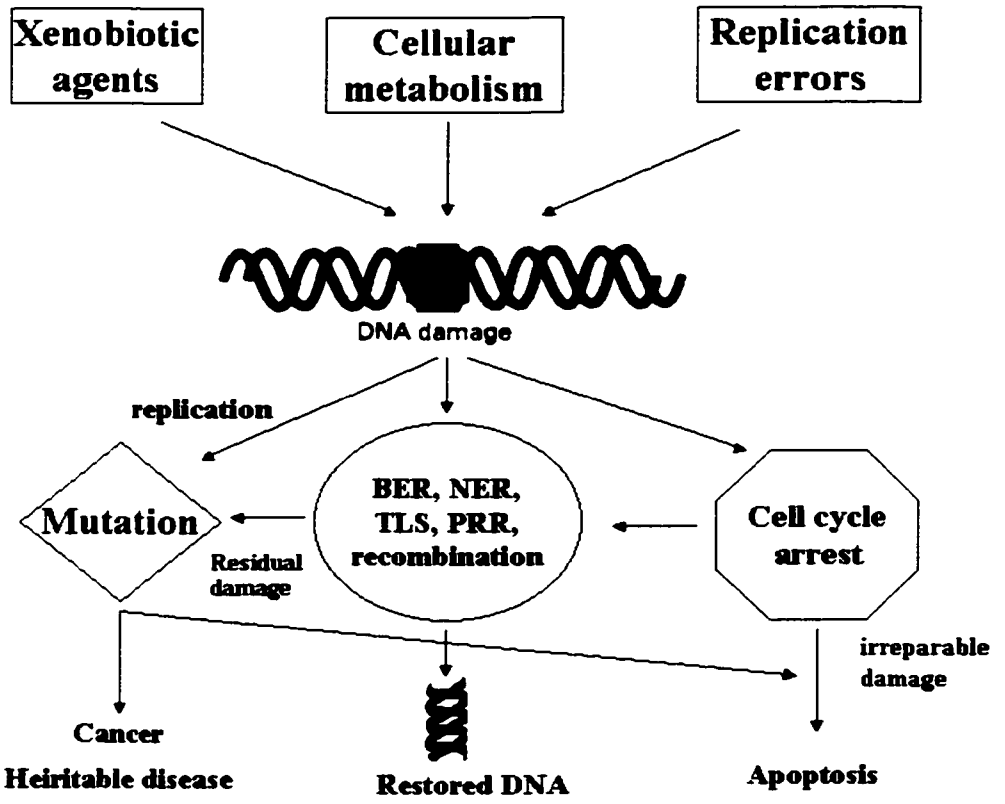

Figure 2. Sources of DNA damage, repair pathways and possible consequences to the cell. DNA is under continual attack from the environment and intracellular processes, which can lead to the production of reactive oxygen species. Cells have evolved repair mechanisms to bypass lesions or stop cell cycle progression to allow for DNA repair before proceeding with replication and transcription.

DNA repair mechanisms

Oxidative DNA damage has commonly thought to be processed almost exclusively through the BER pathway.[59] Evidence now shows that damaged DNA is processed through several types of repair systems including BER, NER, TLS, PRR and recombination. The classic model of BER involves the removal of the damaged base by a specific glycosylase, leaving an apyrinic/apyrimidinic (AP) site. The AP site is subsequently cleaved by an AP endonuclease, DNA polymerase fills in the gap with a new base and DNA ligase seals the ends together. Some of these glycosylases contain the endonuclease activity (i.e., bacterial FPG) and some do not. Other examples of glycosylases known to be involved in BER are Ntg1 and Ntg2 in *Saccharomyces cerevisiae*, and hOGG1 in human.

NER involves removal of DNA lesions and has been shown to remove products of oxidative damage once thought exclusively removed via BER.[55] NER works by nicking the DNA at points both 5' and 3' to the damaged area and removing the oligonucleotide. DNA polymerase then fills in the gap and DNA ligase joins the ends.[60] Examples of NER enzymes include Rad1 and Rad 2 in *S. cerevisiae* and UvrABC in *E. coli*.

PRR involves the repair of single strand breaks caused by damage on the opposing DNA strand. The damaged DNA base is bypassed to allow for repair of the gap. PRR in bacterial systems requires RecA and RecA-mediated SOS response.[61] TLS also involves a certain amount of damage tolerance by allowing the bypass of lesions on the DNA by polymerases in order to allow the cell to survive. In *E. coli*, Pol II, IV and V have all been shown to be involved in TLS.[62]

Recombination takes place in the presence of single or double strand DNA breaks. Recombination is also involved in immunoglobin class-switching.[62,63] Recombination can serve as a damage *tolerance* rather a damage removal by allowing the damaged bases to remain in the genome process.[55] Recently, it was found that oxidative damage could induce illegitimate recombination – a connection that may exist between Rad52 and ROS-induced processes.[64] A good review of these processes can be found in Harris, et al.[63]

Hypothesis and purpose of study

Paraquat (1,1'-dimethyl-4, 4'-bipyridinium, PQ) was selected for this study due to its cyclic oxidation and reduction in tissues leading to oxidative DNA damage. [21,65,66] Despite its known production of ROS within the cell, PQ has not been generally found to be mutagenic[67] until recently.[68,69]. It was hypothesized that if PQ produced oxidative DNA damage then mutagenicity had to occur and be detectable with a sensitive methodology. The methodology selected therefore was the sensitive A_L mutation assay developed by Waldren, et al.[70-78] The study of PQ mutability also held importance from a public health point of view. PQ is use is widespread and incidences of acute poisonings are well documented. The genotoxic effects of low dose exposures however, have been few yet, are highly significant for the healthcare concerns of field workers, residents in farming communities and anyone that consumes of fruit and vegetables dusted with PQ.

This study also involved the role of the BER enzyme, formamidopyrimidine glycosylase (FPG), also known as MutM, FAPY-DNA glycosylase and 8-hydroxyguanine-DNA-glycosylase in PQ genotoxicity in mammalian cells. If

mammalian cells were able to remove and repair more DNA damage than normal from their genome, it was hypothesized that survival of these cells would increase and PQ mutagenicity decrease. FPG is a base excision repair N-glycosylase first cloned in *E. coli* by Boiteux, et al.[79] It was initially characterized as a glycosylase that removed imidazole ring-opened (Fapy) structures from the DNA[79] but since then it has been shown to bind to 8-hydroxy structures,[80] 5-hydroxycytosine[81] and apyrinic/apyrimidinic sites.[82] Purification of FPG from bacteria and cloning of the fpg gene by mass screening of a plasmid library made it possible to characterize its structure and biological functions.[57,79] The bacterial gene that encodes for FPG was transfected into a line of mammalian cells (A_LH). This vector also contained a neomycin-resistant gene therefore, selection of clones containing the inserted gene were possible by growing in media + neomycin. After confirming that the transformed cell lines not only expressed the fpg gene but also produced an active FPG protein, PQ was used to induce oxidative damage. Survival and induced mutant fraction (M_f) were measured and compared in A_LH and fpg transformants exposed to PQ. Fpg expression suppressed mutation and survival increased. These results are evidence that repair of oxidative DNA damage is essential to the prevention of mutation in mammalian cells. An impaired or mutated repair system, caused by genetic predisposition or as a result of exposure, would have detrimental effects to the overall health of an individual's cell, leading in some cases to disease.

B. Paraquat (PQ)

Production, Industrial Use and Public Health

PQ is a widely used contact herbicide used in the control of broad-leaf weeds and grasses. PQ is also used as an aquatic herbicide where it is absorbed by aquatic plants, silt and fish. It is also used as a desiccant for pineapples, sugar cane and soya beans to accelerate the drying process.

PQ was first synthesized in 1882.[66] In 1955, PQ was commercially produced by Imperial Chemical Company (ICL) Laboratories, a company now known as Zeneca. Zeneca is the world's largest producer of PQ and mass-produces PQ in the United Kingdom, the United States, Brazil, India, Thailand, and Malaysia. Zeneca produces formulations of PQ containing 24-36% active ingredient for commercial use and less potent formulations of 2.5% for home use.[66] Recent concern over environmental and health risks of PQ has resulted in its being banned in Norway, Hungary, Finland, Austria and Sweden. Use remains high (and continues to grow) in the United States, Japan, Malaysia, Mexico, France and Brazil. PQ poses health problems in countries such as Taiwan and Thailand, where it has been the leading cause of accidental death.[83]

PQ is used in a variety of commercial products and can be found for sale under the names Crisquat, Cyclone, Dextrone, Dexuron, Gramaxone Extra, Herbaxone, Ortho Weed and Spot Killer and Sweep.[65] In the 1970's PQ was used by the US Drug Enforcement Agency to spray *Cannabis sativa* fields in Mexico in an attempt to reduce the amount of *Cannabis* reaching the US.[84,85]. Several individuals were hospitalized after smoking marijuana containing PQ residues resulting in a ban of its use by the US government in this capacity.

Chemical Properties

PQ is a member of the bipyridyl group of chemicals and thus is almost completely insoluble in organic solvents but highly soluble in water. It is a non-volatile, ionic compound that is oxidation-reduction (redox)-cycled in tissues generating an abundance of free radicals. It acts non-selectively and is highly toxic to both plants and animals. Paraquat dichloride is produced from pyridine in the presence of sodium in anhydrous ammonia by quarterizing the 4,4'-dipyridyl with methyl chloride.[86] Table 1 lists the chemical properties and shows the structure of PQ.

Mode of Action

PQ produces both superoxide anion (O_2^{-} •) and hydrogen peroxide (H_2O_2)(Figure 1). These ROS are generated by the reduction of $PQ^{2+} \rightarrow PQ^{+}$ in the presence of NADPH and NADPH cytochrome reductase supplied by microsomes (Figure 1). Oxidation is coupled with the reduction of molecular oxygen to superoxide anion radicals and generates a large quantity of free radicals with a single molecule of PQ.

Table 1. Chemical Properties of Paraquat.

Chemical Name	Paraquat
	1,1'-dimethyl-4, 4'-bipyridinium
	$C_{12}H4Cl_2N_2$
Molecular Weight	186.2
CAS Number	4685-14-17
Solubility @ 20°C	
Water	561 g/L
Methanol	144 g/L
Ethanol	1.7 g/L
Acetone	200 mg/L
Physical State	Solid white
Specific gravity	1.24-1.26
Melting point	175°-180°C
Stability	Stable on exposure to hot acids Unstable in alkalis Photosensitive
Flash point	Non-explosive, nonflammable
Volatility	Nonvolatile

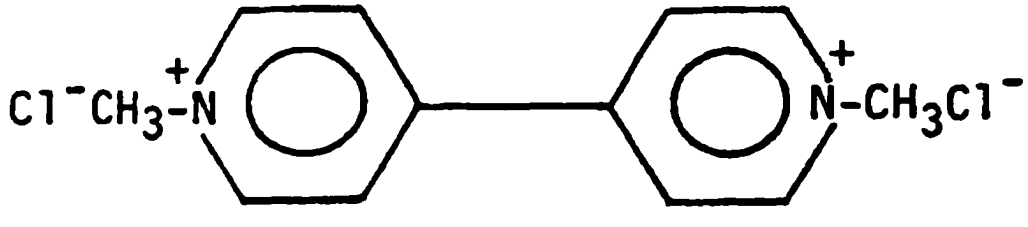

Toxicity

PQ is highly toxic and listed as an EPA Class I toxic substance.[87] Oral ingestion of PQ causes burning and abdominal pain leading to convulsions and, in most cases death. Reports have listed the lethal dose of active PQ for human as a single teaspoonful (~5 ml).[65] PQ enters the cells of animals and plants via passive diffusion[88] and once absorbed, is distributed through the bloodstream. It is excreted fairly rapidly in organisms (~90% in 2 days), although there are delayed toxic effects, some of which can lead to cell death. PQ ingestion produces toxicity to multiple organs in mammal including the lungs, heart, liver, kidneys, cornea, adrenal glands, skin and the digestive system. The main target of PQ toxicity however, is the lung where it produces irreversible pulmonary fibrosis. [89-91]. Redox cycling of PQ can occur rapidly in the lungs due to the abundant supply of oxygen and death occurs as a result of lung edema and fibrosis. Although several therapies have been attempted (i.e., N-acetylcysteine), no treatment is known that can effectively protect living tissues from the toxic effects of PQ exposure.

Little is known about long-term or chronic PQ exposure or long-term effects on genome integrity. Chronic long-term exposure to PQ has gained attention recently as possibly playing a role in several oxidatively-induced diseases including cancer and neurodegenerative diseases.[92] Reviews on the environmental and toxicological aspects of PQ include those of Kimbrough,[91] Smith and Heath.[86,91,93-99].

Acute toxicity

PQ is highly toxic when ingested. Accidental poisoning with PQ is cause of concern among factory workers or field sprayers who come into contact with it. Oral LD_{50} values have been reported at 110-150 mg/kg in rats, 50 mg/kg in monkeys, 48 mg/kg in cats and 50-70 mg/kg in cows.[100,101]. Lethal doses for humans have been reported as 35 mg/kg[100] and death can occur up to 30 days after ingestion. Most exposures to PQ are either dermal or respiratory and result from exposure in fields where the chemical is applied as an herbicide. Precautions such as respiratory protection and skin coverings have been employed to cut down the risks of PQ exposures to workers.

Chronic Toxicity

Long-term exposure of field workers to PQ has been shown to cause skin sensitivity and irritation, minor eye and nose irritations[100] and in some cases, even ulcerations. Spray operators can develop fingernail deformities, discolorations and loss of nails. Rats showed no chronic effects after exposure to 1.25 mg/kg/day for 2 years however, dogs developed lung deterioration at doses of 34 mg/kg/day for 2 years.[100] Overall, studies of long-term effects to workers exposed to PQ have been poorly conducted, focusing on acute reactions and grossly overlooking long-term molecular aspects of PQ metabolism which may cause less visible but more serious risks involved in redox chemistry of the cell.

Carcinogenicity

The US Environmental Protection Agency (EPA) called for carcinogenicity studies of PQ in 1987 using the Ames Test.[87] Studies of rats fed doses of PQ developed lung, thyroid, skin and adrenal tumors.[102] Results of the testing were positive and the EPA has classified PQ as weakly carcinogenic.[103,104]. Despite the "weak" classification, PQ is listed as one of the "Dirty Dozen" Pesticides by the World Health Organization and many watchdog groups would like to eliminate or diminish use.[65]

Teratogenicity

PQ is not considered a risk for causing birth defects at realistic exposure levels.[65] However, studies of pregnant mice exposed to high doses of PQ during the organ-forming period had offspring with less complete bone development than offspring whose mothers were exposed to lower does.[65]

Mutagenicity

In 1987 the US EPA requested mutagenicity testing on PQ using the Ames Test. Eight of sixteen tests were negative, four were weakly positive and four were positive.[102] The EPA has, therefore, listed PQ as being weakly genotoxic. Most studies conducted outside of the EPA have concluded that PQ is not mutagenic[67] however, recent evidence,[68] including this study find that it is mutagenic.

Ecotoxicity

Environmental fate – Ultraviolet light (UV) and sunlight degrade PQ into less toxic compounds.[65] PQ is not mobile in soil once bound but can be transported in runoff and enters aquatic systems.[100] Soil particles exhibit a strong affinity for binding with PQ and the bound particles can persist for extended periods of time. Half-lives of greater than 1000 days have been reported.[105,106]. PQ is not considered a risk for groundwater contamination since only one of 721 groundwater samples collected nation-wide in the US contained PQ (20 mg/L).[102] PQ can bind to sediments in aquatic systems and its persistence in water is greater due to the lack of oxygen required for metabolism. PQ dichloride has been shown to exhibit a half-life of 23 weeks.[102] Following application of PQ to vegetation it decomposes readily in UV light. Only trace amounts of PQ residue have been detected on foods grown for human consumption. However, when PQ is used as a desiccant levels of up to 0.2 mg/kg have been found.[66]

Environmental effects – the most obvious effects of PQ in the environment are the killing of plants and weeds. Since PQ acts non-selectively, any vegetation it comes into contact with it readily absorbs it. Redox cycling occurs in an effort to detoxify PQ, ROS are produced as a by-product of the detoxification and cell death follows. Of great concern is the effect PQ may have on wild animals, including birds and aquatic species. The effects of PQ depend greatly upon species of animal, its weight and exposure level. A good review which lists toxic effects of PQ to particular species is "Paraquat Hazards to Fish, Wildlife and Invertebrates: A Synoptic Review" by Ronald Eisler.[66]

Molecular Studies Using Paraquat

PQ has recently gained popularity in basic research laboratories as a useful tool in oxidation studies.[67-69,107,108] Due to redox cycling, one molecule of PQ can cycle several times producing one molecule of superoxide radical with each cycle (see Figure 1). The dose of PQ can be controlled and due to its solubility in water, it is easily applied. PQ has been used to study lipid peroxidation,[109] effects of antioxidants such as melatonin,[110] N-acetylcysteine, Bis-sulfoxamine (BSO), catechin and epigallocatechin,[111] aging,[112] cancer,[108] neurological disease,[113] uncoupling of nitric oxide synthase,[114] catalase,[68] membrane function,[109] and glutathione.[115] A variety of oxidation effects are caused by PQ, such as chromosomal aberrations yet, it generally has not been considered mutagenic or genotoxic. This study, however, clearly demonstrates that PQ is indeed mutagenic in mammalian cells.

C. Formamidopyrimidine glycosylase (FPG)

Formamidopyrimidine glycosylase (FPG) is also known as MutM, FAPY-DNA glycosylase and 8-hydroxyguanine-DNA-glycosylase. FPG is a base excision repair N-glycosylase that was first cloned in *E. coli* by Boiteux, et. al.[79] It was initially characterized as a glycosylase that removed imidazole ring-opened (Fapy) structures from the DNA but since then it has been shown to bind to 8-hydroxy structures,[80] 5-hydroxycytosine[81] and apyrinic/apyrimidinic sites.[82] Purification of FPG from bacteria and cloning of the fpg gene by mass screening of a plasmid library[79] made it possible to characterize it's structure and biological functions.[57,116]

Physical and structural properties of FPG protein

The FPG protein is a monomer of 30.2 kDa and contains 269 amino acids. It has a stoke radius of 2.5 nm and an isoelectric point of 8.6.[117] Atomic absorption shows that it contains one zinc atom per molecule with the motif (-Cys-X_2-Cys-X16-Cys-X_2-Cys) on the C-terminus.[117,118] FPG contains an invariant N-terminal sequence of Pro-Glu-Leu-Pro-Glu-Val- and invariant lysines Lys52 and Lys147.[116] The N-terminal proline of FPG appears to be critical to repair by linking to the damaged DNA and initiating the catalytic incision of a damage base.[119] Recent crystallography data has confirmed this.[120] The encoding gene, fpg, is highly conserved across aerobic bacteria (*E coli, Therm. Therm.*)[120] and homologs of FPG protein have been found both in *S. cerevisiae* (OGG1, OGG2)[40], mouse (mOGG1) [121]and humans (hOGG1) [122]. These homologs display a similar binding specificity for 8oxoG and Fapy ring-opened bases in DNA despite differences in their primary sequences.[121,123] OGG1, which functions like FPG to remove 8oxoG from double stranded (ds) DNA, shows greater sequence similarity to *E. coli* endonuclease III (endoIII) protein, a protein associated with repair of UV-irradiation damage.[124]

The weight of evidence suggests that fpg plays an important role as a redox regulatory mechanism. *In vitro*, FPG has been show to excise purines, including imidazole ring-opened adenines and guanines and 8-oxoG.[80,116] The structure of the damaged base does not appear to be the only recognition factor for FPG. Studies of Fapy residues embedded in β-DNA show efficient repair but when Fapy residues are placed in Z-DNA no repair occurs.[125] Similarly, when 8-oxoG is paired with adenine it is excised at a much lower rate than when it is paired with cytosine. Thus, both base pairing and

structure appear to play an important role in damage recognition by FPG. *In vivo*, FPG has been shown to have an antimutator effect.[126] In E. coli it is transcribed as part of an operon triggered by E. coli lacking both thioredoxin and glutathione.[127,128] Other studies have shown that strains of bacteria with mutations in the *mutM* (FPG) gene exhibit a 10-fold increase in GC→TA transversions over wild type.[126] Still other studies have shown that the presence of FPG of cells causes an increased resistance to thiopeta,[129] aztridine[130] and gamma rays.[131]

In *E. coli*, FPG acts in concert with two other DNA glycosylases, MutY and MutT[126 132](Figure 3). These glycosylases form a three-prong line of defense against the mutagenic effects of 8oxoG to maintain genome integrity. FPG acts to remove 8oxoG: cytosine mispairs prior to replication, MutY acts specifically to remove 8oxoG past replication in the 8oxoG: adenine configuration and MutY T works to prevent the effects of oxidization on the nucleotide pool, specifically by suppressing the incorporation of d8oxoGMP into the DNA template opposite an adenine.[133] DNA analyzed from a *mutM (fpg) MutT* double mutant showed large quantities of accumulated 8oxoG, amounts exceeding those found in single mutator strains.[132] The contribution of d8oxoGTP to 8oxoG content in DNA was estimated to be four molecules/chromosome,[132] evidence that the rate of 8oxoG accumulation is as much influenced by incorporation of oxidized nucleotides, as it is the direct oxidation of DNA.

Mode of Action

The FPG protein contains three enzymatic activities: (i) DNA glycosylase activity which recognizes damaged double stranded DNA producing an AP site, (ii) AP lyase

activity which cleaves the 3' phosphodiester bond of AP sites thru β-elimination, leaving a clean gap and (iii) dRpase activity which cleaves the 5'deoxyribose phosphodiester moieties.[116]

Crystal structure and catalytic mechanism

In 2000, the crystal structure of FPG was published.[120] It was made from *Thermus thermophilus* HB8, an extremely thermophilic bacterium. X-ray crystallography was determined at 1.9 Å resolution with multiwavelength anomalous diffraction phrasing using the intrinsic Zn^{2}+ ion located in the zinc finger motif.[120] The crystal structure of FPG in a complex with dsDNA has revealed a zinc finger motif, a helix-two-turns-helix (H2TH) motif and catalytic residues that are similar to those of other DNA glycosylases. As other studies have revealed, FPG contains an N-terminal domain with two alpha sequences, a C-terminal domain with four alpha helices and a B-hairpin loop of the zinc finger motif. Good reviews of the FPG structure and catalytic mechanism include Bhagwat and Gerlt[134] and Sugahara, et al.[120]

Based upon the three-dimensional crystal structures, a catalytic mechanism of FPG was proposed and is summarized as the following:

i) FPG binds to a GO structure on the DNA with a "gripping" motion at the hinge region. The ammonium cation of Lys52 acts as a proton donor for cutting of the glycosidic bond on the nucleotide to release the damaged base.

ii) This leaves a carbonium ion at C1' of deoxyribose which is attacked by the N-terminal amino group of Pro1 on FPG. Hydrogen bonding then stabilizes the cation.

iii) The pentose ring of deoxyribose is broken by protonation and a Schiff base is formed between Pro1 of the FPG and the C1' atom of the opened deoxyribose ring.

iv) The enamine forms via mesomeric equilibrium and 3'-phosphoester breakage occurs along with B-elimination.

v) Proton withdrawal by Glu2 causes transfer of the conjugated diene.

vi) δ-elimination esterifies the 5'-phosphoester bond

vii) Protonation of Lys52 and release of the deoxyribose product leave a one-nucleotide gap in the dsDNA.

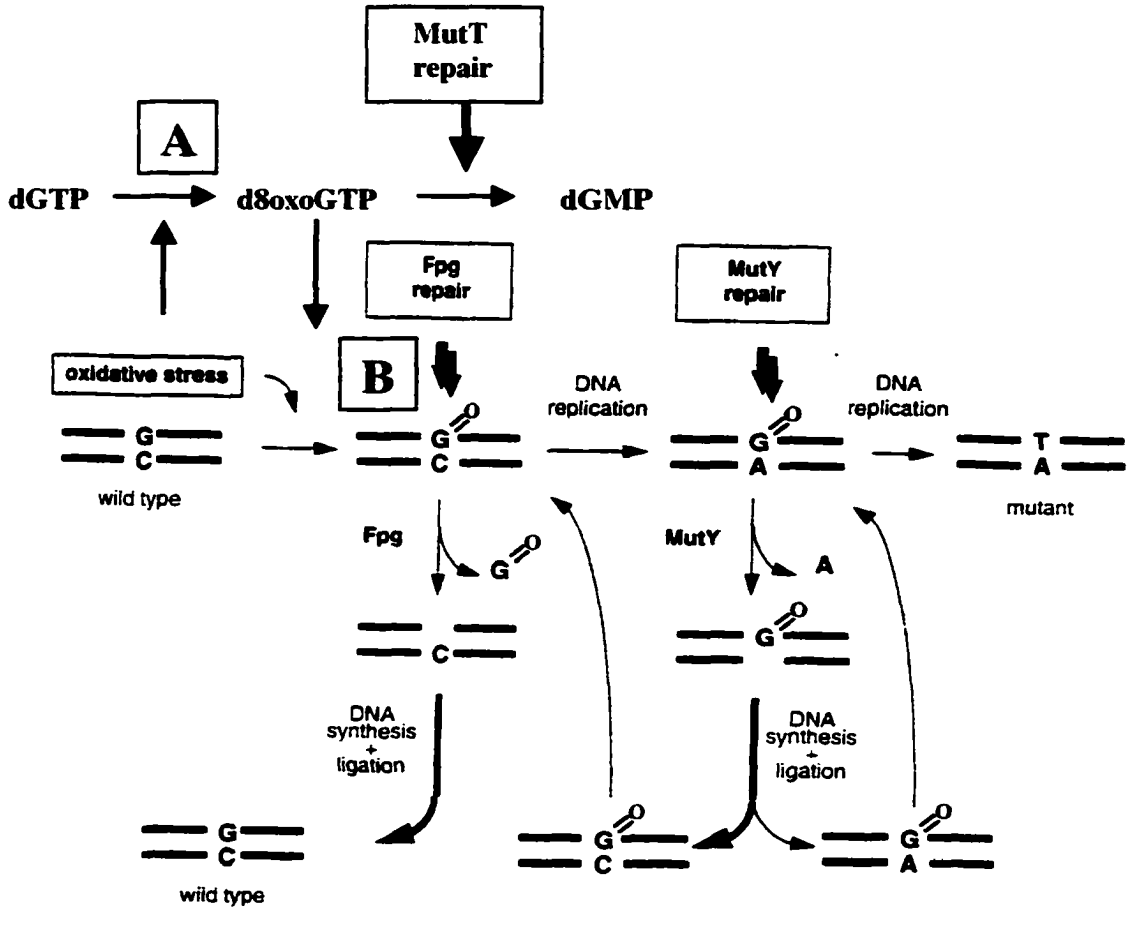

Figure 3. Overlapping functions of FPG, MutT and MutY in the removal of 8oxoG from DNA. Oxidation can occur both in the nucleotide pool (A) and directly to DNA structure (B). Both have deleterious effects to the integrity of the genome.

Chapter II

Materials and Methods

A. Cells Studied

Human x Chinese hamster ovary (CHO) hybrid cells (A_L) were used throughout the experiments.[78] These cells contain a standard set of CHO chromosomes and a single copy of human chromosome 11. A method was developed and has been described[78,135] for the quantification of single gene mutations and large and small deletions in these mammalian cells. The assay involves the use of somatic cell hybrids containing a single copy of human chromosome 11, most of which is not essential for cell reproduction and therefore can be mutated without affecting cell survival. The method was developed by fusing Chinese hamster ovary (CHO) cells with human fibroblasts.[78,135] The resulting hybrid contained a standard set of CHO chromosomes plus a single copy of human chromosome 11 (Figure 4). Markers used to quantify mutants and define mutant spectra have been identified on both the short and long arm of chromosome 11, including RAS, HBE, CD59 and APO-Ai (see Figure 5).

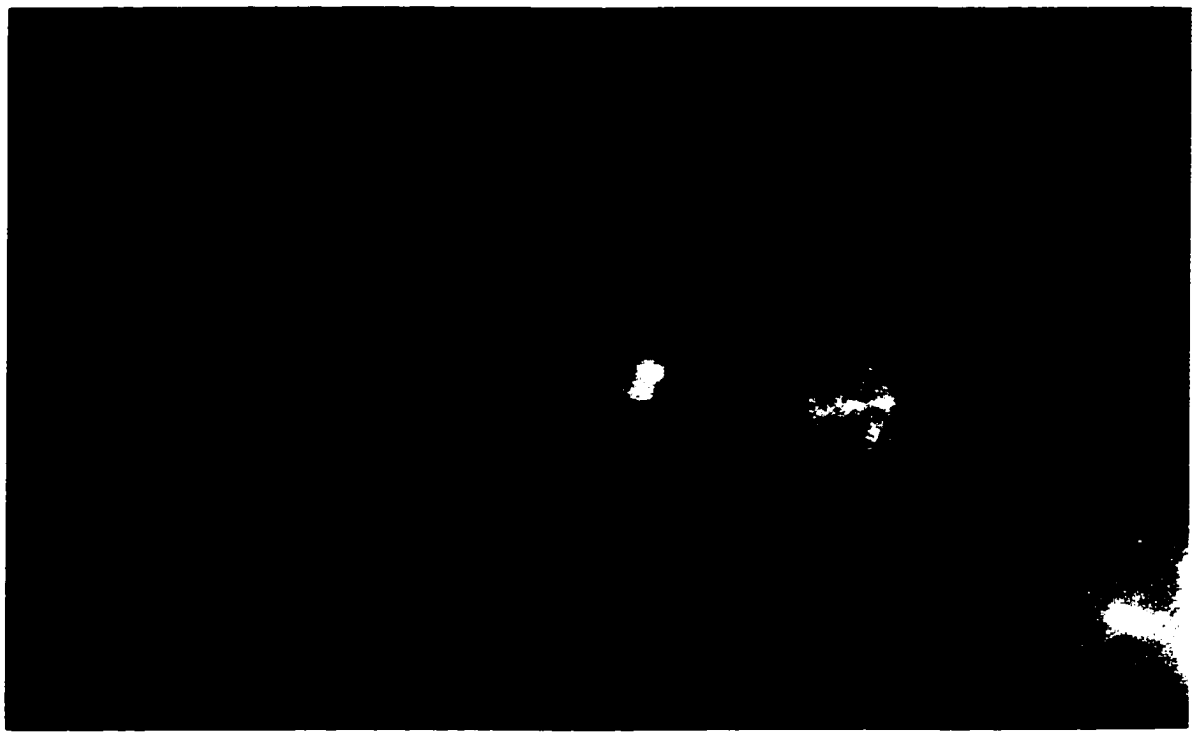

Figure 4. Fluorescent *in situ* hybridization (FISH) image of A_L cells. FISH methodology confirmed the presence of a single copy of a human chromosome. The fluorescent probe used was specific for human chromosome 11.

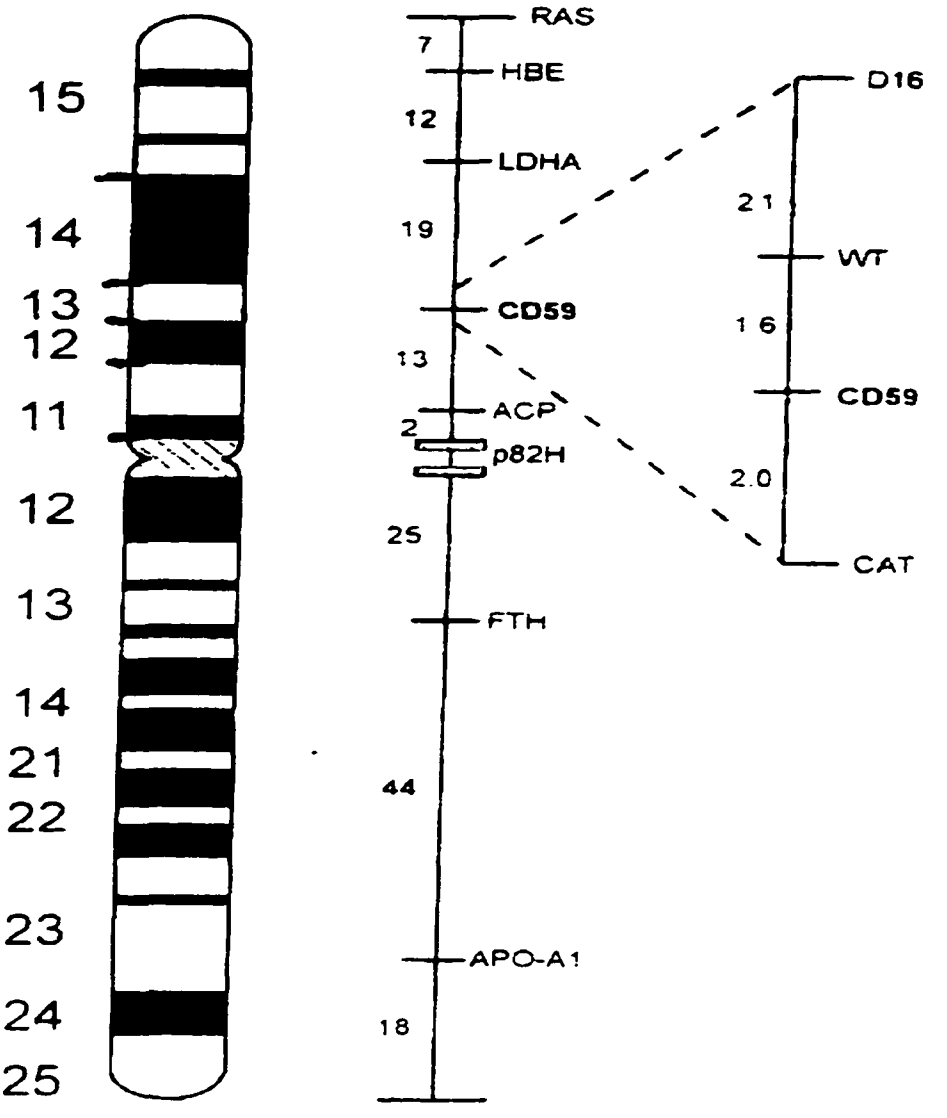

Figure 5. Schematic of human chromosome 11 and marker identification. Human chromosome 11 is used in the A_L mutation assay. Identification of markers used on chromosome 11 are identified as follows: RAS, v-Ha-ras Harvey rat sarcoma viral oncogene homolog; HBE, hemoglobin; LDHA, lactose dehydrogenase A; D16, anonymous probe S11 D16; WT, Wilms' tumor; CD59, cyclin-dependent protein 59; CAT, catalase; ACP, acid phosphatase 2; p82H, pericentric centromeric probe; FTH, Heavy-ferritin protein; APO-A1, apolipoprotein A-I.

Chromosome 11 contains CD59 (or MIC1),[136] the gene that encodes the cell surface antigen CD59 (referred to previously as S1). CD59 is a regulator that protects cells from cytoltic attack (self-lysis) by the membrane attack complex MAC.[136] CD59 has been crystallized and sequenced. It was shown to contain four exons.[137] Primers to these exons have been developed by Waldren, et al. Studies of CD59 have also shown that it inhibits binding of C9 to exon C5b-8, resulting in the MAC complex not being formed.[137]

Mutation at the CD59 locus in the A_L cells was studied via a complement-mediated lysis analysis using monoclonal antibodies, which kill $CD59^+$ cells in the presence of rabbit serum complement E7.1[136] but not $CD59^-$ cells. After exposure of cells to a mutational event, a 10-day expression period was allowed before adding antibody + complement. Surviving mutant colonies were fixed, stained and counted to produce a mutant induction curve.

Tissue culture conditions

- Cells were maintained using Ham's F12 media containing 7% fetal calf serum, 3% new born serum, 0.5% penicillin/streptomycin, and 1.5% HEPES.
- Iron content of the media was $Fe(NO_3)_3$ 0.000005 g/L; $FeSO_4$ 0.000417 g/L.
- Cells were plated in either 60 mM or 100 mM plates using 4 and 8 ml of media respectively and maintained in an incubator at 37°C and humidified at 5% CO_2/95% air.
- Cells were harvested via trypsinization every two days and re-plated.

- Periodically (once per month) hygromycin was added to each plate to selectively kill mutant cells that did not contain the hygromycin-resistant vector. Clones containing a neomycin-resistant vector were selected with neomycin.

B. Transfection of the fpg gene into A_LH cells

To produce A_LH cells in culture with an increased BER capacity, transfection of the fpg gene was done using the psv2neofpg plasmid provided by Dr. Jacques Laval, Unit 347, INSERM Le Kremlin Bicetre, France. To maintain the plasmid it was first transfected into *E. coli* JM109 competent cells (Promega, Madison, WI) using the Promega Standard Transformation Kit protocol (TB095). In this procedure 50 µL of JM109 cells were placed in three separate tubes and 0, 10 and 40 µg of plasmid added to the tubes. DNA binding was allowed for 10 minutes on ice the cells were heat-shocked for 50 seconds in a 45° water bath. The tubes were returned to ice and 900 µL of Terrific Broth (TB) solution (Difco Laboratories, Detroit, MI), made up of 23.8 g TB and 7.5 g agar was added. After incubating for 1 hour in a shaking 37°C water bath, cells were plated on ampicillin plates and incubated overnight. Colonies were chosen randomly by eye, trypsinized and frozen.

Next, the psv2neofpg plasmid was transformed into wild type cells, A_LH, using the Gibco BRL Lipofectin® Transfection Kit protocol (Gibco BRL, Gaithersburg, MD). In this procedure, A_LH cells were plated @ 3×10^5 on two 60 mm plates and grown to 40% confluence. One µg of the psv2neofpg plasmid was diluted in Ultraculture medium containing no serum (Biowhittaker, Walkersville, MA). An additional mixture of Lipofectin® Reagent was mixed with medium and allowed to sit for 30 minutes. The

two solutions were mixed and incubated at room temperature for 15 minutes. The cells were washed with Ultraculture medium once and the cell pellets, resuspended in 1.8 mls of Ultraculture medium, added to the 60 mm plates containing the A_LH cells and incubated for 24 hours at 37°C. The medium was changed to the normal F12 growth medium (see tissue culture section above) and returned to the incubator for 24 hours. Cells were then subcultured at 3 x 10^5 cells in 100 mM plates and selected with 800 µg neomycin. Clones were selected, numbered and named AHF-*n*. Thirty clones were selected, expanded and frozen for future use.

A blank neomycin vector was also transfected into A_LH cells using the Gibco procedure described above for the fpg transformants. Clones were selected, numbered "AHneo-*n*" and used as controls for later experiments.

C. Confirmation of transformation and FPG activity

1. PCR of fpg cDNA

DNA was extracted from clones using the Genomic Tip and Buffer Kit (Qiagen Inc., 9600 De Soto Avenue, Chatsworth, CA). Purity of each sample was confirmed via UV-vis at A260/280 with a preset range for purity of 1.6-1.9.

Two sets of forward and reverse primers were designed and used for polymerase chain reaction (PCR). Primer set 1 was designed using the Primer3 Output website located at the internet address **www.genome.wi.mit.edu/cgi-bin/prmier/primer3.cgi** and provided by the Massachusetts Institute of Technology. By entering the fpg sequence the Primer3 Output program provides selections of forward and reverse primer sequences.

Primer Set 1 sequences:

fpg forward: 5' GGTCAGCACATTATGCCCTT 3'

fpg reverse: 5' TACCGTTTAAGCGACCAACCC 3'

predicted molecular weight (mw) of product: 125 base pairs (bps)

Primer set 2 sequence was taken from a manuscript [128].

Primer Set 2 sequences:

Fpg forward: 5' AAATAGCCCGGTTTACCATCACTTT 3'

fpg reverse: 5' CGGCTGGCGTCATCACTGTC 3'

predicted molecular weight (mw) of product: 250 base pairs (bps)

Primer Sets 1 and 2 were made by Macromolecular Resources (Colorado State University, Dept. of Biochemistry, Fort Collins, CO).

PCR conditions were carried out using the Invitrogen cDNA Cycle Kit (Invitrogen Corp., 1600 Faraday Avenue, Carlsbad, CA) using the following conditions:

PCR Mix per Sample: sterile water, 8.7 µL, 10X Qiagen buffer 2 µL, dNTPs 2 µL, forward primer 2 µL, reverse primer 2 µL, magnesium chloride 1 µL, solution "Q" 2 µL, taq 0.3 µL.

PCR conditions: 94°C 5 minutes, 30 cycles of 94°C denaturing (30 seconds), 60°C annealing (30 seconds) and 72°C extension (30 seconds) and 72°C 10 minutes.

Following PCR, samples were run on a 2% agarose gel (GenePure 3:1 agarose, ISC Bioexpress, Kaysville, UT) and visualized by UV light.

2. RT-PCR

Reverse transcription (RT)-PCR (Diffenbach 1995) is a technique that combines the synthesis of cDNA from RNA templates with PCR. RT-PCR was carried out using the cDNA Cycle Kit (Invitrogen Corporation, Carlsbad, CA). RNA was extracted from each sample using the RNeasy Kit (Qiagen Inc., Chatsworth, CA). Quantitation of each sample was confirmed via UV-vis at absorbance A260 and quality of the RNA confirmed by Northern gel analysis.

Northern Gel Analysis:

- A Northern gel was poured using 1 gram agarose, 10 mls 10X MOPS and 85 mls diH_2O. Mixture was boiled and 5.4 mls 35% formaldehyde and 6.6 µL 10 mg/ ethidium bromide added.
- 2 µg of RNA were diluted with 2 volumes of 1.5X sample buffer (622.6 mls formamide, 211.7 mls formaldehyde, 124.5 mls 10X MOPS, 41.2 mls DEPC-treated water).
- The RNA was denatured for 5 minutes by heating in a 68°C water bath. Denaturing was stopped by placing samples on ice immediately.
- 10X formamide loading dye was added to a final concentration of 1X in MOPS buffer.
- Samples were loaded onto the gel and run at 65 volts for 1 hour.

- The gel was transferred to a nitrocellulose membrane in 10X SSC Buffer for 24 hours.
- The membrane was pre-hybridized for 5 hours at 42°C in 15 mls of Prehybridization Solution (100 mls formamide, 70 mls 20% SDS, 24 mls 1 M sodium pyrophosphate, pH= 7.2 and 6 mls H_2O).
- The prehybridization solution was removed and 15 mls of fresh solution added.
- RNA probe was added and hybridization was run at 42°C overnight.
- The membrane was washed 3 times as follows:
- 1st rinse: 2 XSSC, 0.1% SDS 10 minutes at 42°C
- 2nd rinse: 0.5X SSC, 0.1% SDS 15 minutes at 42°C
- 3rd rinse: 0.1X SSC, 0.1% SDS 30 minutes at 50°C
- The membrane was wrapped in plastic wrap to prevent drying and a picture taken.

RT Reaction:

- 10 ng of RNA for each sample were placed in a tube on ice. A test mRNA was provided in the kit to be used a control for the RT procedure.
- Sterile water was added to bring the volume up to 11.5 µL and 1 µL of random primer was added.
- The tubes were heated at 65°C for 10 minutes and then placed on ice for 2 minutes.

- Following a short centrifugation, 1.0 µL RNase inhibitor, 4.0 µL 5X RT Buffer, 1.0 µL 100 mM dNTPs, 80 mM sodium pyrophosphate and 0.5 µL AMV Reverse Transcriptase was added to each tube.
- The tubes were incubated at 42°C for 1 hour and then at 95°C for 2 minutes.
- PCR conditions were carried out using the Invitrogen cDNA Cycle Kit (Invitrogen Corp., 1600 Faraday Avenue, Carlsbad, CA) and the following conditions:

PCR Mix per Sample: 1 µL sample, 8.7 µL sterile water, 10X Qiagen buffer 2 µL, dNTPs 2 µL, forward primer 2 µL, reverse primer 2 µL, magnesium chloride 1 µL, solution "Q" 2 µL, taq 0.3 µL.

PCR conditions: 94°C 5 minutes, 30 cycles of 94°C denaturing (30 seconds), 60°C annealing (30 seconds) and 72°C extension (30 seconds) and 72°C 10 minutes.

PCR Mix for mRNA control: 2 µL sample, 37 µL sterile water, 5 µL 10X PCR buffer, 1 µL 100 mM dNTPs, 2 µL forward primer, 2 µL reverse primer, 0.5 µL taq.

PCR conditions for mRNA control: 30 cycles of 94°C 1 minute, 55°C 2 minutes and 72°C extension 3 minutes.

- Samples were then run on a 2% GenePure 3:1 agarose gel (ISC Bioexpress 420 N. Kays Drive, Kaysville, UT) and visualized by UV light.

3. *In Vitro* Cleavage of 8oxoG by FPG Protein

A base cleavage assay,[138] using a ^{32}P-labeled oligonucleotide (oligo), was used to determine if the FPG protein made in the clones was active (able to recognize and bind 8oxoG) and to quantitate levels of its activity. An oligo was designed containing a single 8oxoG, one of the lesions excised *in vitro* by active FPG. The oligo was end-labeled with ^{32}P and incubated in a reaction mixture with cell extracts and run on a polyacrylamide gel. If active, FPG will cut the oligo at the 8oxoG, releasing a piece of DNA containing the ^{32}P label. The released piece of DNA will represent a smaller molecular weight than the un-cut oligo and will produce a second lower band on the gel. Quantitation of the bands is possible using the Molecular Dynamics STORM computer program. The polyacrylamide gel is exposed to the specially designed Molecular Dynamics screen, which reads radioactivity in a gel. The screen is then placed on a STORM scanner and a computer image is generated. The software calculates band intensities, reported as the percentage of ^{32}P in the control band.

The oligo was kindly provided by Dr. Rita Ghosh, AMC Cancer Research Center, Denver, Colorado, and contained the construct:

- 5' ATA CGT ACG GG*G CGG GGC GTG C 3'
- 3' TAT GCA TGC CC C GCC CCG CAC G 5'

End-labeling of oligonucleotide:

Bacteriophage T4 Polynucleotide Kinase was used to attach the radioactive label to the 5' end of the oligonucleotide. Twenty microcuries were used to label 1 µg of SP-1 8-oxodG with PNKinase. The reaction was allowed to proceed for one hour at 37°C. The reaction was terminated by adding 1 µL of 0.5 M EDTA. The reaction mixture was passed through a NICKTM column (Amersham) to purify the labeled oligo. Pure oligo was collected in 200 µL of TE Buffer. Five µL of the oligo were saved for gel analysis. Approximately 1 µg of the complementary SPI oligo was added to the 195 µL of the labeled oligo. The reaction was done at 90°C for 90 minutes and annealing efficiency checked on a 20% native acrylamide gel using 20,000 cpm per lane of the single stranded and double stranded oligo. The presence of two bands, representing both single- and double-stranded DNA was used to confirm annealing.

Excision Assay

- The concentration of total protein in each sample was determined using the BCA Protocol (see above) and a plate reader. Aliquots of 5, 10, 20, 40, 60 & 80 µg of protein were made for each sample and the volume brought up to a total of 31 µL with sterile water.
- Cells extracts were incubated at 37°C for 45 minutes in a reaction mixture containing: 5X OGG1 Cleavage Buffer, ^{32}P-labeled double-stranded oligonucleotide (20,000 cpms) and cellular extracts (31 µL). The reaction then took place by incubating in a 37° water bath for 45 minutes.

- The reaction was terminated by adding 10X formamide to each reaction to a final volume of 1X. Add 5 µL 50% glycerol to each sample to aid in loading.
- Samples were subsequently run on a 12% denaturing polyacrylamide gel that contained:
    - 30 mls 20X gel mix
    - 20 mls water
    - 80 µL 30% Ammonium Persulfate (APS) (Sigma)
    - 30 µL TEMED –(Gibco BRL, Grand Island, NY)
- The gel was pre-run by placing in a medi gel box, adding 1000 mls 1X TBE and running at 100 volts for 30 minutes.
- Samples were loaded onto a gel and run at 75 volts for approximately 5 hours or until formamide had run ~ 15 cm down the gel.
- The gel was removed from the glass plates, covered with plastic wrap to avoid dehydration and exposed to X-ray film overnight at -80°C.
- Film was exposed overnight to a PhosphorImager (Molecular Dynamics, 928 East Arques Avenue, Sunnyvale, CA) plate and scan into computer using the STORM (Molecular Dynamics) computer scanner.

4. Western Blot Analysis

The FPG polyclonal antibody was provided by Trevigen (Trevigen, Inc., 8405 Helgerman Court, Gaithersburg, MD). Clones were grown to confluence on 60 mm plates and placed in a lysis buffer containing Tris-HCl (ph 8), 2 M NaCl, 50 mM EDTA,

20 % SDS, 0.1 µL/samples proteinase K and deionized water. An aliquot was taken for total protein analysis and the remaining saved for Western Blotting and base excision repair assays (see below).

Total Protein Analysis Assay:

This protocol was used to determine protein concentrations in cell extracts using a 96-well plate reader and the Pierce BCA Protein Assay Kit (Pierce PO Box 117, Rockford, IL). A standard curve was made using 2 mg/ stock BSA provided by the kit and aliquoted into the 96-well plate in triplicate. Triplicates of each unknown sample were made by aliquoting 10 µL of each sample into three separate wells. Two hundred µL of BCA reagent was added to each well and the samples placed in the plate reader. Concentrations were given as µg/ml.

Western Blot Analysis:

Western blot analysis was based on the methods of Okayasu, et al.[139] Cells from clones and controls (1-2 x 10^6) were lysed in lysis buffer containing 50 mM Tris, 150 mM NaCl, 2 mM EDTA, 2 mM EGTA, 25 mM NaF and 25 mM ß-glycerolphosphate, pH 7.5, 0.2% Triton-X 100, 0.3% NP-40, 0.1 mM sodium vanadate, 0.1 mM PMSF, leupeptin (5 µg/ml) and aprotinin (5µg/ml) (fresh) (Song, et al 1996). Ten µg protein was applied per sample for 10% SDS-polyacrylamide gel electrophoresis (SDS PAGE. The amount of protein from each extract was quantified using the BCA protocol described above. Each sample was loaded onto a gel by a microsyringe. The separated gels were transferred to nitrocellulose membranes for 24 hours at 4°C. The membrane

was washed with 1 x TBST (25 mM Tris, pH 8.0, 125 mM NaCl, 0.025% Tween 20) and incubated in blocking buffer containing 25 mM Tris pH 8.0, 125 mM NaCl, 0.025 % Tween 20, and 5% dry milk for 1 h at room temperature. The primary antibodies were applied for 1h at room temperature. The membranes were washed and incubated with horseradish peroxidase-labeled secondary antibodies in blocking solution for 1 h. Subsequently, the membranes was washed and incubated in ECL Western blotting detection reagent (Amersham RPN 2106) for 1 minute. The blot was exposed onto x-ray film for 5-45 minutes.

D. Cell Survival

Survival Assay

Survival curves – survival curves were determined using exponentially growing cells in 60 mm plates. Standard procedures were as described previously.[78] Clonogenic survival was determined by fixing colonies with a mixture of 95% ethanol, acetic acid and H_2O and stained with 1% crystal violet. Colonies were counted by eye. A colony was defined as having fifty or more cells.

Chemicals

H_2O_2

30% Hydrogen peroxide (H_2O_2) was purchased from Sigma Chemical Company (Sigma-Aldrich, PO Box 355, Milwaukee, WI) and used in varying concentrations to determine survival curves (see results).

Paraquat

Paraquat (PQ, methyl viologen) was purchased from Sigma Chemical Company and used in varying concentrations to determine survival curves. 4 mM stock was made by diluting 18.3 g PQ in 25 mls F12 growth medium and stored away from light. Fresh PQ stock was used for each experiment.

N-acetylcysteine (NAC)

NAC was purchased from Sigma Chemical Company and diluted into a 200 mM stock solution with diH_2O. 40 µL of stock was added to each plate containing 4 mls of F12 media for a final concentration of 20 mM.

Bis-sulfoxyamine (BSO)

BSO was purchased from Sigma Chemical Company and diluted into a 4 mM stock solution with diH_2O. 10 µL of stock was added to each plate containing 4 mls of F12 media for a final concentration of 10 mM.

Dimethylsulfoxide (DMSO)

DMSO was purchased from Sigma Chemical Company and was added to each plate containing 4 mls for a final v/v concentration of 1%.

E. Induced Mutation

Mutation Assay:

The mutation assay has been described.[78,135,140-144] 5 x 10^5 cells were plated for PQ or H_2O_2 exposure in 100 mm plates and allowed to adhere for 3 hours. Plates were incubated with 2 x 10^5 cells. The cells were then treated with PQ or H_2O_2 for the prescribed time and then rinsed three times with Hank's Balanced Salt Solution (HBSS) (Mediatech, Inc., 13884 Park Center Road, Herndon, VA). Every two days, the cells were subcultured to allow for expression over the following ten days.

To determine mutant fraction, 2 x 10^5 cells per dose were plated 100 mm plates containing 7 of Ultraculture growth medium (Biowhittaker, Walkersville, MD). Additional cells were plated to determine plating efficiency and to subculture for a second challenge following the same procedure in two days. After a three-hour period, to allow the cells to attach to the plates and to recover from trypsinization, 2% complement and 0.3% antiserum (v/v) were added to each plate. Complement by itself was added to the plating efficiency plates to measure killing by complement. Mutant fractions (M_f) were calculated by determining the average and standard numbers of mutants in two separate experiments and expressed as mutant/10^5 cells.

$$M_f = \frac{\text{number of mutants}}{\text{number of cells plated}} \times \frac{1}{\text{P.E. (complement alone)}}$$

F. Glutathione Studies

Procedures used for the detection of glutathione in A_L cells were based upon those of Vandeputte, et al.[145]

Experimental Design for GSH/GSSG Measurement in A_L Cells After Exposure to PQ

1. A_LH cells were used as controls and AHF-10 clone cells were used as test samples.
2. Cells were trypsinized and replated @ 1 x 10^5 cells in 8 mls F12 media (20% fetal calf serum) as outlined below.

Plate#*	PQ (μM)	BSO	NAC
1	0	-	-
2	0	+	-
3	0	-	+
4	50	-	-
5	50	+	-
6	50	-	+
7	100	-	-
8	100	+	-
9	100	-	+
10	125	-	-
11	125	+	-
12	125	-	+

*each plate should be done in triplicate.

3. Cells were allowed to adhere for 3 hours.
4. PQ and BSO or NAC was added and cells returned to the incubator.
5. After 4 days, the media was removed and each plate was rinsed 1 time with HBSS + 1% Hepes.
6. GSH/GSSG was measured as described below.

GSH/GSSG Assay

Solutions

4 mM PQ stock

50 µL = 50 µM

100 µL = 100 µM

125 µL = 125 µM

4 mM BSO stock

Add 20 µL to each plate

200 mM NAC stock

Add 40 uL to each plate

- Cells were plated and dosed as outlined above.
- Cells were trypsinized and dissolved in 10 mM HCl
- Cells were lysed by a freeze-thaw cycle in ethanol/water bath then spun @ 2000 rpm for 5 minutes.
- 50 uL of supernatant was aliquoted from each sample for total protein analysis and the remaining supernatant transferred to a new microfuge tube.
- 50 uL 6.5% (w/v) 5-sulfosolicylic acid (SSA) was added to each tube, the tubes were placed on ice for 10 minutes to precipitate proteins and the tubes were then centrifuged @2000 rpm for 15 minutes.
- Supernatants were collected and placed in a new tube and samples stored at -70°C.

Assay Reagents:

Stock Buffer

143 mM NaH_2PO_4

6.3 mM EDTA

pH = 7.4

DTNB Ellman reagent 5,5'-dithiobis- (2-nitrobenzoic acid)

10 mM DTNB in stock buffer (4 mg/ml)

NADPH (nicotinamide adenine dinucleotide phosphate)

2 mM in stock buffer (1.7. mg/ml)

GSSH reductase (GR)

8.5 Units/ml in stock buffer

50 mM GSH stock (in 10 mM HCL and 1.3% SSA)

154 mg GSH

8 ml 10 mM HCl

2 ml 6.5% SSA

Assay Buffer

5 ml DTNB

8.5 ml NADPH

36.5 ml stock buffer

Assay Protocol:

- 20 µL samples, standards and blanks were added to 96-well plate in triplicate.
- Standards of GSH were made at 0, 0.2, 0.5, 1.0, 2.0, 5.0, 10.0, and 20.0 µM.
- 20 µL stock buffer was added to each well to neutralize the pH.
- 200 µL assay buffer added to each well for 5 minutes.
- The reaction was started by adding 40 µL GSSH reductase to each well.
- The plate was incubated at room temperature for 2 minutes then read @ 405 nM by a plate reader.
- Determinations were given as µg GSH or GSSG and ratioed against total protein readings to give a µg GSH or GSSG/nmol total cellular protein.

Chapter III

Results

A. Cell Transformation

The transformation of A_LH cells to fpg transformants was undertaken to produce a cell line with increased BER capability in which to study PQ toxicity and mutability. As shown in Section II of this chapter (Cell Survival Results), the initial experiments in this study demonstrated that some of the fpg transformants had increased survival and virtually no mutation induced by PQ when compared to wild type, A_LH cells. Due to the problems associated with the Western blots (see Section D of this chapter) the experiments described below (PCR, RT-PCR and 8oxoG cleavage) were actually performed after the survival and mutation studies. For the sake of simplicity in presentation and discussion, results describing the success of the fpg transformation are presented first.

In addition, one will notice that some survival and mutation analyses were conducted on AHF10 while others were conducted using AHF3. The explanation for this seemingly erratic shift between cell lines is simply – until the base cleavage studies were conducted that showed AHF3 to more efficiently excise 8oxoG, AHF10 cells were used

based on the results available, which were the survival curves (Figure 18). Fpg transformants had been randomly selected from fifteen different clones for experiments and AHF3 was not included in that initial survival study. As a consequence, it was not included in the 16-hour mutation studies that followed but AHF10 cells were. Once the cleavage studies were conducted AHF3 stood out from the other transformants and was flagged for further studies.

1. PCR of DNA from fpg transformants

Prior to RT-PCR of RNAs, PCR conditions were tested using DNA extracted from fpg transformants, using the psv2neofpg vector as a cDNA positive control. These results are presented in Figure 6, which is a computer image of a PCR gel. Lane 1 contains the molecular weight (mw) markers, Lane 2 is the reaction mixture with no DNA added and Lane 3 is the reaction mixture plus the cDNA control. As expected, no band is seen in Lane 2. A band is seen in Lane 3 at mw = 125 for the cDNA control. This is the predicted weight of the PCR product as predicted by primer design. The bands below mw = 100 are unused primers.

Figure 7 is a computer image of a PCR gel of DNA extracted from a series of A_LH clones transformed with the fpg gene. Lane 2 is the cDNA control. Lanes 3-8 contain DNA from fpg transformants. A band of DNA is seen in all the samples at molecular weight 125 as expected. These results confirmed that the fpg transformants contained the fpg gene and that the PCR conditions chosen worked for RT-PCR.

A second set of fpg primers was also used (see Materials and Methods) designed to give a PCR product of 250 base pairs (bp). This alternative primer set was used to

confirm the presence of the fpg gene in the transformed A_LH cells. Figure 8 shows the results of PCR using fpg primer set 2 and is similar to those using fpg primer set 1 for the fpg transformants. In addition, results show that A_LH cells which contain no bacterial fpg gene, have very little binding affinity for the fpg primers as expected.

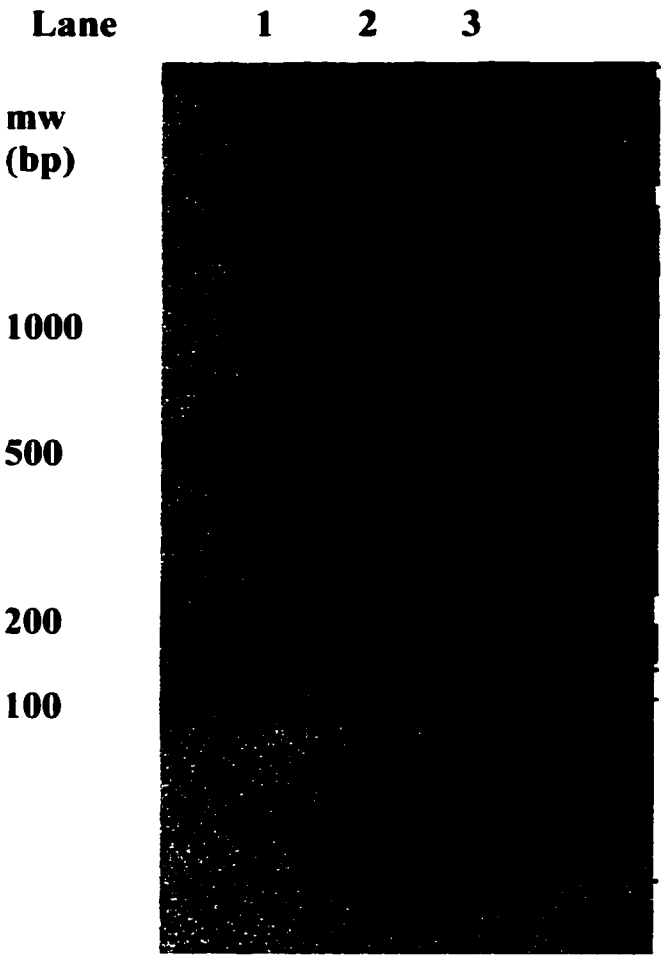

Figure 6. PCR of the psv2neofpg plasmid used to transform A_LH cells to fpg transformants. Lane 1 contains molecular weight markers, Lane 2 contains primer mix with no DNA added and Lane 3 contains the psv2neo fpg plasmid + primer mix.

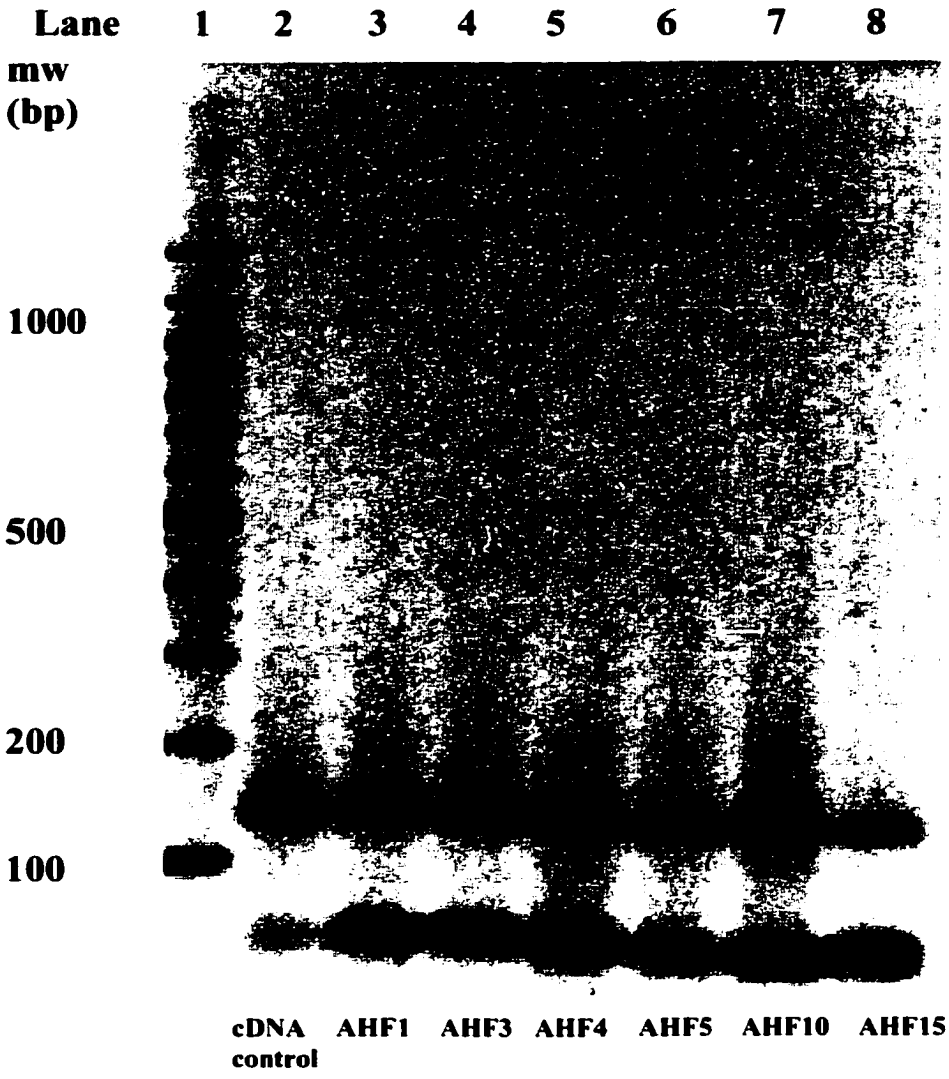

Figure 7. PCR of the psv2neofpg plasmid and DNA from fpg transformants. Lane 1 contains molecular weight markers, Lane 2 contains the cDNA fpg control (arrow), Lanes 3-8 contain DNA extracted from fpg transformants. The bands seen below mw = 100 are unused primers.

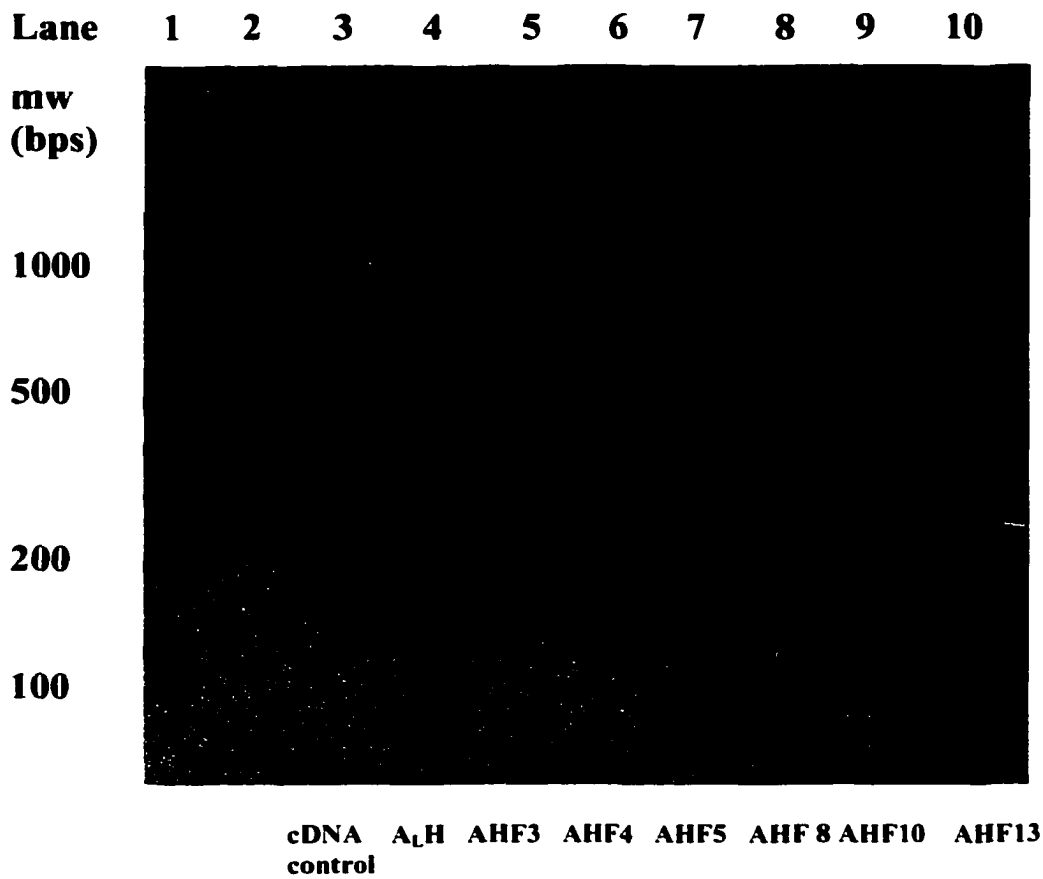

Figure 8. PCR of DNA extracted from fpg transformants and A_LH cells using fpg primer set 2. Lane 1 contains molecular weight markers, Lane 2 is a blank, Lane 3 is the cDNA control, Lane 4 is the DNA from wild type (A_LH) cells, which does not contain the fpg gene, Lanes 5-10 contain the fpg transformants and show varying degree of affinity for fpg primers. The bands are at mw = 250, the predicted size of the DNA from the primers used.

2. RT-PCR of RNA

Reverse transcriptase (RT)-PCR was conducted to confirm the presence of the fpg vector in the fpg transformants. Prior to RT-PCR the quality of the RNA extracted from the cells was checked by Northern analysis as described in Materials and Methods by Dr. Leia Smith of Colorado State University. Figure 9 is a picture of a Northern gel of RNA extracted from the fpg transformants and A_LH cells. The 28S and 18S designations refer to ribosomal markers used when checking RNA integrity. Two μg of RNA were run for each cell line. The gel shows that the RNA used for RT-PCR was of good quality and not degraded. Better RT-PCR controls should have been used (attempts to use this control were not successful for reasons still unresolved). The addition of primers for β-actin, a protein made by almost all cells, is commonly used as an internal "housekeeping" control. The presence of this control allows bands to be normalized and makes possible quantitation of band intensities. Without this control, it is impossible to conclude with certainty that the intensity of the band(s) seen in an ethidium bromide stained gel are reflective of expression levels. However, it seems clear that some of the fpg transformants expressed bacterial fpg and that A_LH does not.

In this study, the RT-PCR products were not used for quantitation but for supportive data with the 8oxoG cleavage assay. The RNA used for all RT-PCR experiments in this study was taken from the aliquots analyzed in the Northern blot shown in Figure 9.

Figure 10 shows computer images of results from two RT-PCR procedures. Figure 10 (a) shows a band at mw = 125 as expected. The cDNA control is in Lane 3 and served as a PCR control for the RT-PCR reaction. The mRNA in the RT-PCR kit

provided the RT control. It is in Lane 4 and produced a band at mw = 900 as expected. The fpg transformants showed varying degrees of affinity for the fpg primers as indicated by the intensity of the bands at mw = 125.

Figure 10 (b) shows the results of the RT-PCR for fpg transformants and A_LH. The cDNA obtained from A_LH RNA (Lane 10) showed less primer binding than the fpg transformants, confirmation that the transformant cells contained the fpg gene and the wild type (A_LH) cells do not.

Figure 9. Northern gel analysis of RNA from fpg transformant and A_LH cells. 28S and 18S indicate the ribosomal markers used for checking the integrity of RNA. When both bands are present the RNA is considered of good quality and not degraded. The samples were loaded as follows: Lane 1, A_LH; Lane 2, AHF1; Lane 3, AHF3, Lane 4, AHF4; Lane 5, AHF5; Lane 6, AHF8; Lane7, AHF10; Lane 8, AHF12; Lane 9' AHF14; and Lane 10, AHF15.

Figure 10. RT-PCR of RNA from fpg transformants and wild type ($A_L H$) cells. (a) results using the fpg transformant RNA for RT-PCR. Lane 1 contains molecular weight markers. Lane 2 is a blank well. Lane 3 contains the PCR control. Lane 4 contains the RT control and Lanes 5-8 contain the fpg transformants. (b) Results of RT-PCR using both fpg transformant and $A_L H$ RNA for RT-PCR. Lane 1 contains molecular weight markers. Lanes 2 and 3 are blank wells. Lane 4 contains the cDNA control. Lanes 5-9 contain the fpg transformants and Lane 10 contains the wild type. $A_L H$.

a

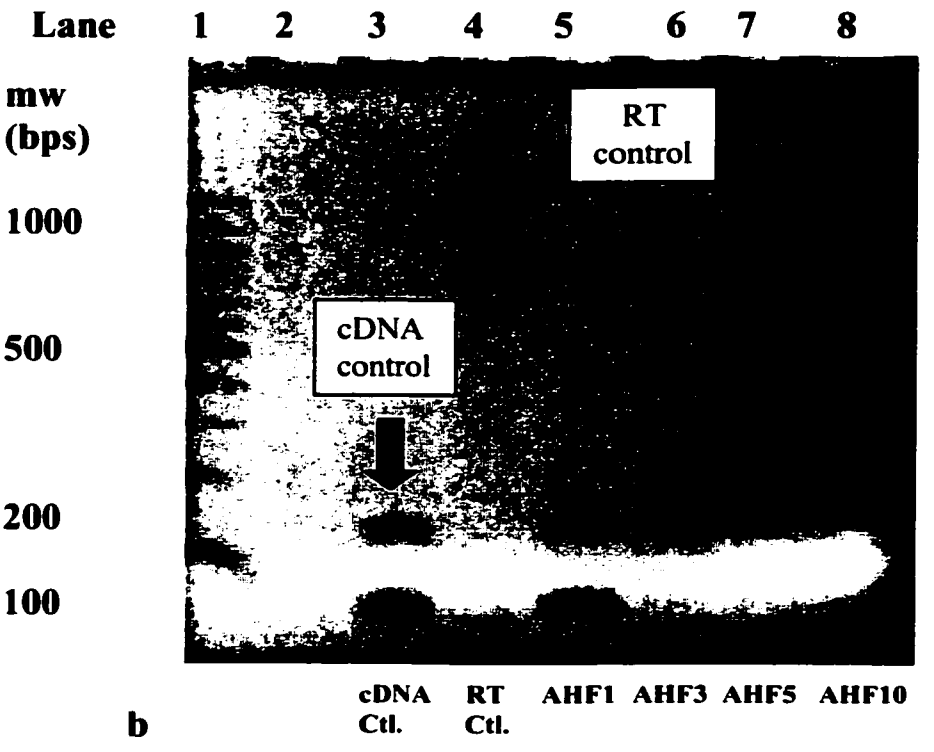

b

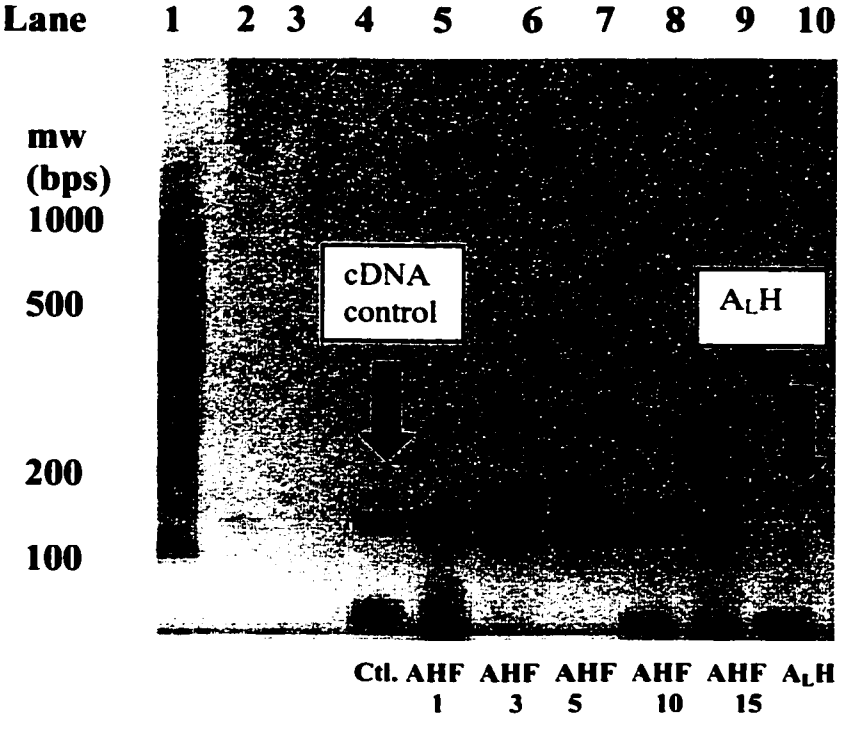

3. *In Vitro* Cleavage of 8oxoG by FPG Protein

The fraction of ^{32}P-8oxoG oligonucleotide cleaved by FPG protein from DNA of fpg transformants and A_LH cellular extracts is compared in Figures 11 and 12. This assay was used to determine if the FPG protein shown to be present in the fpg transformants by RT-PCR analysis was enzymatically active and if so, to estimate at what level of activity. Transformants were selected for this assay based on RT-PCR data. Concentrations of 5, 10, 20, 40, 60 and 80 μg of total cellular protein from A_LH and the selected transformants were incubated in a reaction mixture (See Materials and Methods) containing the ^{32}P-8oxoG oligo.

During the one-hour incubation, repair proteins in the cellular extracts specific for 8oxoG (i.e., FPG) recognize and bind to the damaged portion of the oligo. The protein then cleaves the oligo at the damaged base, releasing two smaller pieces of DNA; one being end-labeled with ^{32}P, which is visible on X-ray film. Quantitation of the bands is possible using the Molecular Dynamics STORM computer program. The polyacrylamide gel is exposed to the specially designed Molecular Dynamics screen that reads radioactivity in a gel. The screen is then placed on a STORM scanner and a computer image is generated. The software then allows you to measure band intensities. The band intensities were reported as percentages of the ^{32}P control band.

Figure 11 is a computer image of a polyacrylamide gel after incubation of cellular extracts of 20, 40 and 60 μg with a ^{32}P-labeled 8oxoG oligo. The upper band in each lane indicates uncleaved oligo and the lower band indicates cleaved oligo. Once cleaved the released portion of oligonucleotide migrates further down the gel than the larger, uncleaved piece of oligo DNA, making two bands visible. As concentration was

increased (from left to right in the gel), meaning the amount of FPG protein in the reaction mixture also increased. fpg transformants showed dose-dependent cleavage of the 8oxoG oligo. A_LH cells showed a lower overall amount of cleavage even at higher concentrations.

Figure 12 is a plot showing the fraction of 8oxoG oligonucleotide cleaved at increasing concentrations of cellular protein. As concentration of total protein increased, fpg transformants and A_LH cells showed increasing amount of 8oxoG oligonucleotide cleavage. Extracts of transformant, AHF3, were more active than the others.

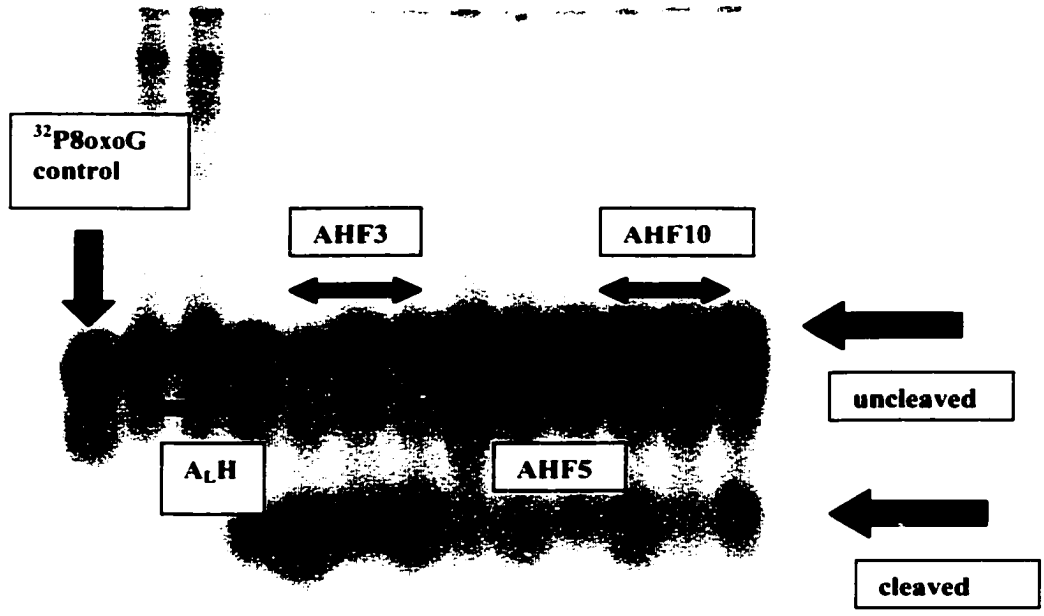

Figure 11. Computer image of a polyacrylamide gel showing the cleavage efficiency of 8oxoG by A_LH and fpg transformants. The ^{32}P-8oxoG control is the oligonucleotide incubated with sterile water. Three samples were run from each cell line in increasing amounts of total cellular protein (20, 40 and 60 μg from left to right). The upper band is the uncleaved oligo and the lower band indicates the portion of the oligo that has been cleaved and released by FPG protein.

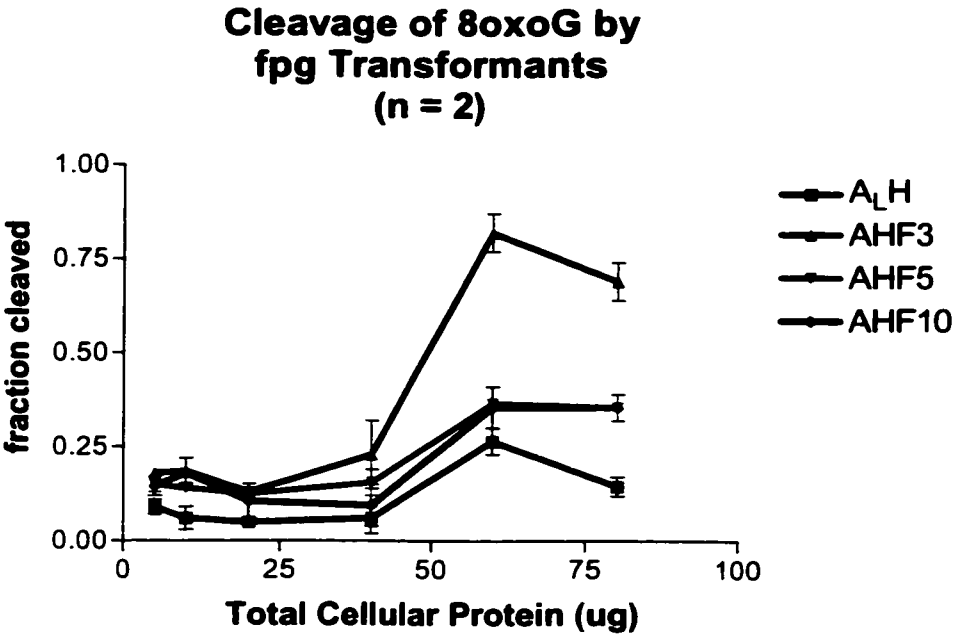

Figure 12. Dose response plot of FPG activity in A_LH and fpg transformants. The fraction of ^{32}P-8oxoG oligonucleotide cleaved and released by fpg-transformant and A_LH reaches a maximum at approximately 60 µg of cellular extract.

Fraction Levels of 8oxoG Cleavage by fpg Transformants and A_LH Cells

µg protein	A_LH assay 1	A_LH assay 2	AHF3 assay 1	AHF3 assay 2	AHF5 assay 1	AHF5 assay 2	AHF10 assay 1	AHF10 assay 2
5	0.07	0.11	0.17	0.19	0.13	0.17	0.12	0.17
10	0.09	0.03	0.15	0.22	0.13	0.15	0.14	0.22
20	0.04	0.06	0.11	0.15	0.14	0.11	0.06	0.15
40	0.02	0.1	0.14	0.32	0.12	0.19	0.04	0.15
60	0.23	0.3	0.77	0.87	0.36	0.37	0.3	0.41
80	0.17	0.12	0.74	0.64	0.39	0.32	0.32	0.39

µg	A_LH Mean	A_LH SD	AHF3 Mean	AHF3 SD	AHF5 Mean	AHF5 SD	AHF10 Mean	AHF10 SD
5.00	0.09	0.03	0.18	0.01	0.15	0.03	0.15	0.04
10.00	0.06	0.04	0.19	0.05	0.14	0.01	0.18	0.06
20.00	0.05	0.01	0.13	0.03	0.13	0.02	0.11	0.06
40.00	0.06	0.06	0.23	0.13	0.16	0.05	0.10	0.08
60.00	0.27	0.05	0.82	0.07	0.37	0.01	0.36	0.08
80.00	0.15	0.04	0.69	0.07	0.36	0.05	0.36	0.05

4. Western Blotting

Western blotting of fpg transformant and A_LH proteins was done from FPG protein polyclonal antibody as described in Materials and Methods and Figure 13 shows the results. Lane 1 contains the protein from A_LH cells. Since the ALH cells do not express the bacterial fpg gene and therefore do not make FPG protein, A_LH cells should not have bound the FPG antibody. There was however, binding in all lanes, including the A_LH lane. The most reasonable explanation for this result is that the FPG antibody used showed a high degree of non-specific binding for proteins other than FPG and that it was unable to distinguish between the bacterial FPG protein and the CHO homolog.

Modifications of the protocol were made by varying the concentration of antibody used and shortening/lengthening the time of exposure in an attempt to increase specificity but, binding to control A_LH cells continued to be seen. In an attempt to remove CHO proteins in the extract that were contributing to the non-specificity, the FPG antibody was incubated with CHO cell extract. Again, non-specific binding occurred. Since better FPG antibodies were not available the FPG antibody work was abandoned in favor of the base excision assay, which would be able to provide me with protein activity data.

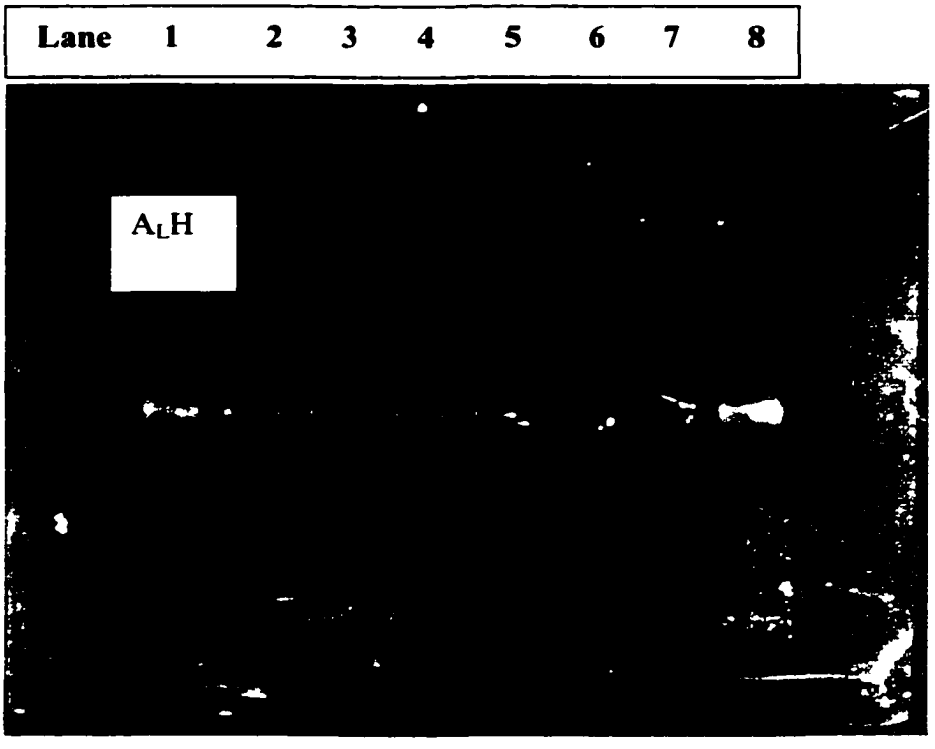

Figure 13. Computer image of a western blot from fpg transformants and A_LH cellular extracts using FPG polyclonal antibody. Binding was non-specific and did not discriminate A_L cells from fpg transformants. Lane 1 contains A_LH cellular extracts; Lane 2 AHF1; Lane 3, AHF3; Lane 4, AHF4; Lane 5, AHF5; Lane 6, AHF8; Lane 7, AHF10; and Lane 8, AHF12.

B. Cell Survival

A_LH survival after PQ exposure

Survival curves were constructed to quantitate levels of PQ cytotoxicity in A_LH cells. Cells were exposed to concentrations of 400, 600 and 800 μM PQ for 16 hours, 1, 2, 3, 4, and 7 days. Figure 14 shows survival curves of A_LH cells. Killing is increased at longer exposures time. This is possibly due to redox cycling of PQ, resulting in the generation of a continual concentration of ROS within the cells or to the depletion of intracellular antioxidants. After 4 days of PQ exposure no cells survived even at the lowest concentration of PQ.

A_LH survival after PQ exposure +/- BSO, NAC or DMSO

Since PQ is known to be redox cycled in cells to produce ROS, experiments were conducted using the antioxidant chemicals BSO, NAC and DMSO to see if each affected PQ cytotoxicity, as measured by survival percentage. Figures 15, 16 and 17 shows the results of these experiments. As expected, BSO, a chemical that blocks the glutathione cycle and thus reduces the amount of ROS-scavenging by glutathione, increased killing of PQ significantly. NAC, a chemical that acts as both a ROS scavenger and boosts the glutathione cycle as a precursor to cysteine, increased the survival of A_LH cells. An unexpected result was that DMSO, a ROS-scavenging chemical, however, did not increase or decrease survival at all.

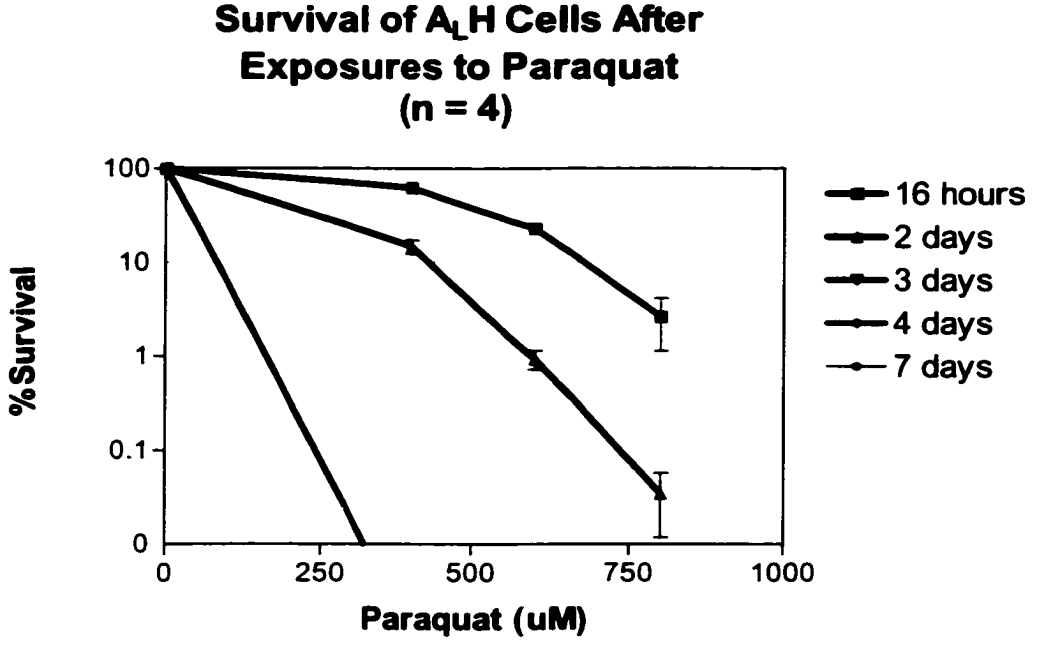

Figure 14. Survival curves for A_LH cells exposed to PQ for different time periods. The shoulder of the curve indicates that at low doses A_LH cells are able to effectively deal with oxidative stress. As PQ dose increases however, killing increases so that at after 4- and 7-day exposures no cells survived.

Data for Survival Curves of A_LH Cells After Exposure to PQ for Various Time Periods.

	16 hours			2 days			3 days		
µM PQ	a	b	c	a	b	c	a	b	c
	100	100	100	100	100	100	100	100	100
400	64	66	70	50	12	22	13	12	1.00E-03
600	30	20	22	19	0.9	1.5	0.8	0.5	1.00E-03
800	0.5	2	1	7	3.00E-03	3.00E-02	5.00E-03	0.1	1.00E-03

PQ (uM)	16 hours		2 days		3 days	
	Mean	SD	Mean	SD	Mean	SD
0.00	100.00	0.00	100.00	0.00	100.00	0.00
400.00	62.50	8.70	14.75	4.86	0.00	0.00
600.00	22.75	4.99	0.93	0.42	0.00	0.00
800.00	2.63	2.98	0.03	0.05	0.00	0.00

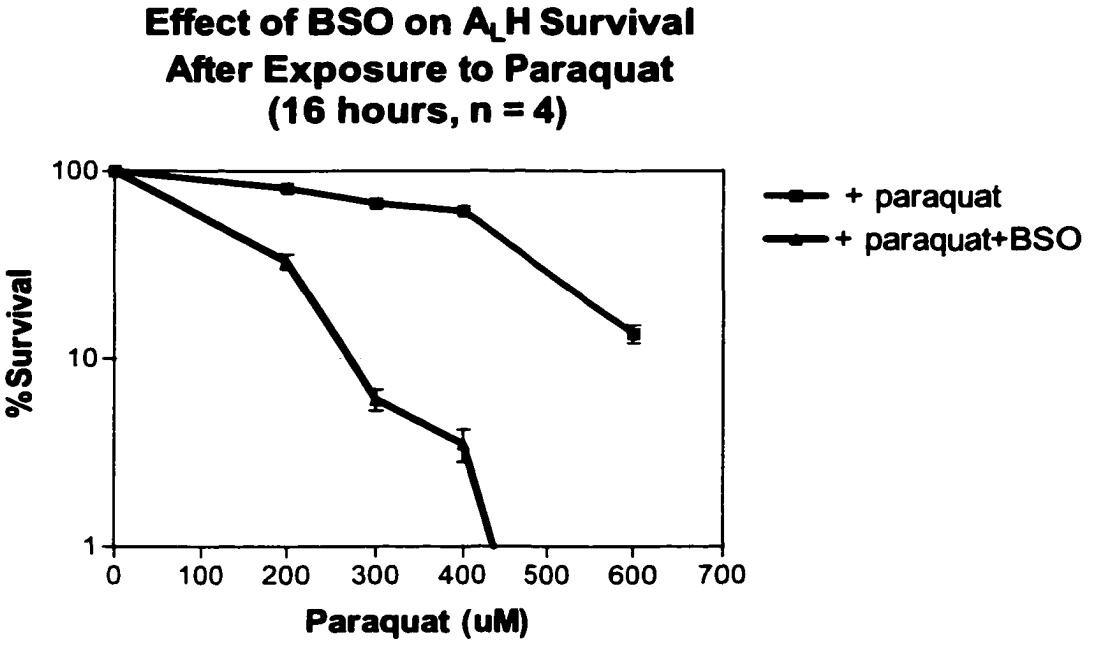

Figure 15. Survival curve of A_LH cells exposed to PQ +/- BSO for 16-hours. The addition of BSO, a competitive inhibitor of the glutathione precursor cysteine, increases cell killing by PQ.

Data for the Effect of BSO on A_LH Survival After Exposure to PQ.

	PQ				PQ + BSO			
µM PQ	a	b	c	D	a	b	c	d
0	100	100	100	100	100	100	100	100
200	80	83	87	75	34.5	39.8	25.6	32.4
300	68.6	75	62	63	5.1	5.9	8.3	4.9
400	59	62	58	66	2.2	2.5	5	4.3
600	10.3	17	15	12	0.01	0.00	0.00	0.00

PQ (uM)	+ PQ		PQ + BSO	
	Mean	SD	Mean	SD
0.00	100.00	0.00	100.00	0.00
200.00	81.25	5.06	33.08	5.88
300.00	67.15	5.99	6.05	1.56
400.00	61.25	3.59	3.50	1.36
600.00	13.58	3.00	0.00	0.00

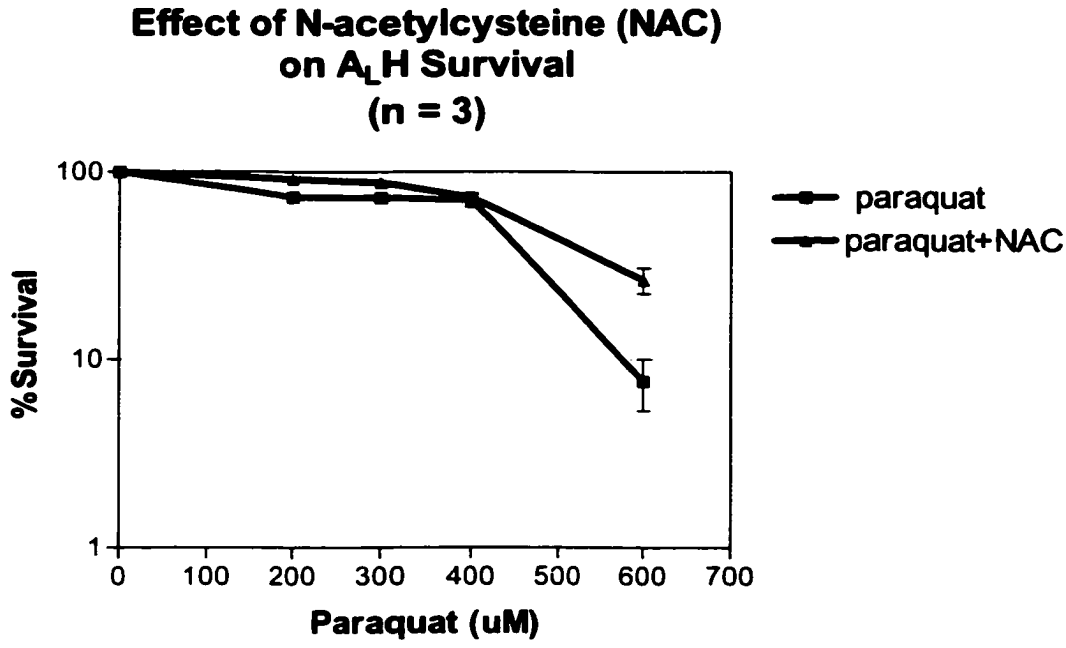

Figure 16. Survival curve of A_LH cells exposed to PQ +/- NAC for 16-hours. NAC, an intracellular antioxidant increases cell survival following the induction of oxidative stress by PQ.

Data for the Effect of NAC on A_LH Survival After Exposure to PQ.

	PQ			PQ + NAC		
µM PQ	a	b	c	A	b	c
0	100	100	100	100	100	100
200	80	69	70.9	88	100	86.9
300	68.6	69	81.3	89.6	82.16	92.16
400	59	75.4	78.1	73.3	72.6	72.6
600	10.3	9.7	3	19.3	26.80	33.70

PQ (uM)	PQ		PQ + NAC	
	Mean	SD	Mean	SD
0.00	100.00	0.00	100.00	0.00
200.00	73.30	5.88	91.63	7.27
300.00	72.97	7.22	87.97	5.19
400.00	70.83	10.34	72.83	0.40
600.00	7.67	4.05	26.60	7.20

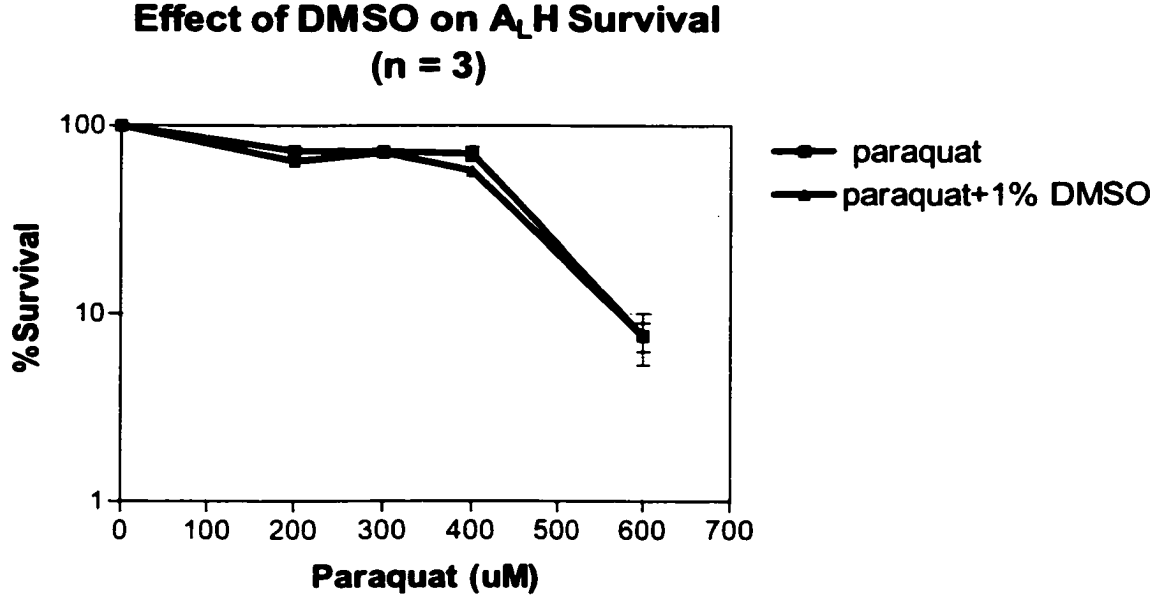

Figure 17. Survival curve of A_LH cells exposed to PQ =/- DMSO for 16-hours. DMSO, an intracellular antioxidant, did not alter cell survival.

Data for the Effect of DMSO on A_LH Survival After Exposure to PQ.

	PQ			PQ + DMSO		
µM PQ	a	b	c	a	b	c
0	100	100	100	100	100	100
200	80	69	70.9	69.5	61.2	63.3
300	68.6	69	81.3	70.9	66.4	79
400	59	75.4	78.1	50.3	62.3	59.9
600	10.3	9.7	3	10.2	6.70	5.90

PQ (uM)	PQ		PQ+ DMSO	
	Mean	SD	Mean	SD
0.00	100.00	0.00	100.00	0.00
200.00	73.30	5.88	64.67	4.32
300.00	72.97	7.22	72.10	6.39
400.00	70.83	10.34	57.50	6.35
600.00	7.67	4.05	7.60	2.29

fpg transformant survival after PQ exposure

Survival of A_LH cells was compared to survival in cells containing and expressing the bacterial fpg gene. A random sampling of fpg transformants was selected. Figure 18 shows the survival curves. The fpg-transformants had increased survival percentages after 16-hour PQ exposure when compared to the A_LH control. While cell survival studies were merely suggestive and unable to point to the addition of the fpg in the cells as the reason for better survival, they illustrate an inherent difference exists between the cell types which other, more sensitive methodologies might be able to elucidate.

To show that it was not the transformation assay causing a genetic alteration that increased survival percentage, a blank neomycin vector was transfected into A_LH cells and clones picked and designated AHneo-*n*. Figure 19 illustrates that the transfection of a blank vector alone does not increase survival following PQ exposure.

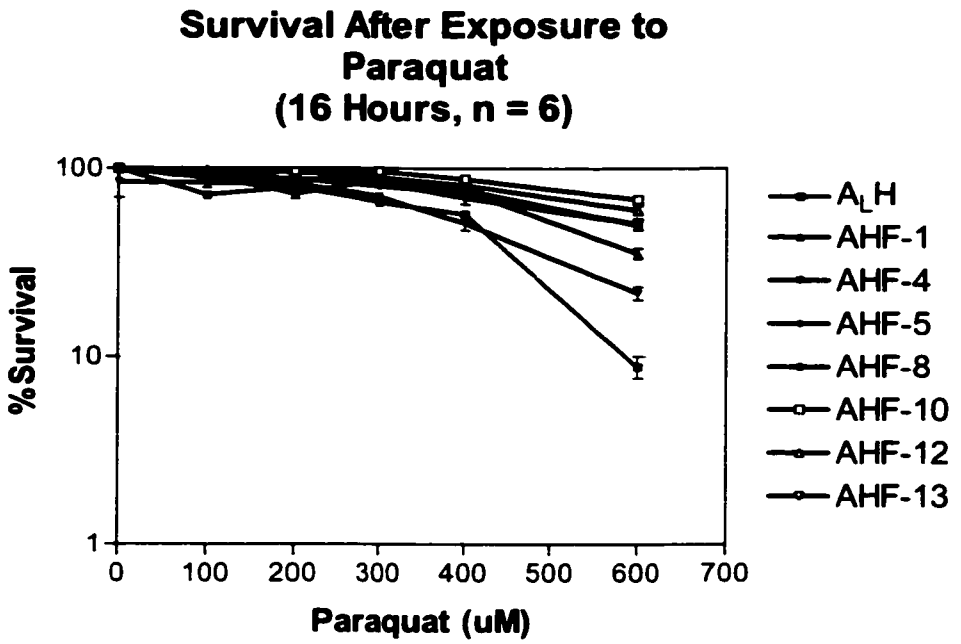

Figure 18. Survival curves for A_LH and fpg transformants exposed to PQ 16-hours. The fpg-transformants showed increased survival after exposure to PQ when compared to A_LH cells.

Data for Survival Curves of A_LH and fpg Transformants Exposed to PQ for 16-hours.

	ALH					
0	100.00	100.00	100.00	100.00	100.00	100.00
100.00	79.30	67.60	71.20	62.10	77.50	78.00
200.00	80.00	81.30	74.10	77.70	80.60	85.00
300.00	68.60	66.80	62.30	58.00	68.80	74.50
400.00	59.00	59.80	62.30	45.60	58.00	58.90
600.00	3.00	9.70	8.50	10.20	10.90	10.70
	AHF1					
µM PQ	a	B	c	d	e	f
0.00	100.00	100.00	100.00	100.00	100.00	100.00
100.00	97.30	93.96	90.48	88.90	72.60	93.60
200.00	93.60	93.50	98.20	80.80	92.80	69.20
300.00	93.30	91.20	71.10	84.20	87.70	93.50
400.00	82.60	75.40	73.50	78.10	75.40	75.40
600.00	38.00	38.70	39.00	32.10	25.90	39.00
	AHF4					
µM PQ	a	B	c	d	e	f
0.00	100.00	100.00	100.00	100.00	100.00	10.00
100.00	95.30	64.20	90.00	95.50	80.00	81.20
200.00	91.00	89.70	81.90	68.10	94.00	73.80
300.00	78.60	77.70	60.70	74.60	67.60	67.60
400.00	57.60	31.30	52.90	57.20	48.30	61.48
600.00	22.60	19.70	17.00	29.00	19.30	23.20
	AHF5					
µM PQ	a	B	c	d	e	f
0.00	100.00	100.00	100.00	100.00	100.00	100.00
100.00						
200.00	98.50	86.60	93.60	82.70	81.60	85.10
300.00	91.80	86.20	78.80	75.70	75.00	79.20
400.00	85.50	71.90	69.20	72.60	72.60	74.24
600.00	58.10	49.10	52.20	53.36	49.10	43.30

(continued...)

	AHF8					
µM PQ	a	b	c	d	e	f
0.00	100.00	100.00	100.00	100.00	100.00	100.00
100.00	100.00	97.40	98.60	90.80	90.10	77.30
200.00	58.70	82.60	85.10	74.24	72.69	68.44
300.00	94.50	92.40	85.84	89.32	93.57	68.44
400.00	83.50	75.40	79.20	76.20	80.40	68.10
600.00	54.60	52.90	40.90	48.70	53.36	
	AHF10					
µM PQ	a	b	c	d	e	f
0.00	100.00	100.00	100.00	100.00	100.00	100.00
100.00	100.00	100.00	100.00	95.80	90.09	77.33
200.00	98.00	100.00	95.80	98.90	90.00	
300.00	95.40	96.60	97.80	99.70	94.70	95.50
400.00	88.90	85.80	86.20	76.56	100.00	90.80
600.00	67.80	68.00	65.30	65.70	71.50	72.70
	AHF12					
µM PQ	a	b	c	d	e	f
0.00	100.00	100.00	100.00	100.00	100.00	100.00
100.00	102.00	100.00	100.00	100.00	92.80	100.00
200.00	97.00	97.80	93.96	98.90	92.40	93.96
300.00	85.10	81.90	93.96	90.48	98.20	90.40
400.00	81.20	88.90	77.70	71.92	90.10	80.00
600.00	60.00	49.10	54.50	70.40	57.60	69.20
	AHF13					
µM PQ	a	b	c	d	e	f
0.00	100.00	100.00	100.00	100.00	100.00	100.00
100.00	98.30	81.90	98.90	95.80	80.40	81.20
200.00	96.10	81.90	82.70	91.20	84.68	85.80
300.00	93.00	80.40	75.70	87.70	86.60	
400.00	82.50	46.00	71.90	76.90	76.56	66.50
600.00	55.50	64.50	44.00	44.46	53.70	42.10

(continued...)

PQ (uM)	ALH		AHF-1		AHF-4		AHF-5	
	Mean	SD	Mean	SD	Mean	SD	Mean	SD
0.00	100.00	0.00	100.00	0.00	85.00	36.74	100.00	0.00
100.00	72.62	6.86	89.47	8.77	84.37	11.92		
200.00	79.78	3.66	88.02	10.90	83.08	10.37	88.02	6.65
300.00	66.50	5.72	86.83	8.49	71.13	7.00	81.12	6.57
400.00	57.27	5.90	76.73	3.23	51.46	10.86	74.34	5.71
600.00	8.83	2.98	35.45	5.38	21.80	4.20	50.86	4.98

PQ (uM)	AHF-8		AHF-10		AHF-12		AHF-13	
	Mean	SD	Mean	SD	Mean	SD	Mean	SD
0.00	100.00	0.00	100.00	0.00	100.00	0.00	100.00	0.00
100.00	92.37	8.45	93.87	8.99	99.13	3.20	89.42	9.11
200.00	73.63	9.62	96.54	3.97	95.67	2.58	87.06	5.51
300.00	87.35	9.79	96.62	1.86	90.01	5.88	84.68	6.73
400.00	77.13	5.31		7.64	81.64	6.89	70.06	12.95
600.00	50.09	5.60	68.50	3.02	60.13	8.34	50.71	8.72

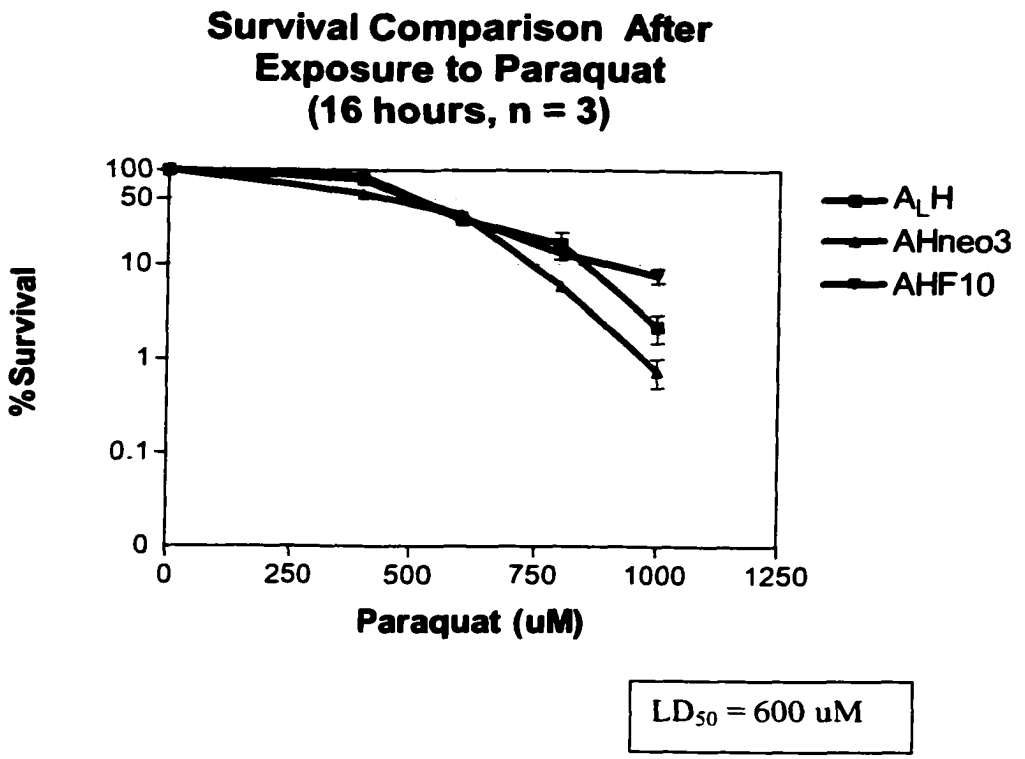

Figure 19. Survival curves for A_LH, AHF3 and AHF10 cells exposed to PQ 16-hours. Survival of AHneo3 cells, which contained a blank neomycin vector, was not significantly different from wild type, A_LH cells.

Data for Survival Curves of A_LH, AHneo3 and AHF10 Cells After Exposure to PQ.

	ALH			AHneo3			AHF10		
µM PQ	a	b	c	a	b	c	a	b	c
0.00	100.00	100.00	100.00	100.00	100.00	100.00	100.00	100.0	100.00
400.00	80.00	83.50	78.50	58.00	51.00	61.90	87.00	91.10	81.80
600.00	23.80	34.60	31.65	43.00	33.00	27.00	27.50	35.20	32.40
800.00	12.60	26.86	10.20	6.00	5.00	6.80	9.50	16.10	13.90
1000.0	2.56	0.80	3.22	0.99	1.00	0.24	9.00	8.90	5.00

PQ (uM)	ALH		AHneo3		AHF-10	
	Mean	SD	Mean	SD	Mean	SD
0.00	100.00	0.00	100.00	0.00	100.00	0.00
400.00	80.67	2.57	56.97	5.52	86.63	4.66
600.00	30.02	5.58	34.33	8.08	31.70	3.90
800.00	16.55	9.01	5.93	0.90	13.17	3.36
1000.00	2.19	1.25	0.74	0.44	7.63	2.28

A_LH and fpg transformant survival after H_2O_2 exposure

Survival in A_LH and fpg-transformants exposed to hydrogen peroxide (H_2O_2) was measured (Figure 20). H_2O_2 is known to produce ROS within the cell via the iron-catalyzed Fenton reaction and was used as a control for the effects of exposure to ROS. The media used for cell culture contained sufficient iron concentrations for the Fenton Reaction to occur (see tissue culture conditions in Chapter II).

In contrast to the finding that survival of fpg-transformants was higher than controls when exposed to PQ, there was no difference in survival when H_2O_2 was used. This result is likely due to the generation of superoxide anion ($^{\cdot}\bullet O_2$) by PQ (see Figure 1) in addition to the production of H_2O_2 when it is redox cycled, meaning in effect, that more free radicals are present in the cellular environment. Redox cycling of PQ may cause more killing by increasing total oxidation within the cell. The concentration of PQ used was higher, LD_{50} = 600 μM compared to H_2O_2, LD_{50} = 300 μM but levels of killing were about the same. The data obtained are really not complete enough to make a true observation of whether or not fpg expression can increase survival after exposure to H_2O_2.

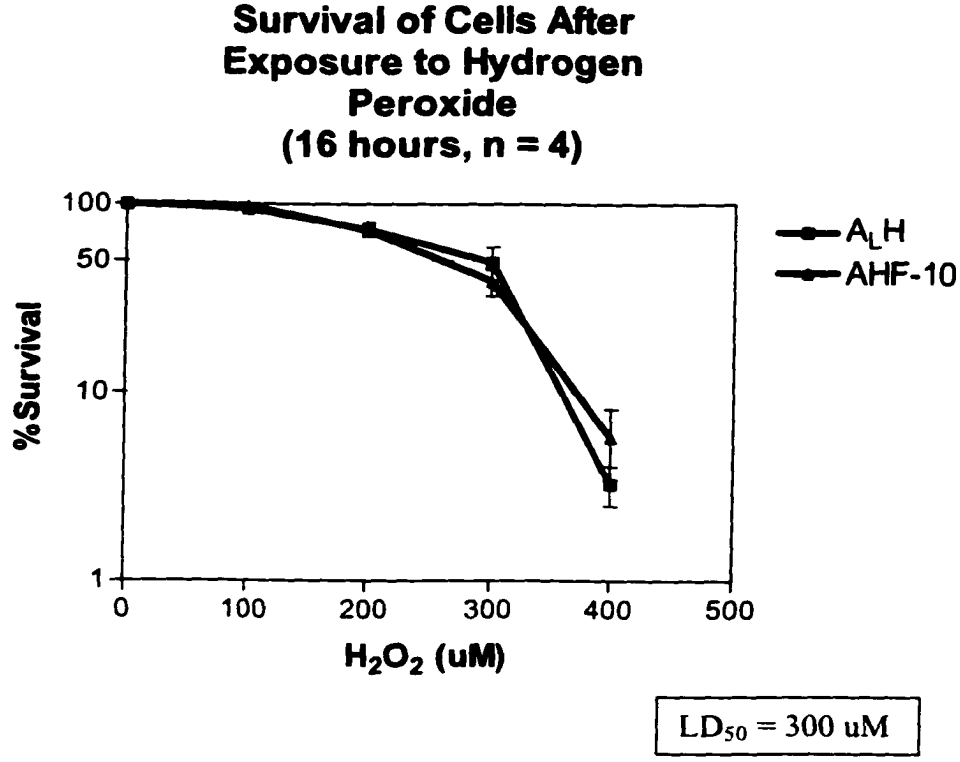

Figure 20. Survival curves for A_LH and AHF10 cells exposed to H_2O_2 16-hours. Survival after H_2O_2 exposure was not different between the two cell types.

Data for Survival Curves of A_LH and AHF10 Cells After Exposure to PQ.

H_2O_2 (μM)	A_LH				AHF-10			
	a	b	c	d	a	b	c	d
0.00	100.00	100.00	100.00	100.00	100.00	100.00	100.00	100.00
100.00	92.00	98.80	96.30	91.80	97.00	98.80	98.30	98.50
200.00	63.00	69.00	91.20	71.20	73.00	63.20	85.00	69.00
300.00	22.00	70.60	53.40	49.90	30.00	28.00	54.30	42.90
400.00	5.00	2.70	1.40	3.90	12.00	1.90	2.20	7.00

H_2O_2 (μM)	A_LH		AHF-10	
	Mean	SD	Mean	SD
0.00	100.00	0.00	100.00	0.00
100.00	94.73	3.42	98.15	0.79
200.00	73.60	12.23	72.55	9.22
300.00	48.98	20.13	38.80	12.26
400.00	3.25	1.55	5.78	4.76

A_LH and fpg transformant survival after 4-day exposure to PQ

Survival was also measured after a 4-day exposure to PQ. Figure 21 shows the survival curves for A_LH and two different fpg-transformants. Survival of one transformant, AHF10, was like that of A_LH, whereas survival of AHF3, was greater (LD_{50} = 110 μM vs. 60 μM respectively). Differences in gene function between these two transformants cannot be determined from survival data alone but, studies of FPG activity (Figure 12) show that AHF3 possessed a higher level of active FPG protein than AHF10, the other transformants and A_LH. It seems reasonable therefore that the increased ability to repair oxidative damage may explain the increased survival of AHF3 cells.

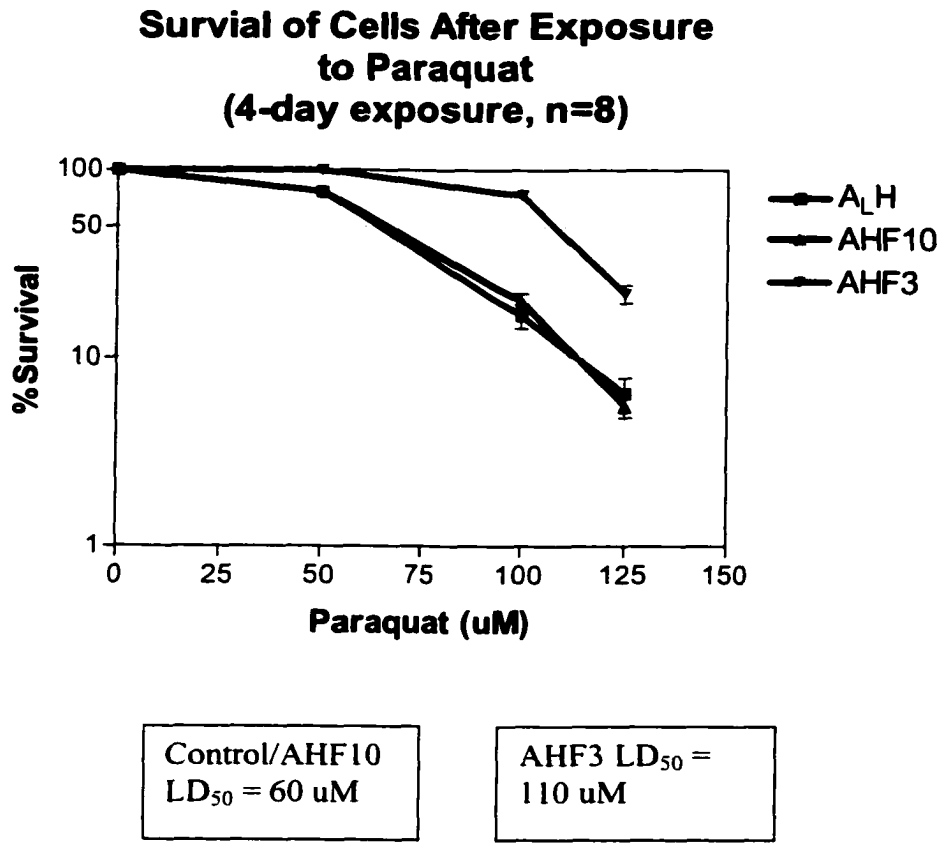

Figure 21. Survival curves for A_LH, AHF3 and AHF10 cells exposed to PQ for 4-days. AHF3 cells showed significantly increased survival than A_LH and AHF10 cells. Most likely this increased survival is due to a greater activity of FPG protein in the AHF3 cells.

Data for Survival Curve for A_LH, AHF10 and AHF3 Cells After 4-day Exposure to PQ.

	ALH							
μM PQ	a	b	c	d	e	f	g	h
0.00	100.00	100.00	100.00	100.00	100.00	100.00	100.00	100.00
50.00	90.00	70.00	69.00	60.00	81.00	71.00	90.00	85.00
100.00	20.00	15.00	8.00	16.00	32.00	12.00	16.00	16.00
125.00	10.00	5.00	3.00	5.00	14.00	3.00	7.00	5.00
	AHF10							
μM PQ	a	b	c	d	e	f	g	h
0.00	100.00	100.00	100.00	100.00	100.00	100.00	100.00	100.00
100.00	93.00	65.00	69.00	66.00	75.00	67.00	89.00	90.00
200.00	32.00	15.00	20.00	20.00	15.00	18.00	21.00	20.00
300.00	7.00	5.00	4.00	4.00	7.00	3.00	5.00	10.00
	AHF3							
μM PQ	a	b	c	d	e	f	g	h
0.00	100.00	100.00	100.00	100.00	100.00	100.00	100.00	100.00
100.00	100.00	100.00	100.00	100.00	100.00	100.00	100.00	100.00
200.00	82.00	72.00	56.00	66.00	75.00	88.00	81.00	70.00
300.00	27.00	17.00	12.00	15.00	22.00	30.00	28.00	24.00

PQ (μM)	A_LH		AHF10		AHF3	
	Mean	SD	Mean	SD	Mean	SD
0.00	100.00	0.00	100.00	0.00	100.00	0.00
50.00	77.00	11.06	76.75	11.96	100.00	0.00
100.00	16.88	7.04	20.13	5.33	73.75	10.12
125.00	6.50	3.78	5.63	2.26	21.88	6.58

C. Induced Mutation Studies

Mutation after 16-hour PQ and H_2O_2 exposures

Induction of CD59$^-$ mutants was measured in A_LH and in the fpg-transformant, AHF10, exposed to PQ at concentrations determined as appropriate by cell survival experiments (Figure 22). Results for mutant induction by H_2O_2 are shown in Figure 23. AHF10 was used in these studies because preliminary survival curves showed it to be more resistant to PQ cytotoxicity after 16 hours than the other fpg transformants (Figure 18). Cells were exposed to PQ for 16 hours then subcultured for a 10-day expression period (see Materials and Methods), after which CD59 antisera + complement was added.

CD59$^-$ mutants were induced by PQ in A_LH cells but not in AHF10 cells. The elimination of induced mutation in this fpg transformant was unexpected. Cell survival studies had shown the fpg transformants to be more resistant to PQ cytotoxicity but cell death did occur. Given that these same lethal concentrations of PQ were used for the mutant induction studies, some level of mutation was expected to occur.

These results indicate that the type of DNA damage induced by PQ is mutagenic. In addition, since cells expressing fpg were able to avoid mutant induction by PQ, the types of DNA damage removed by the FPG protein are mutagenic.

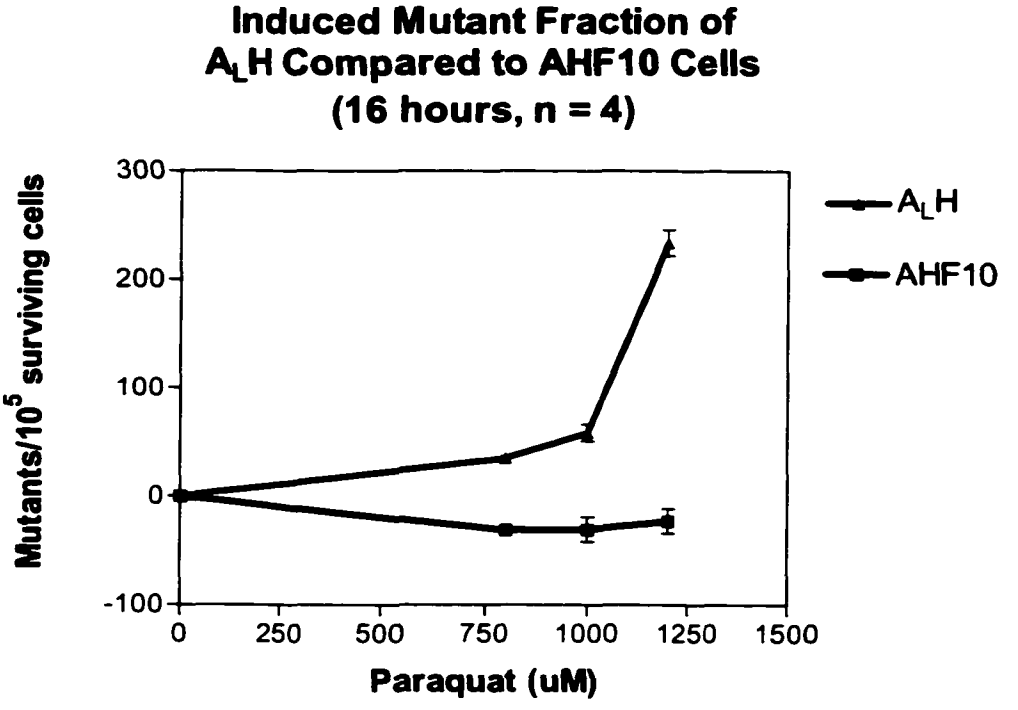

Figure 22. M_f for CD59- mutants induced in A_LH and AHF10 cells after exposure to PQ 16-hours. AHF10 cells, which express bacterial fpg, do not develop mutations even at the highest exposure levels.

Data for M_f for $CD59^-$ Mutants Induced A_LH and AHF10 Cells After Exposure to PQ.

PQ (μM)	AHF10 Challenge 1	AHF10 Challenge 2	A_LH Challenge 1	A_LH Challenge 2
0.00	0.00	0.00	0.00	0.00
800.00	-25.90	-35.90	34.00	36.40
1000.00	-41.90	-19.06	66.00	50.82
1200.00	-34.00	-11.60	222.00	246.00

PQ (μM)	AHF10 Mean	AHF10 SD	A_LH Mean	A_LH SD
0.00	0.00	0.00	0.00	0.00
800.00	-30.90	7.07	35.20	1.70
1000.00	-30.48	16.15	58.41	10.73
1200.00	-22.80	15.84	234.00	16.97

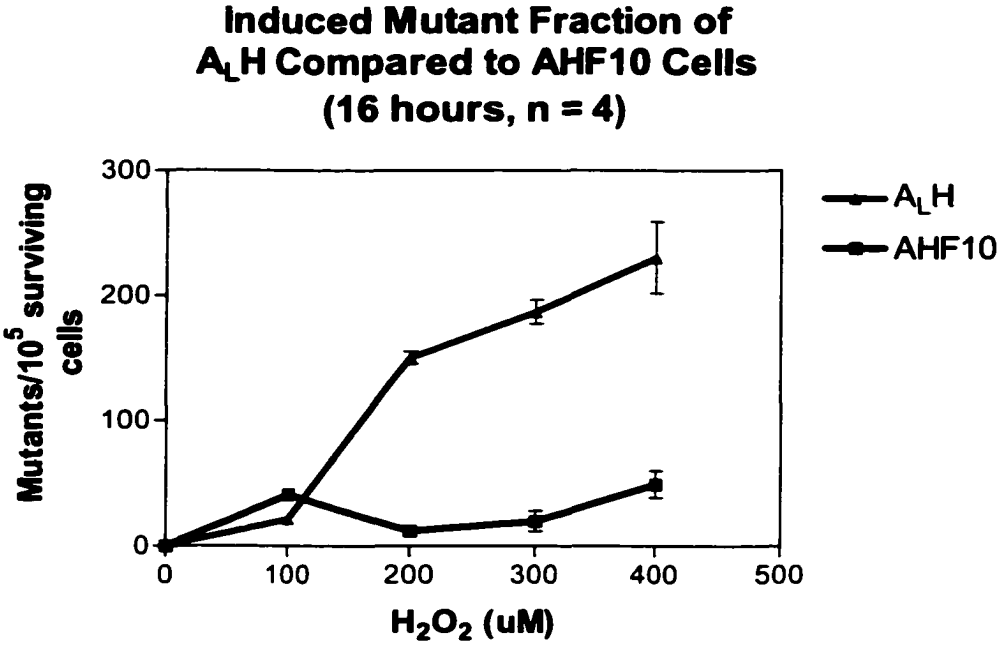

Figure 23. M_f for CD59- mutants induced in A_LH and AHF10 cells after exposure to H_2O_2 16-hours. AHF10 are able to avoid mutant induction even at the highest dose.

Data for M_f for $CD59^-$ Mutants Induced A_LH and AHF10 Cells After Exposure to H_2O_2.

	AHF10		ALH	
PQ (μM)	Challenge 1	Challenge 2	Challenge 1	Challenge 2
0.00	0.00	0.00	0.00	0.00
100.00	41.00	41.82	22.00	21.40
200.00	10.30	13.91	145.00	155.15
300.00	28.00	11.80	177.40	196.30
400.00	60.00	38.50	201.50	258.80

H_2O_2 (μM)	AHF10		A_LH	
	Mean	SD	Mean	SD
0.00	0.00	0.00	0.00	0.00
100.00	41.41	0.58	21.70	0.42
200.00	12.11	2.55	150.08	7.18
300.00	19.90	11.46	186.85	13.36
400.00	49.25	15.20	230.15	40.52

Mutation after 4-day exposure

Mutant induction was determined in A_LH cells after a 4-day exposure to PQ and compared to results found for a 16-hour exposure. As shown in Figure 24, the longer exposure to PQ increased mutant yields. For example, as many mutants were induced at 50 μM PQ in a 4-day exposure as at 1250 μM PQ for 16 hours.

Figure 25 shows the survival curve and mutant induction in AHF3, the fpg transformant with the highest FPG activity (Figure 12), compared to A_LH cells. The upper portion of the figure shows differences in survival curves and the lower portion shows differences in mutant induction. AHF3 cells have greater resistance to PQ toxicity and have no more mutants than the background levels measured in controls.

The presence of active FPG protein appears to give the AHF3 cells an advantage against the detrimental effects of ROS-generating exposures. Mutation of AHneo3 (blank vector) cells was measured and showed levels of mutant induction similar to those seen in A_LH. PQ induced mutation in AHneo3 cells, therefore ruling out the possibility that the transfection procedure could account for the results observed in the fpg transformants.

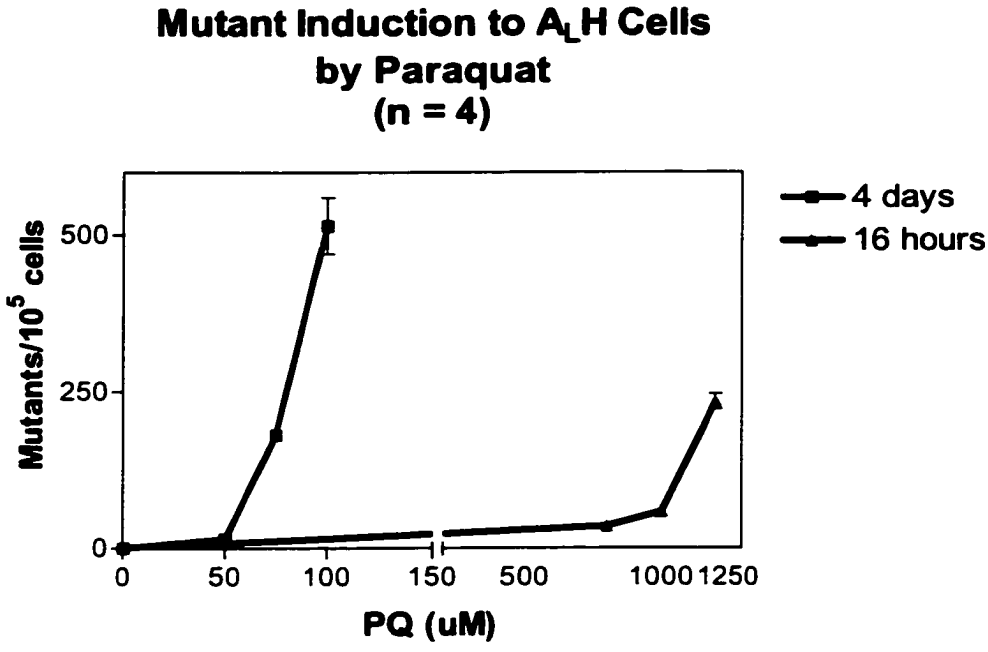

Figure 24. M_f for CD59$^-$ mutants induced A_LH after exposure to PQ 16-hours and 4-days. As exposure time to PQ increases, the number of mutants also increases.

Data for M_f for $CD59^-$ Mutants Induced A_LH After Exposure to PQ.

PQ (μM)	16-hours Challenge 1	16-hours Challenge 2	4-days Challenge 1	4-days Challenge 2
0.00	0.00	0.00	0.00	0.00
800.00	14.70	14.80	34.00	36.40
1000.00	174.90	187.14	66.00	50.82
1200.00	469.60	559.90	222.00	246.00

PQ (μM)	4 days Mean	4 days SD	16 hours Mean	16 hours SD
0.00	0.00	0.00	0.00	0.00
800.00			35.20	1.70
1000.00			58.41	10.73
1200.00			234.00	16.97
50.00	14.75	0.07		
75.00	181.02	8.65		
100.00	514.75	63.85		

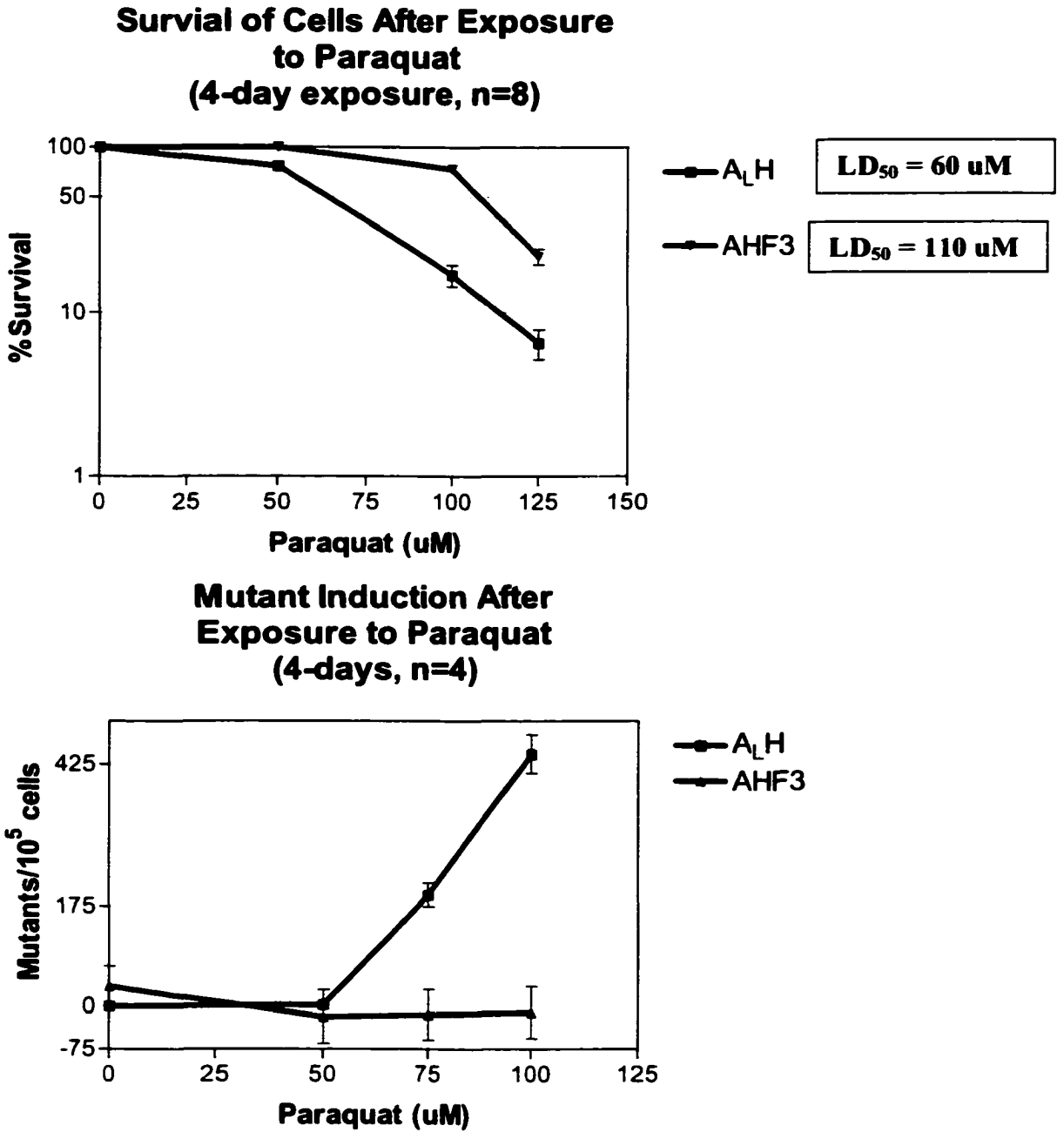

Figure 25. Comparison of survival curves and induced mutant fraction of A_LH and AHF3 cells exposed to PQ for 4-days. AHF3 cells efficiently cleaved 8oxoG as shown in Figure 12, supporting the idea that efficient DNA repair increases PQ resistance and decreases mutant induction.

Data for Survival Curves and M_f for CD59$^-$ Mutants Induced A_LH and AHF3 Cells After Exposure to PQ.

Cell Survival

	A_LH			AHF10		
µM PQ	A	b	c	a	b	C
0.00	100.00	100.00	100.00	100.00	100.00	100.00
50.00	90.00	70.00	72.00	93.00	65.00	70.50
100.00	20.00	20.50	13.00	20.10	20.00	11.00
125.00	10.00	3.00	6.70	7.00	4.50	7.90

PQ (uM)	A_LH		AHF3	
	Mean	SD	Mean	SD
0.00	100.00	0.00	100.00	0.00
50.00	80.00	14.14	100.00	0.00
100.00	16.00	5.66	76.00	8.49
125.00	6.50	4.95	23.50	4.95

Mutant Induction

	A_LH			AHF3			
PQ (µM)	Chall 1	Chall 2	Chall 3	Chall 1	Chall 2	Chall 3	Chall 4
0.00	0.00	0.00	0.00	0.00	0.00	0.00	139.87
50.00	1.97	3.00		-48.60	-87.01	-59.87	120.70
75.00	164.60	186	235.00	-87.17	-55.68	-31.52	114.01
100.00	480.79	470	376.00	-90.20	-62.16	-7.50	115.77
100.00	442.30	33.29		11.02	45.62		

PQ ((µM)	A_LH		AHF3	
	Mean	SD	Mean	SD
0.00	0.00	0.00	34.97	69.94
50.00	2.48	0.73	-18.70	94.32
75.00	195.03	36.16	-15.09	89.03
100.00	442.30	57.66	-11.02	91.23

D. Glutathione Measurements After Exposure to Paraquat

Glutathione (GSH) levels were measured in A_LH cells exposed to PQ for 16-hours (Figure 26). The addition of BSO decreases baseline levels of GSH within the cells. After the addition of 400 μM PQ for 16 hours, GSH levels were increased but dropped with the addition of BSO, as expected. The measurement of GSH levels after exposure to a chemical or an agent is suggestive of the involvement of ROS-generation in the system being studied. BSO and NAC both affect GSH levels, though in opposing ways, so that their addition can be used to shed light on the effect of the chemical or agent being studied. Figure 27 shows levels of GSH and glutathione disulfide (GSSG), which refer to un-oxidized and oxidized glutathione respectively.

The upper portion of the figure ("a") shows that after exposure to PQ for 4 days, PQ (0-125 μM) did not alter GSH. The addition of BSO decreases the baseline levels (no PQ added) but concentrations of GSH rise with each increase in PQ concentration. The addition of PQ is likely inducing transcription of GSH in response to the production of ROS within the cell. The initial drop in concentration with the addition of NAC was unexpected but may indicate that after a long-term (4-day) exposure to PQ, NAC is unable to boost the GSH cycle enough to affect it.

The lower portion of Figure 27 ("b") shows the levels of GSSG measured in the A_LH cells after a 4-day exposure to PQ. No real difference in concentration levels was observed except when BSO and PQ were added. All levels of exposure (0 to 125 uM) show higher concentrations of GSSG in the cells when BSO is added. This is likely due to the block of the GSH-GSSG cycle and concentrations of GSSG are unable to cycle, thus resulting in their higher overall concentration.

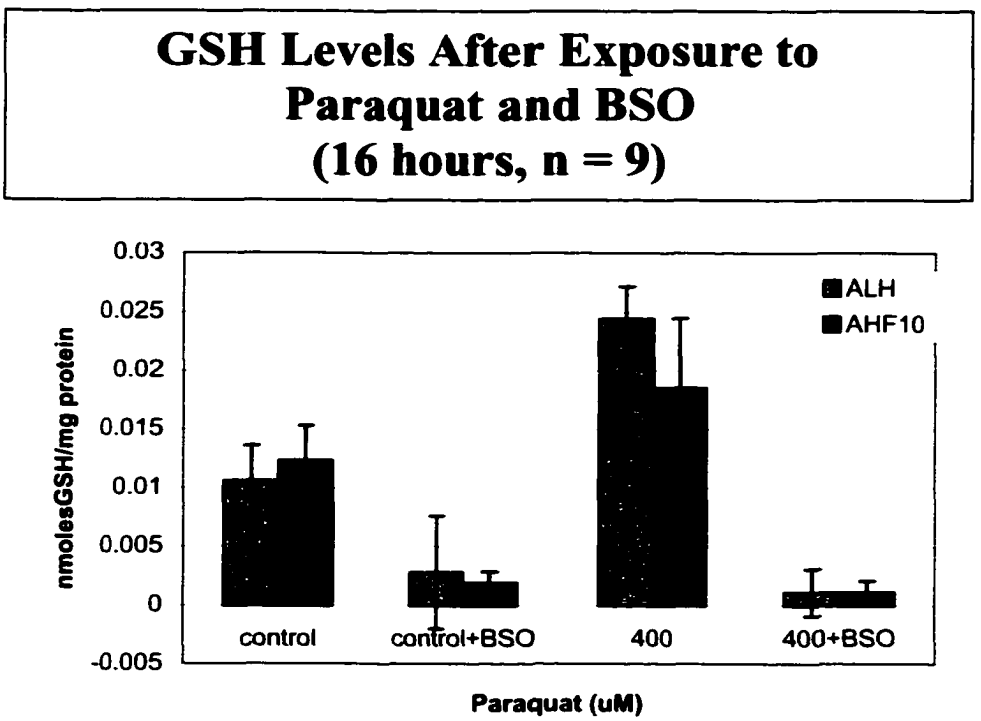

Figure 26. GSH levels in A_LH cells exposed to PQ +/- BSO for 16 hours. GSH appears to be induced by PQ addition.

Data for GSH Levels in A_LH Cells Exposed to PQ +/- BSO for 16-hours.

	A_LH	AHF10
	Mean	Mean
control	0.0106	0.0123
control+BSO	0.0028	0.0019
400 μM PQ	0.0244	0.0185
400+BSO	0.0011	0.0011
600 μM PQ	0.0114	0.0094
600+BSO	0.0047	0.0009
800 μM PQ	0.027	0.0284
800+BSO	0.0037	0.002

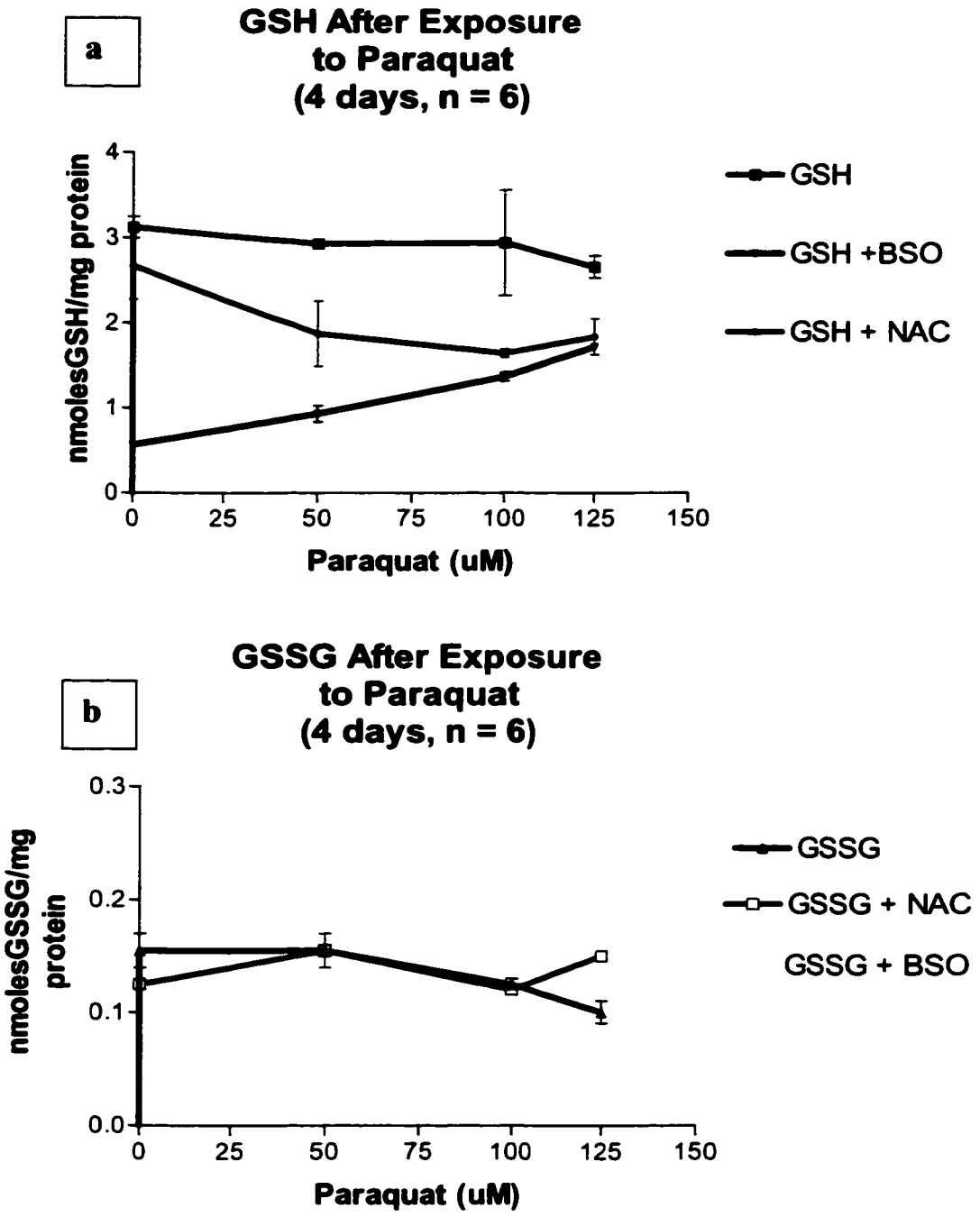

Figure 27. Oxidized (GSH) and un-oxidized (GSSG) glutathione levels in A_LH cells exposed to PQ +/- BSO for 16-hours.

Data for Levels of GSH and GSSG in A_LH Cells After Exposure to PQ.

GSH	GSH		GSH +BSO		GSH + NAC	
PQ (μM)	assay 1	assay 2	Assay 1	assay 2	assay 1	assay 2
0	3.25	3	0.568		2.28	3.06
50	2.98	2.88	1.03	0.84	2.26	1.49
100	3.56	2.32	1.42	1.32	1.6	1.69
125	2.79	2.53	1.74	1.7	2.05	1.63

PQ (uM)	GSH		GSH +BSO		GSH + NAC	
	Mean	SEM	Mean	SEM	Mean	SEM
0.00	3.13	0.13	0.57	0.00	2.67	0.39
50.00	2.93	0.05	0.93	0.10	1.88	0.39
100.00	2.94	0.62	1.37	0.05	1.65	0.05
125.00	2.66	0.13	1.72	0.02	1.84	0.21

GSSG	GSSG		GSSG + BSO		GSSG + NAC	
PQ (μM)	assay 1	assay 2	Assay 1	assay 2	assay 1	assay 2
0	0.14	0.17	0.21		0.13	0.12
50	0.15	0.16	0.24	0.19	0.14	0.17
100	0.12	0.13	0.13	0.17	0.12	0.12
125	0.11	0.09	0.16	0.2	0.15	0.15

PQ (uM)	GSSG		GSSG + BSO		GSSG + NAC	
	Mean	SEM	Mean	SEM	Mean	SEM
0.00	0.16	0.02	0.21	0.00	0.13	0.00
50.00	0.16	0.00	0.22	0.03	0.16	0.02
100.00	0.13	0.00	0.15	0.02	0.12	0.00
125.00	0.10	0.01	0.18	0.02	0.15	0.00

Chapter IV

Conclusions and

Discussion

I investigated the genotoxic effects of PQ and compared the results to transformants of A_LH containing the bacterial fpg gene. I found that:

1. A_LH cells expressing bacterial fpg cleaved more 8oxoG than wild type A_LH cells when incubated with a ^{32}P-labeled oligonucleotide containing 8oxoG.

Protein extracts from some transformed cells cleaved the ^{32}P-8oxoG oligo to a greater percentage than that from A_LH cells as measured by the release of a ^{32}P-labeled fragment. Prior to carrying out the cleavage experiments, my RT-PCR results indicated that some of the fpg transformants expressed the fpg gene (Figure 10). RT-PCR cannot, of course, provide evidence as to whether or not the FPG protein in these cells was enzymatically active. This was shown in the *in vitro* cleavage experiments. The cDNA made from mRNA of A_LH cells does not bind to the fpg primers (Figure 10b). But without a housekeeping gene such as β-actin as an internal PCR control, it is not possible

to state that no binding occurred in the wild type cells or that different transformed clones had more or less message for the bacterial fpg. A possible explanation for the low level of binding of A_LH to PCR primers for a gene not present in it is that A_LH cells contain a gene with repair capacity[146] with homology for fpg. Since this gene is known to be evolutionarily-conserved, A_LH cells probably contain a gene similar enough in structure to fpg to bind fpg-specific primers. I found that PCR conditions required "fine-tuning" to increase specificity for the fpg message which could reflect sequence similarities between the bacterial fpg gene and a CHO homolog.

Further support for the presence of a homolog of fpg in A_LH cells was provided by the cleavage experiments which showed that protein extracts from A_LH cells cleaved 8oxoG, though to a lower percentage than the most efficient fpg transformant (Figure 12). The presence of a protein with similar enzymatic function, if not exact sequence to the bacterial FPG protein, would be expected in the A_LH cells since the need to recognize and remove oxidative DNA damage is vital to genomic stability and long-term survival of any species. In this regard, enzymes with functions like that of FPG are seen in both *S. cerevisiae* OGG1 and the human homolog hOGG1. The proteins in these eukaryotic cells have been shown to function in the removal of 8oxoG from dsDNA but, are more closely homologous in sequence to bacterial endoIII than to FPG.[116] This could be the case for A_LH (CHO) cells as well.

When considering the results of the cleavage experiments, it is important to note that they represent a "snapshot in time," not a kinetic study. The incubation of the cell extracts with the ^{32}P-labeled 8oxoG was terminated after an hour and immediately run on a denaturing polyacrylamide gel (see Materials and Methods). What is visualized on the

gel reflects the amount of 8oxoG cleaved during this time. *In vivo*, an equilibrium exists between DNA nicking and DNA repair. The question could be raised that perhaps the A_LH cells more efficiently repair DNA nicking caused by FPG protein than do the fpg transformant cells and therefore the 8oxoG cleavage assay is not a true picture of repair capacity. But, even if protein extracts from A_LH cells were able to reseal DNA nicks more efficiently than that of the fpg transformants, the ^{32}P released when FPG protein nicks the DNA would not be re-incorporated into the DNA when the nicks were re-sealed. Rather, it would remain part of a 15-base piece of DNA (see Materials and Methods for details of the oligo construct) and this piece would migrate at a different rate than the longer (30-mer) dsDNA, and be seen as a distinct band in the gel. Additionally, I conducted control studies with vectors that contained the neomycin plasmid but not the fpg plasmid and found that both survival and mutation in these control cells was similar to that of the A_LH cells, not the fpg transformants. These "empty vector" controls indicate that the fpg gene was responsible for the phenotype observed. Further, it is unlikely that the transfection procedure would of itself alter ligase activity in a manner that would not be reflected in cell survival or mutant induction results.

8oxoG cleavage experiments showed that the FPG protein in the transformants was enzymatically active for 8oxoG. Thus, results obtained for survival and mutant induction by PQ, can be considered in terms of an increased repair capacity in some of the fpg transformants. Low concentrations of protein extract did not show significant FPG activity but the amount of 8oxoG cleavage depended on the protein concentration (Figure 12). Cleavage occurs *in vivo* at the lower concentrations but the methodology I

used is limited in sensitivity, making the detection of very low amounts of 8oxoG cleavage impossible.

Since the FPG polyclonal antibody experiments were not definitive, it was impossible from these experiments to say what concentration of FPG protein was present in the cell extracts. So, I used low and high concentrations of cell extract in the cleavage experiments. FPG cleavage of 8oxoG was undetectable at low concentrations but, at approximately 40 μg of protein, differences in cleavage were observed and at approximately 60 μg, FPG activity appeared to level off.

It should be noted that the extract concentrations used were *total protein* so that the amount of FPG present in each extract from each individual cell line examined was unknown. Despite this limitation, the data provide evidence that different fpg transformants exhibited different levels of cleavage efficiency and showed that at least one transformant had a very high level of activity. These differences in activity may reflect differing numbers of fpg inserts in each different cell line or that fpg inserts were controlled by promoters of different strength. AHF3, in particular, showed levels of cleavage ten times greater than that of A_LH cells.

The difference in A_LH and AHF3 cells in 8oxoG cleavage efficiency provided the basis for the most important results obtained in my study. That is, the differences in cell survival and mutant induction by PQ correlate with cleavage efficiency so that important insight was provided into the role of DNA repair capacity in mutagenesis and cell killing.

An additional interesting observation can be made from results of the experiments involving the cleavage and genotoxicity in the fpg transformant, AHF10. Although the fraction of 8oxoG cleavage seen with AHF10 surpasses that of A_LH cells, the difference

in activity was not significant (Figure 12). Despite this, AHF10 cells were significantly more resistant than A_LH to mutant induction by both PQ and H_2O_2 (Figures 22 and 23). Since a fine balance exists between DNA damage and repair in cells, it is reasonable that the amount of oxidative damage in A_LH cells is enough higher than that in the AHF10 cells to result in mutation. In other words, AHF10 cells may exhibit only a little more DNA repair capacity than A_LH but the difference is sufficient to prevent mutation. Likewise, when considering this result in terms of human health, individual susceptibility to oxidatively-induced disease may be governed by very small differences in DNA repair capability. Small differences in individual DNA repair capacity could, therefore, could be important to the outcome of exposure to ROS-generating compounds, like PQ.

It would be interesting to correlate the 8oxoG cleavage efficiency in individual human subjects with disease status (i.e., normal vs. benign cancer vs. metastatic cancer). The assessment of an individual's DNA repair capability could possibly be used as a risk indicator and used in cooperation with biomarkers of disease susceptibility.

AHF3 cells were not analyzed for survival or mutant induction by PQ prior to the cleavage assay, therefore it was important to backtrack and measure these endpoints for comparison with A_LH cells. Since mutation was virtually eliminated in AHF10 cells, the comparison that could be made in terms of mutant induction with AHF3 cells was limited and not undertaken. It would be useful, however, to continue these studies and repeat mutant induction studies by PQ with these two cell lines for both 16-hour and 4-day exposure periods. Future studies using Southern analysis would also provide new and important information by showing the actual number of inserts contained in each fpg transformant. Correlations between fpg insert number and FPG protein activity to

survival curves and mutant fraction could be important. An additional study would involve the removal of the fpg gene from the fpg transformant cells. Since insertion of the bacterial fpg gene made cells resistant to PQ mutation, then removal or shut down of the gene would be expected to reverse the effect.

2. PQ is lethal in mammalian cells at low doses.

PQ toxicity is associated mostly with incidents of accidental ingestion by humans or accidental spillage into streams and wildlife habitats. In those cases, the amount of PQ involved can be in the kilogram quantity. Toxicity to living species is usually acute so that killing occurs in a few days. In contrast, I investigated PQ toxicity at μM concentrations for relatively short exposure times of hours or days. I found that PQ was quite lethal to cells in culture and that lengthening the exposure time (increasing the dose) increased lethality (Figure 14).

An important question is in what way does PQ cause cytotoxicity? Certainly oxidative DNA damage is implicated by the results of this study as well as the work of others.[69,110] Oxidative damage is known to cause a variety of damage to DNA bases and to the deoxyribonucleic backbone. The build up of DNA damage, especially promutagenic 8oxoG, likely plays a role in PQ cytotoxicity. A key to PQ cytotoxicity however, may involve the formation of the imidazole ring-opened base damage known as "Fapy." *In vitro*, Fapy DNA damage halts replication by blocking DNA polymerases[30] and prevents mRNA transcription.[35] The production of DNA and shortened proteins are considered a likely source of Fapy cytotoxicity and may be the source of PQ cytotoxicity as well.

As shown in Figure 14, the shoulder of the survival curve for A_LH cells was quite broad. This suggests that at low doses of PQ, these A_LH cells are able to effectively deal with the lethal effects of PQ. CHO cells, which are the parent cells to A_LH, possess inherent BER mechanisms and have been shown for example, to repair 8oxoG base damage induced by gamma irradiation when given sufficient time.[147] The somewhat odd shape of the survival curves for A_LH cells is most likely explained by CHO defense mechanisms against oxidative damage. Levels of enzymes that deal with oxidative stress in A_LH cells have been measured:*

SOD	5.92 +/- 0.3 units/mg protein
Catalase	89.6 +/- 2.0 nmol H_2O_2 consumed/min/mg protein
Glutathione peroxidase	21.41 +/-1.6 nmols/mg protein
Glutathione reductase	26.2 +/-2.1 nmols/mg protein

*Dr. Daniel L. Gustafson, unpublished data

If A_LH cells were not able to efficiently handle normal levels of oxidative stress the accumulation of mutation would be likely. An interesting study that could be initiated along these lines would involve measuring DNA repair capacity in BALB/c versus C57BL/6 mice. BALB/c mice have been shown to be deficient in double-stand break repair and prone to cancer development when compared with C57BL/6 mice.[148] The role BER repair in the sensitivity in this strain of mice has not been investigated thoroughly and may well prove to be an important aspect of their susceptibility to oxidative stress.[149,150]

ROS generation by PQ is suggested by the alteration in survival curves when the ROS modulators, NAC or BSO, were added in the medium. NAC, an antioxidant in cells,[151] increased survival (Figure 16) whereas BSO, which blocks the GSH cycle, another antioxidant defense system in cells, decreased survival (Figure 15). Further, H_2O_2, a known source of intracellular ROS, produced survival curves similar in slope to those obtained with PQ (Figure 20). My studies with GSH levels also indicated that PQ induced ROS. GSH levels were increased in A_LH cells after the addition of PQ and dropped with the addition of BSO (Figures 26 and 27). The rise in GSH levels after PQ exposure is a cellular response to increased ROS generation. Likewise, the negative effect of BSO on GSH levels reflects the inhibition of the GSH cycle, preventing the conversion of GSSG (oxidized GSH) to its un-oxidized form (see Figure 1).

The role redox cycling plays in PQ cytotoxicity could be examined by growing cells under anaerobic conditions. By removing oxygen, redox cycling of PQ through the NADPH cycle would not occur. It would be expected that cytotoxicity of PQ would diminish, although alternate effects of PQ on cells are unknown. Could PQ be processed through an alternative biotransformation pathway that does not require oxygen? Would PQ bind to cellular components? Would that binding be deleterious to the cell? These are all questions that would be revealed by these experiments.

Although it is interesting to look at PQ lethality per se, the real purpose of using PQ in this study was as a tool for measuring PQ oxidation effects in mammalian cells. The A_LH cells containing and expressing fpg provided a means to examine the role of BER in cell survival and mutagenesis.

Survival studies were conducted on the fpg transformants. Some of the fpg transformants showed greater survival than A_LH cells after PQ exposure. Given the evidence from my studies and others that PQ generates ROS and evidence in the literature that FPG can repair oxidative DNA damage, these results were expected. However, there was no difference in survival of A_LH and AHF10 cells after exposure to H_2O_2. It may well be therefore, that PQ and H_2O_2 cause oxidation through different pathways. H_2O_2 is converted into H_2O and O_2 by catalase (See Chapter I) and it can produce the damaging •OH through the Fenton Reaction. PQ, on the other hand, is able to produce a variety of ROS including $^{\cdot}\bullet O_2$, •OH and H_2O_2. This could mean that PQ is generating a larger *quantity* of ROS than H_2O_2 (via redox cycling) as well as a different *quality* of ROS. Although the survival curves were merely suggestive, the difference in ROS generation by PQ and H_2O_2 may explain the results obtained.

3. Expression of the FPG protein in mammalian cells increases survival and prevents mutant induction by PQ.

PQ induces mutations at the CD59 locus of A_LH cells in a dose-dependent manner (Figure 22, Figure 25). The A_L mutation assay measures induction of CD59- mutants. The CD59 gene is located on human chromosome 11, a chromosome not vital to cell reproduction of this hybrid. Several CHO genes are also required for expression of the CD59 cell surface antigen and these are also known to be targets of mutation to CD59- phenotype. Some mutation assays measure mutant induction in a single gene (i.e., the *hprt*- assay). This methodological design of the A_L assay increases the sensitivity of mutant detection and has been successful in providing evidence of mutant induction by

agents that at one time were thought to be non-mutagenic (e.g., arsenic and asbestos).[142,152] Like PQ, the mutagenic effects of arsenic and asbestos were shown to depend on the generation of ROS.

My results point to PQ as being a weak mutagen. The number of mutants induced at the CD59 loci is low when compared to some other mutagens such as benzo (a) pyrene (B(a)P). B(a)P mutant induction was previously measured in A_L cells.[78] The yield was 130 mutants/10^5 clonable cells by B(a)P ($D_0 \approx 20$ μM) compared to 70 mutants/10^5 clonable cells for PQ ($LD_{50} = 60$ μM). PQ, by this measure, is half as mutagenic as B(a)P. Mutant induction has also been measured at the *hprt*- loci of CHO cells[153] yielding 248 mutants/10^6 and 456/10^6 clonable cells after exposure to 30 and 100 ng/ml B(a)P, respectively. Prior studies that compared the CD59 and *hprt*- locus showed the CD59 loci to be 28-fold more sensitive for the measurement of mutant induction by arsenic.[142] If this holds true for PQ, the *hprt*- assay would be unable to detect mutant induction by PQ.

This relatively low mutagenicity of PQ, compared to its lethal effect, may explain why it is classified a "weak carcinogen" after EPA testing. Cigarette smoke and cigarette smoke condensate (CSC) are negative in the Ames' Test but both are strong carcinogens. Based upon my results, high doses of PQ would be required to produce enough mutants to be detectable by most conventional testing methods (those other than the A_L assay). In this regard, PQ most likely would induce damage that was cytotoxic long before it could be expressed in a carcinogenic manner.

As I found with cell killing, the mutagenic effect of PQ increases with exposure time. Mutant induction at 4-days was much higher than 16-hour exposures; despite the

use of lower concentrations of PQ (Figure 24). This is likely due to redox cycling of PQ generating deleterious ROS. It may be that over time repair and defense mechanisms are overwhelmed so that cytotoxic and genotoxic damage accumulates. The most relevant studies in this regard would involve long-term exposure (weeks and months) to very low doses of PQ. It would be of interest to determine if repair enzymes in A_LH cells would gradually "win back" the fight against ROS and as time passed the amount of mutagenic DNA damage measured would decrease. These kinds of studies unfortunately are not done to test chemicals by the FDA or any other agency.

The fpg transformant cells I created contained an additional enzyme for defense against ROS-generating compounds. When exposed to PQ and H_2O_2 mutant induction in some of the fpg transformants was not seen at a level above background (Figures 22, 23, 25). Thus, the presence of active FPG protein appears to play a key role in suppressing mutant induction by PQ.

The gene for catalase on human chromosome 11 is in proximity to CD59 ($\approx$ 2 megabases, see Figure 5). It may be, therefore, that both catalase and CD59 are sometimes mutated together by PQ (as by deletion), thus, decreasing the mutant's ability to neutralize $\bullet O_2^-$. Mutant spectra studies would be an important addition to the results of my study and should further elucidate the genotoxic effects of PQ. Additionally, transfecting a bacterial catalase gene (HPI) into A_LH cells and subsequently deactivating it could provide insight into the importance of endogenous H_2O_2 in PQ genotoxicity. PQ may be causing deleterious effects to cells mainly through the production of $\bullet O_2^-$ rather than by production of H_2O_2. Both $\bullet O_2^-$ and H_2O_2 have the ability to produce $\bullet$OH (see Figure 1) but, it is possible that they use different pathways to damage cells. If the

catalase gene is mutated by PQ in conjunction with CD59, then its ability to act as an oxidative stress defense mechanism is impaired. This could explain part of the differences observed between the two chemicals in terms of survival curves and mutant induction.

4. FPG protein excises DNA damage that causes mutation.

The fact PQ did not induce CD59- mutants in the fpg transformants is an important indicator that the types of damage caused by PQ and H_2O_2, namely, oxidative damage to DNA, are the types of damages that cause mutation. Bacterial FPG protein has been found to bind and excise 8oxoG, FapyG and FapyA and 8oxoA, to a lesser extent.[52] Therefore, it may be that these types of damage to DNA may be the principal DNA damage that is mutagenic in cells treated with PQ. It is important to note that FPG protein excises Fapy adducts. Many of the studies looking at DNA adducts and their mutagenicity and relation to carcinogenesis focus solely on the known mutagen, 8oxoG. However, the relationship between Fapy and 8oxo adducts is important but, often overlooked in scientific studies. Fapy or 8oxo adducts are formed depending upon the redox status of the cell.[154] Recent studies have found that the *ratio* between the two different types of damage (Fapy:8oxo) correlated to the disease status of cancerous and normal tissues.[45,155] That is, Fapy adducts predominate in normal tissues whereas 8oxo adducts predominate in cancerous tissues. The balance between DNA damage and repair certainly plays an important role in cell health but there is also a balance in the redox status of the cell between the utilization of reductive and oxidative states. In the reductive pathway ROS can form ring-opened Fapy adducts whereas oxidative pathways

form 8oxo products. This utilization of the reductive pathway and formation of types of DNA damage that stop replication and are cytotoxic allow the cell to avoid the production of genotoxic forms of DNA (i.e., 8oxoG). The cells used in this study are not cancerous in origin and may, therefore, preferentially shuttle oxidative stress through reductive pathways to form Fapy adducts.

There have been reports of mutant strains of mice that lack the DNA glycosylase needed to excise 8oxoG.[156] These mice accumulated large quantities of 8oxoG, yet did not develop cancer.[156] These studies question the importance of 8oxoG as a factor in carcinogenesis. However, it is important to note that Fapy adducts were not measured in these studies. The production of Fapy adducts may be the important link to the lack of cancer development in these mice. It may be that these mice do not develop cancer because of the preferential use in their cells of the reductive, cytotoxic formation of Fapy adducts rather than the oxidative, genotoxic pathway which forms 8oxo adducts. Further, the ogg1 gene, a homolog of fpg, was mutated in these mice. This gene encodes for the protein, OGG1, which almost exclusively cleaves 8oxoG whereas FPG cleaves both 8oxoG and FapyG with equal specificity. Additional repair enzymes have been identified in yeast and humans, OGG2 and hOGG2, respectively,[157] which share homology and function with FPG, in that they cleave to oxidatively-induced DNA base damage. These enzymes may play an important role in the prevention of carcinogenesis in the mutant mice as well as in humans. In addition, the transcription of proteins such as bacterial FPG specifically designed for the recognition and removal of 8oxoG from the genome are conserved from bacteria up to humans. It is unlikely then that if the removal of

8oxoG were not of utmost importance in evolutionary terms that it would have been left in the genome.

My results give evidence that individual susceptibility and risk may be associated not only with levels of DNA damage (exposure to oxidative stress) but also with repair capacity. Genetic predisposition to cancer may be linked to one's ability to produce active DNA repair enzymes.

In summary, the most important results I obtained are the suppression of mutant induction by PQ in AHF3 and AHF10 cells and the correlation with cell survival curves and 8oxoG cleavage studies. Although these results are not conclusive, it is not unreasonable to make the connection with cleavage efficiency of 8oxoG and mutant suppression. It is also important to remember that the experiments conducted in this study were *in vitro* studies. The relevance to *in vivo* situations is not known but certainly my studies offer important clues. I showed that PQ is a mutagen in mammalian cells and provided new insights into the role of DNA repair in the prevention of mutagenic changes in DNA by PQ and H_2O_2.

References

1. Krokan, H. E., Standal, R., and Slupphaug, G. DNA glycosylases in the base excision repair of DNA. Biochem.J., *325 (Pt 1)*: 1-16, 1997.

2. McCord, J. M. and Fridovich, I. The utility of superoxide dismutase in studying free radical reactions. I. Radicals generated by the interaction of sulfite, dimethyl sulfoxide, and oxygen. J.Biol.Chem., *244*: 6056-6063, 1969.

3. Rhee, S. G. Redox signaling: hydrogen peroxide as intracellular messenger. Exp.Mol.Med., *31*: 53-59, 1999.

4. Imlay, J. A., Chin, S. M., and Linn, S. Toxic DNA damage by hydrogen peroxide through the Fenton reaction in vivo and in vitro. Science, *240*: 640-642, 1988.

5. Zaho, M. J., Jung, L., Tanielian, C., and Mechin, R. Kinetics of the competitive degradation of deoxyribose and other biomolecules by hydroxyl radicals produced by the Fenton reaction. Free Radic.Res., *20*: 345-363, 1994.

6. Djuric, Z., Heilbrun, L. K., Reading, B. A., Boomer, A., Valeriote, F. A., and Martino, S. Effects of a low-fat diet on levels of oxidative damage to DNA to human peripheral nucleated blood cells. J.Natl.Cancer Inst., *83*: 766-769, 1991.

7. Falck, F., Jr., Ricci, A., Jr., Wolff, M. S., Godbold, J., and Deckers, P. Pesticides and polychlorinated biphenyl residues in human breast lipids and their relation to breast cancer. Arch.Environ.Health, *47*: 143-146, 1992.

8. Floyd, R. A., Watson, J. J., Harris, J., West, M., and Wong, P. K. Formation of 8-hydroxydeoxyguanosine, hydroxyl free radical adduct of DNA in granulocytes exposed to the tumor promoter, tetradecanoylphorbolacetate. Biochem.Biophys.Res.Commun., *137*: 841-846, 1986.

9. Kuchino, Y., Mori, F., Kasai, H., Inoue, H., Iwai, S., Miura, K., Ohtsuka, E., and Nishimura, S. Misreading of DNA templates containing 8-

hydroxydeoxyguanosine at the modified base and at adjacent residues. Nature, *327*: 77-79, 1987.

10. Lim, J. S., Frenkel, K., and Troll, W. Tamoxifen suppresses tumor promoter-induced hydrogen peroxide formation by human neutrophils. Cancer Res., *52*: 4969-4972, 1992.

11. Nackerdien, Z., Olinski, R., and Dizdaroglu, M. DNA base damage in chromatin of gamma-irradiated cultured human cells. Free Radic.Res.Commun., *16*: 259-273, 1992.

12. Olinski, R., Zastawny, T., Budzbon, J., Skokowski, J., Zegarski, W., and Dizdaroglu, M. DNA base modifications in chromatin of human cancerous tissues. FEBS Lett., *309*: 193-198, 1992.

13. Troll, W. and Wiesner, R. The role of oxygen radicals as a possible mechanism of tumor promotion. Annu.Rev.Pharmacol.Toxicol., *25*: 509-528, 1985.

14. Malins, D. C., Holmes, E. H., Polissar, N. L., and Gunselman, S. J. The etiology of breast cancer. Characteristic alteration in hydroxyl radical-induced DNA base lesions during oncogenesis with potential for evaluating incidence risk. Cancer, *71*: 3036-3043, 1993.

15. Halliwell, B. and Gutteridge, J. M. Role of free radicals and catalytic metal ions in human disease: an overview. Methods Enzymol., *186*: 1-85, 1990.

16. Thompson, L. H. and Schild, D. The contribution of homologous recombination in preserving genome integrity in mammalian cells. Biochimie, *81*: 87-105, 1999.

17. Free Radicals: A Practical Approach.Oxford: IRL Press, 1996.

18. Halliwell, B. Superoxide-dependent formation of hydroxyl radicals in the presence of iron chelates: is it a mechanism for hydroxyl radical production in biochemical systems? FEBS Lett., *92*: 321-326, 1978.

19. Fridovich, I. The biology of oxygen radicals. Science, *201*: 875-880, 1978.

20. Casarett and Doull's Toxicology The Basic Science of Poisons, 5th ed.New York: McGraw Hill, 1996.

21. Hathway, D. E. Toxic action/toxicity. Biol.Rev.Camb.Philos.Soc., *75*: 95-127, 2000.

22. Kelly, K. A., Havrilla, C. M., Brady, T. C., Abramo, K. H., and Levin, E. D. Oxidative stress in toxicology: established mammalian and emerging piscine model systems. Environ.Health Perspect., *106*: 375-384, 1998.

23. Dizdaroglu, M. Chemical determination of free radical-induced damage to DNA. Free Radic.Biol.Med., *10*: 225-242, 1991.

24. Floyd, R. A., Watson, J. J., Wong, P. K., Altmiller, D. H., and Rickard, R. C. Hydroxyl free radical adduct of deoxyguanosine: sensitive detection and mechanisms of formation. Free Radic.Res.Commun., *1*: 163-172, 1986.

25. Chetsanga, C. J. and Grigorian, C. In situ enzymatic reclosure of opened imidazole rings of purines in DNA damaged by gamma-irradiation. Proc.Natl.Acad.Sci.U.S.A, *82*: 633-637, 1985.

26. Viswanathan, A. and Doetsch, P. W. Effects of nonbulky DNA base damages on Escherichia coli RNA polymerase- mediated elongation and promoter clearance. J.Biol.Chem., *273*: 21276-21281, 1998.

27. Boiteux, S. and Laval, J. Imidazole open ring 7-methylguanine: an inhibitor of DNA synthesis. Biochem.Biophys.Res.Commun., *110*: 552-558, 1983.

28. Cheng, K. C., Cahill, D. S., Kasai, H., Nishimura, S., and Loeb, L. A. 8-Hydroxyguanine, an abundant form of oxidative DNA damage, causes G---- T and A----C substitutions. J.Biol.Chem., *267*: 166-172, 1992.

29. Fraga, C. G., Shigenaga, M. K., Park, J. W., Degan, P., and Ames, B. N. Oxidative damage to DNA during aging: 8-hydroxy-2'-deoxyguanosine in rat organ DNA and urine. Proc.Natl.Acad.Sci.U.S.A, *87*: 4533-4537, 1990.

30. Klein, J. C., Bleeker, M. J., Saris, C. P., Roelen, H. C., Brugghe, H. F., van den, E. H., van der Marel, G. A., van Boom, J. H., Westra, J. G., Kriek, E., and . Repair and replication of plasmids with site-specific 8-oxodG and 8- AAFdG

residues in normal and repair-deficient human cells. Nucleic Acids Res., *20*: 4437-4443, 1992.

31. Moriya, M., Ou, C., Bodepudi, V., Johnson, F., Takeshita, M., and Grollman, A. P. Site-specific mutagenesis using a gapped duplex vector: a study of translesion synthesis past 8-oxodeoxyguanosine in E. coli. Mutat.Res., *254*: 281-288, 1991.

32. Shibutani, S., Takeshita, M., and Grollman, A. P. Insertion of specific bases during DNA synthesis past the oxidation- damaged base 8-oxodG. Nature, *349*: 431-434, 1991.

33. Kamiya, H., Miura, H., Murata-Kamiya, N., Ishikawa, H., Sakaguchi, T., Inoue, H., Sasaki, T., Masutani, C., Hanaoka, F., Nishimura, S., and . 8-Hydroxyadenine (7,8-dihydro-8-oxoadenine) induces misincorporation in in vitro DNA synthesis and mutations in NIH 3T3 cells. Nucleic Acids Res., *23*: 2893-2899, 1995.

34. Malins, D. C., Holmes, E. H., and Gunselman, S. J. 8-Hydroxydeoxyguanosine levels in DNA of human breast cancers are not significantly different from those of non-cancerous breast tissues by the HPLC-ECD method. Cancer Letters 90, 157-162. Cancer Lett., *94*: 233, 1995.

35. Koch, K. S., Fletcher, R. G., Grond, M. P., and Leffert, H. L. A 43-base-pair complementary DNA sequence homology and triplet repeat motif among putative polymeric immunoglobulin receptor messenger RNAs in regenerating rat liver. Hepatology, *18*: 226-228, 1993.

36. O'Connor, T. R., Boiteux, S., and Laval, J. Ring-opened 7-methylguanine residues in DNA are a block to in vitro DNA synthesis. Nucleic Acids Res., *16*: 5879-5894, 1988.

37. Tudek, B., Boiteux, S., and Laval, J. Biological properties of imidazole ring-opened N7-methylguanine in M13mp18 phage DNA. Nucleic Acids Res., *20*: 3079-3084, 1992.

38. Chetsanga, C. J. and Lindahl, T. Release of 7-methylguanine residues whose imidazole rings have been opened from damaged DNA by a DNA glycosylase from Escherichia coli. Nucleic Acids Res., *6* : 3673-3684, 1979.

39. Chetsanga, C. J., Lozon, M., Makaroff, C., and Savage, L. Purification and characterization of Escherichia coli formamidopyrimidine-DNA glycosylase that

excises damaged 7- methylguanine from deoxyribonucleic acid. Biochemistry, *20*: 5201-5207, 1981.

40. van der Kemp, P. A., Thomas, D., Barbey, R., de Oliveira, R., and Boiteux, S. Cloning and expression in Escherichia coli of the OGG1 gene of Saccharomyces cerevisiae, which codes for a DNA glycosylase that excises 7,8-dihydro-8-oxoguanine and 2,6-diamino-4-hydroxy-5-N- methylformamidopyrimidine. Proc.Natl.Acad.Sci.U.S.A, *93*: 5197-5202, 1996.

41. Asagoshi, K., Yamada, T., Terato, H., Ohyama, Y., Monden, Y., Arai, T., Nishimura, S., Aburatani, H., Lindahl, T., and Ide, H. Distinct repair activities of human 7,8-dihydro-8-oxoguanine DNA glycosylase and formamidopyrimidine DNA glycosylase for formamidopyrimidine and 7,8-dihydro-8-oxoguanine. J.Biol.Chem., *275*: 4956-4964, 2000.

42. Liu, J. and Doetsch, P. W. Escherichia coli RNA and DNA polymerase bypass of dihydrouracil: mutagenic potential via transcription and replication. Nucleic Acids Res., *26*: 1707-1712, 1998.

43. Ames, B. N. Endogenous DNA damage as related to cancer and aging. Mutat.Res., *214*: 41-46, 1989.

44. McCord, J. M. Oxygen-derived radicals: a link between reperfusion injury and inflammation. Fed.Proc., *46*: 2402-2406, 1987.

45. Malins, D. C., Holmes, E. H., Polissar, N. L., and Gunselman, S. J. The etiology of breast cancer. Characteristic alteration in hydroxyl radical-induced DNA base lesions during oncogenesis with potential for evaluating incidence risk. Cancer, *71*: 3036-3043, 1993.

46. Reiter, R. J. The role of the neurohormone melatonin as a buffer against macromolecular oxidative damage. Neurochem.Int., *27*: 453-460, 1995.

47. Halliwell, B. Production of superoxide, hydrogen peroxide and hydroxyl radicals by phagocytic cells: a cause of chronic inflammatory disease? Cell Biol.Int.Rep., *6*: 529-542, 1982.

48. Voehringer, D. W. BCL-2 and glutathione: alterations in cellular redox state that regulate apoptosis sensitivity. Free Radic.Biol.Med., *27*: 945-950, 1999.

49. Blount, B. C., Mack, M. M., Wehr, C. M., MacGregor, J. T., Hiatt, R. A., Wang, G., Wickramasinghe, S. N., Everson, R. B., and Ames, B. N. Folate deficiency causes uracil misincorporation into human DNA and chromosome breakage: implications for cancer and neuronal damage. Proc.Natl.Acad.Sci.U.S.A, *94*: 3290-3295, 1997.

50. Dizdaroglu, M. and Bergtold, D. S. Characterization of free radical-induced base damage in DNA at biologically relevant levels. Anal.Biochem., *156*: 182-188, 1986.

51. Halliwell, B. and Dizdaroglu, M. The measurement of oxidative damage to DNA by HPLC and GC/MS techniques. Free Radic.Res.Commun., *16*: 75-87, 1992.

52. Rodriguez, H., Jurado, J., Laval, J., and Dizdaroglu, M. Comparison of the levels of 8-hydroxyguanine in DNA as measured by gas chromatography mass spectrometry following hydrolysis of DNA by Escherichia coli Fpg protein or formic acid. Nucleic Acids Res., *28*: E75, 2000.

53. Meister, A. Glutathione metabolism and its selective modification. J.Biol.Chem., *263*: 17205-17208, 1988.

54. Friedberg, E. C. Eukaryotic DNA repair: glimpses through the yeast Saccharomyces cerevisiae. Bioessays, *13*: 295-302, 1991.

55. Swanson, R. L., Morey, N. J., Doetsch, P. W., and Jinks-Robertson, S. Overlapping specificities of base excision repair, nucleotide excision repair, recombination, and translesion synthesis pathways for DNA base damage in Saccharomyces cerevisiae. Mol.Cell Biol., *19*: 2929-2935, 1999.

56. Norbury, C. J. and Hickson, I. D. Cellular responses to DNA damage. Annu.Rev.Pharmacol.Toxicol., *41*: 367-401, 2001.

57. Laval, J., Boiteux, S., and O'Connor, T. R. Physiological properties and repair of apurinic/apyrimidinic sites and imidazole ring-opened guanines in DNA. Mutat.Res., *233*: 73-79, 1990.

58. Hoeijmakers, J. H. Genome maintenance mechanisms for preventing cancer. Nature, *411*: 366-374, 2001.

59. Laval, J. Role of DNA repair enzymes in the cellular resistance to oxidative stress. Pathol.Biol.(Paris), *44*: 14-24, 1996.

60. Friedberg, E. C., Walker, G. C., and Siede, S. DNA Repair and Mutagenesis.Washington D.C.: ASM Press, 1995.

61. Broomfield, S., Hryciw, T., and Xiao, W. DNA postreplication repair and mutagenesis in Saccharomyces cerevisiae. Mutat.Res., *486*: 167-184, 2001.

62. Napolitano, R., Janel-Bintz, R., Wagner, J., and Fuchs, R. P. All three SOS-inducible DNA polymerases (Pol II, Pol IV and Pol V) are involved in induced mutagenesis. EMBO J., *19*: 6259-6265, 2000.

63. Harris, R. S., Kong, Q., and Maizels, N. Somatic hypermutation and the three R's: repair, replication and recombination. Mutat.Res., *436*: 157-178, 1999.

64. Onda, M., Hanada, K., Kawachi, H., and Ikeda, H. Escherichia coli mutM suppresses illegitimate recombination induced by oxidative stress. Genetics, *151*: 439-446, 1999.

65. Pesticides Information Profiles: Paraquat. The Pesticide Information Project Oregon State University. 1996.
Ref Type: Report

66. Eisler Ronald. Paraquat Hazards to Fish, Wildlife, and Invertebrates: A Synoptic Review. US Fish and Wildlife Service. 85 (1.22). 1990. Springfield, VA, National Technical Information Service.
Ref Type: Report

67. Kitahara, J., Yamanaka, K., Kato, K., Lee, Y. W., Klein, C. B., and Costa, M. Mutagenicity of cobalt and reactive oxygen producers. Mutat.Res., *370*: 133-140, 1996.

68. Schriner, S. E., Smith, A. C., Dang, N. H., Fukuchi, K., and Martin, G. M. Overexpression of wild-type and nuclear-targeted catalase modulates resistance to oxidative stress but does not alter spontaneous mutant frequencies at APRT. Mutat.Res., *449*: 21-31, 2000.

69. Zienolddiny, S., Ryberg, D., and Haugen, A. Induction of microsatellite mutations by oxidative agents in human lung cancer cell lines. Carcinogenesis, *21*: 1521-1526, 2000.

70. Kraemer, S. M., Kronenberg, A., Ueno, A., and Waldren, C. A. Measuring the spectrum of mutation induced by nitrogen ions and protons in the human-hamster hybrid cell line A(L)C. Radiat.Res., *153*: 743-751, 2000.

71. Hei, T. K., Wu, L. J., Liu, S. X., Vannais, D., Waldren, C. A., and Randers-Pehrson, G. Mutagenic effects of a single and an exact number of alpha particles in mammalian cells. Proc.Natl.Acad.Sci.U.S.A, *94*: 3765-3770, 1997.

72. Ueno, A. M., Vannais, D. B., Gustafson, D. L., Wong, J. C., and Waldren, C. A. A low, adaptive dose of gamma-rays reduced the number and altered the spectrum of S1- mutants in human-hamster hybrid AL cells. Mutat.Res., *358*: 161-169, 1996.

73. McGuinness, S. M., Shibuya, M. L., Ueno, A. M., Vannais, D. B., and Waldren, C. A. Mutant quantity and quality in mammalian cells (AL) exposed to cesium-137 gamma radiation: effect of caffeine. Radiat.Res., *142*: 247-255, 1995.

74. Hei, T. K., Piao, C. Q., He, Z. Y., Vannais, D., and Waldren, C. A. Chrysotile fiber is a strong mutagen in mammalian cells. Cancer Res., *52*: 6305-6309, 1992.

75. Giaccia, A. J., Lewis, A. D., Denko, N. C., Cholon, A., Evans, J. W., Waldren, C. A., Stamato, T. D., and Brown, J. M. The hypersensitivity of the Chinese hamster ovary variant BL-10 to bleomycin killing is due to a lack of glutathione S-transferase-alpha activity. Cancer Res., *51*: 4463-4469, 1991.

76. Waldren, C. A. and Puck, T. T. Steps toward experimental measurement of total mutations relevant to human disease. Somat.Cell Mol.Genet., *13*: 411-414, 1987.

77. Pillidge, L., Musk, S. R., Johnson, R. T., and Waldren, C. A. Excessive chromosome fragility and abundance of sister-chromatid exchanges induced by UV in an Indian muntjac cell line defective in postreplication (daughter strand) repair. Mutat.Res., *166*: 265-273, 1986.

78. Waldren, C., Correll, L., Sognier, M. A., and Puck, T. T. Measurement of low levels of x-ray mutagenesis in relation to human disease. Proc.Natl.Acad.Sci.U.S.A, *83*: 4839-4843, 1986.

79. Boiteux, S., O'Connor, T. R., and Laval, J. Formamidopyrimidine-DNA glycosylase of Escherichia coli: cloning and sequencing of the fpg structural gene and overproduction of the protein. EMBO J., *6*: 3177-3183, 1987.

80. Tchou, J., Kasai, H., Shibutani, S., Chung, M. H., Laval, J., Grollman, A. P., and Nishimura, S. 8-oxoguanine (8-hydroxyguanine) DNA glycosylase and its substrate specificity. Proc.Natl.Acad.Sci.U.S.A, *88*: 4690-4694, 1991.

81. Hatahet, Z., Kow, Y. W., Purmal, A. A., Cunningham, R. P., and Wallace, S. S. New substrates for old enzymes. 5-Hydroxy-2'-deoxycytidine and 5- hydroxy-2'-deoxyuridine are substrates for Escherichia coli endonuclease III and formamidopyrimidine DNA N-glycosylase, while 5- hydroxy-2'-deoxyuridine is a substrate for uracil DNA N-glycosylase. J.Biol.Chem., *269*: 18814-18820, 1994.

82. Castaing, B., Boiteux, S., and Zelwer, C. DNA containing a chemically reduced apurinic site is a high affinity ligand for the E. coli formamidopyrimidine-DNA glycosylase. Nucleic Acids Res., *20*: 389-394, 1992.

83. Satoh, T. and Hosokawa, M. Organophosphates and their impact on the global environment. Neurotoxicology, *21*: 223-227, 2000.

84. Turner, C. E., Elsohly, M. A., Cheng, F. P., and Torres, L. M. Marijuana and paraquat. JAMA, *240*: 1857, 1978.

85. Turner, C. E., Cheng, P. C., Torres, L. M., and Elsohly, M. A. Detection and analysis of paraquat in confiscated marijuana samples. Bull.Narc., *30*: 47-56, 1978.

86. Haley, T. J. Review of the toxicology of paraquat (1,1'-dimethyl-4,4'-bipyridinium chloride). Clin.Toxicol., *14*: 1-46, 1979.

87. US EPA. Paraquat. CASRN 1910-42-5. 10-1-1993. Integrated Risk Information System.
Ref Type: Report

88. Walters, K. A. and Dugard, P. H. The influence of polyoxyethylene ether surfactants on transport of paraquat across isolated gastric mucosa [proceedings]. J.Pharm.Pharmacol., *30 Suppl*: 32P, 1978.

89. Giri, S. N. and Krishna, G. A. The effect of paraquat on guanylate cyclase activity in relation to morphological changes of guinea pig lungs. Lung, *157*: 127-134, 1980.

90. Hampson, E. C., Eyles, D. W., and Pond, S. M. Effects of paraquat on canine bronchoalveolar lavage fluid. Toxicol.Appl.Pharmacol., *98*: 206-215, 1989.

91. Kimbrough, R. D. Toxic effects of the herbicide paraquat. Chest, *65*: Suppl-67S, 1974.

92. Sayre, L. M., Smith, M. A., and Perry, G. Chemistry and biochemistry of oxidative stress in neurodegenerative disease. Curr.Med.Chem., *8*: 721-738, 2001.

93. Autor, A. P. Reduction of paraquat toxicity by superoxide dismutase. Life Sci., *14*: 1309-1319, 1974.

94. Dasta, J. F. Paraquat poisoning: a review. Am.J.Hosp.Pharm., *35*: 1368-1372, 1978.

95. Onyeama, H. P. and Oehme, F. W. A literature review of paraquat toxicity. Vet.Hum.Toxicol., *26*: 494-502, 1984.

96. Smith, J. G. Paraquat poisoning by skin absorption: a review. Hum.Toxicol., *7*: 15-19, 1988.

97. Smith, L. L. Paraquat toxicity. Philos.Trans.R.Soc.Lond B Biol.Sci., *311*: 647-657, 1985.

98. Smith, L. L. The toxicity of paraquat. Adverse Drug React.Acute.Poisoning.Rev., *7*: 1-17, 1988.

99. Smith, P. and Heath, D. Paraquat. CRC Crit Rev.Toxicol., *4*: 411-445, 1976.

100. US Library of Medicine. Hazardous Substances Databank. 2001. Bethesda, MD. Ref Type: Generic

101. Stevens, J. T. and Sumner, D. D. Herbicides. *In* W. J. Hayes, Jr. and E. R. Laws, Jr. (eds.), Handbook of Pesticide Toxicology, pp. 10-88. New York, NY: Academic Press, 1991.

102. US EPA. Health Advisory Draft Report: Paraquat. 1987. Washington, D.C. Ref Type: Report

103. United States Environmental Protection Agency. Federal Register Document for Paraquat. Vol. 64, No. 125, 35067-35070. 6-30-1999. Ref Type: Report

104. US EPA. Pesticide Fact Sheet Number 131: Paraquat. Office of Pesticides and Toxic Substances. 1987. Washington, D.C. Ref Type: Report

105. Wauchope, R. D., Buttler, T. M., Hornsby, A. G., Augustijn Beckers, P. W. M., and Burt, J. P. SCS/ARS/CES Pesticide properties database for environmental decisionmaking. Rev.Environ.Contam.Toxicol., *123*: 1-157, 1992.

106. Weed Science Society of America. Herbicide Handbook, Seventh ed.Champaign, IL: Weed Society of America, 1994.

107. Humphreys, J. M., Hilliker, A. J., and Phillips, J. P. Paraquat selection identifies X-linked oxygen defense genes in Drosophila melanogaster. Genome, *36*: 162-165, 1993.

108. Speit, G., Haupter, S., and Hartmann, A. Evaluation of the genotoxic properties of paraquat in V79 Chinese hamster cells. Mutat.Res., *412*: 187-193, 1998.

109. Tsukamoto, M., Tampo, Y., Sawada, M., and Yonaha, M. Paraquat-induced membrane dysfunction in pulmonary microvascular endothelial cells. Pharmacol.Toxicol., *86*: 102-109, 2000.

110. Ortiz, G. G., Reiter, R. J., Zuniga, G., Melchiorri, D., Sewerynek, E., Pablos, M. I., Oh, C. S., Garcia, J. J., and Bitzer-Quintero, O. K. Genotoxicity of paraquat: micronuclei induced in bone marrow and peripheral blood are inhibited by melatonin. Mutat.Res., *464*: 239-245, 2000.

111. Tanaka, R. Protective effects of (-)-epigallocatechin gallate and (+)-catechin on paraquat-induced genotoxicity in cultured cells. J.Toxicol.Sci., *25*: 199-204, 2000.

112. Ishii, N. Oxidative Stress and Aging in Caenorhabditis Elegans. Free Radic.Res., *33*: 857-864, 2001.

113. Corasaniti, M. T., Strongoli, M. C., Rotiroti, D., Bagetta, G., and Nistico, G. Paraquat: a useful tool for the in vivo study of mechanisms of neuronal cell death. Pharmacol.Toxicol., *83*: 1-7, 1998.

114. Tomita, M., Okuyama, T., Ishikawa, T., Hidaka, K., and Nohno, T. The role of nitric oxide in paraquat-induced cytotoxicity in the human A549 lung carcinoma cell line. Free Radic.Res., *34*: 193-202, 2001.

115. Konstantinova, S. G. and Russanov, E. M. Studies on paraquat-induced oxidative stress in rat liver. Acta Physiol Pharmacol.Bulg., *24*: 107-111, 1999.

116. Boiteux, S. Properties and biological functions of the NTH and FPG proteins of Escherichia coli: two DNA glycosylases that repair oxidative damage in DNA. J.Photochem.Photobiol.B, *19*: 87-96, 1993.

117. O'Connor, T. R., Graves, R. J., de Murcia, G., Castaing, B., and Laval, J. Fpg protein of Escherichia coli is a zinc finger protein whose cysteine residues have a structural and/or functional role. J.Biol.Chem., *268*: 9063-9070, 1993.

118. Boiteux, S., O'Connor, T. R., Lederer, F., Gouyette, A., and Laval, J. Homogeneous Escherichia coli FPG protein. A DNA glycosylase which excises imidazole ring-opened purines and nicks DNA at apurinic/apyrimidinic sites. J.Biol.Chem., *265*: 3916-3922, 1990.

119. Zharkov, D. O., Rieger, R. A., Iden, C. R., and Grollman, A. P. NH2-terminal proline acts as a nucleophile in the glycosylase/AP-lyase reaction catalyzed by Escherichia coli formamidopyrimidine-DNA glycosylase (Fpg) protein. J.Biol.Chem., *272*: 5335-5341, 1997.

120. Sugahara, M., Mikawa, T., Kumasaka, T., Yamamoto, M., Kato, R., Fukuyama, K., Inoue, Y., and Kuramitsu, S. Crystal structure of a repair enzyme of oxidatively damaged DNA, MutM (Fpg), from an extreme thermophile, Thermus thermophilus HB8. EMBO J., *19*: 3857-3869, 2000.

121. Boiteux, S., Dherin, C., Reille, F., Apiou, F., Dutrillaux, B., and Radicella, J. P. Excision repair of 8-hydroxyguanine in mammalian cells: the mouse Ogg1 protein as a model. Free Radic.Res., *29*: 487-497, 1998.

122. Roldan-Arjona, T., Wei, Y. F., Carter, K. C., Klungland, A., Anselmino, C., Wang, R. P., Augustus, M., and Lindahl, T. Molecular cloning and functional expression of a human cDNA encoding the antimutator enzyme 8-hydroxyguanine-DNA glycosylase. Proc.Natl.Acad.Sci.U.S.A, *94*: 8016-8020, 1997.

123. Boiteux, S. and Radicella, J. P. The human OGG1 gene: structure, functions, and its implication in the process of carcinogenesis. Arch.Biochem.Biophys., *377*: 1-8, 2000.

124. Roldan-Arjona, T., Garcia-Ortiz, M. V., Ruiz-Rubio, M., and Ariza, R. R. cDNA cloning, expression and functional characterization of an Arabidopsis thaliana homologue of the Escherichia coli DNA repair enzyme endonuclease III. Plant Mol.Biol., *44*: 43-52, 2000.

125. Lagravere, C., Malfoy, B., Leng, M., and Laval, J. Ring-opened alkylated guanine is not repaired in Z-DNA. Nature, *310*: 798-800, 1984.

126. Michaels, M. L., Cruz, C., Grollman, A. P., and Miller, J. H. Evidence that MutY and MutM combine to prevent mutations by an oxidatively damaged form of guanine in DNA. Proc.Natl.Acad.Sci.U.S.A, *89*: 7022-7025, 1992.

127. Gallardo-Madueno, R., Leal, J. F., Dorado, G., Holmgren, A., Lopez-Barea, J., and Pueyo, C. In vivo transcription of nrdAB operon and of grxA and fpg genes is triggered in Escherichia coli lacking both thioredoxin and glutaredoxin 1 or thioredoxin and glutathione, respectively. J.Biol.Chem., *273*: 18382-18388, 1998.

128. Gifford, C. M. and Wallace, S. S. The genes encoding formamidopyrimidine and MutY DNA glycosylases in Escherichia coli are transcribed as part of complex operons. J.Bacteriol., *181*: 4223-4236, 1999.

129. Gill, R. D., Cussac, C., Souhami, R. L., and Laval, F. Increased resistance to N,N',N"-triethylenethiophosphoramide (thiotepa) in cells expressing the Escherichia coli formamidopyrimidine-DNA glycosylase. Cancer Res., *56*: 3721-3724, 1996.

130. Cussac, C. and Laval, F. Reduction of the toxicity and mutagenicity of aziridine in mammalian cells harboring the Escherichia coli fpg gene. Nucleic Acids Res., *24*: 1742-1746, 1996.

131. Laval, F. Expression of the E. coli fpg gene in mammalian cells reduces the mutagenicity of gamma-rays. Nucleic Acids Res., *22*: 4943-4946, 1994.

132. Tajiri, T., Maki, H., and Sekiguchi, M. Functional cooperation of MutT, MutM and MutY proteins in preventing mutations caused by spontaneous oxidation of guanine nucleotide in Escherichia coli. Mutat.Res., *336*: 257-267, 1995.

133. Akiyama, M., Maki, H., Sekiguchi, M., and Horiuchi, T. A specific role of MutT protein: to prevent dG.dA mispairing in DNA replication. Proc.Natl.Acad.Sci.U.S.A, *86*: 3949-3952, 1989.

134. Bhagwat, M. and Gerlt, J. A. 3'- and 5'-strand cleavage reactions catalyzed by the Fpg protein from Escherichia coli occur via successive beta- and delta-elimination mechanisms, respectively. Biochemistry, *35*: 659-665, 1996.

135. Waldren, C. A. and Puck, T. T. Steps toward experimental measurement of total mutations relevant to human disease. Somat.Cell Mol.Genet., *13*: 411-414, 1987.

136. Wilson, A. B., Seilly, D., Willers, C., Vannais, D. B., McGraw, M., Waldren, C. A., Hei, T. K., and Davies, A. Antigen S1, encoded by the MIC1 gene, is characterized as an epitope of human CD59, enabling measurement of mutagen-induced intragenic deletions in the AL cell system. Somat.Cell Mol.Genet., *25*: 147-157, 1999.

137. Kimura, Y., Furuhata, T., Urano, T., Hirata, K., Nakamura, Y., and Tokino, T. Genomic structure and chromosomal localization of GML (GPI-anchored molecule-like protein), a gene induced by p53. Genomics, *41*: 477-480, 1997.

138. Randerath, K., Zhou, G. D., Somers, R. L., Robbins, J. H., and Brooks, P. J. A {super32}P-postlabeling assay for the oxidative DNA lesion 8,5'-Cyclo- 2'-deoxyadenosine in mammalian tissues: Evidence that four type II I- compounds are dinucleotides containing the lesion in the 3' nucleotide. J.Biol.Chem., 2001.

139. Okayasu, R., Suetomi, K., and Ullrich, R. L. Wortmannin inhibits repair of DNA double-strand breaks in irradiated normal human cells. Radiat.Res., *149*: 440-445, 1998.

140. Hei, T. K., Piao, C. Q., He, Z. Y., Vannais, D., and Waldren, C. A. Chrysotile fiber is a strong mutagen in mammalian cells. Cancer Res., *52*: 6305-6309, 1992.

141. Hei, T. K., Wu, L. J., Liu, S. X., Vannais, D., Waldren, C. A., and Randers-Pehrson, G. Mutagenic effects of a single and an exact number of alpha particles in mammalian cells. Proc.Natl.Acad.Sci.U.S.A, *94*: 3765-3770, 1997.

142. Hei, T. K., Liu, S. X., and Waldren, C. Mutagenicity of arsenic in mammalian cells: role of reactive oxygen species. Proc.Natl.Acad.Sci.U.S.A, *95*: 8103-8107, 1998.

143. McGuinness, S. M., Shibuya, M. L., Ueno, A. M., Vannais, D. B., and Waldren, C. A. Mutant quantity and quality in mammalian cells (AL) exposed to cesium-137 gamma radiation: effect of caffeine. Radiat.Res., *142*: 247-255, 1995.

144. Waldren, C. A. and Patterson, D. Effects of caffeine on purine metabolism and ultraviolet light-induced lethality in cultured mammalian cells. Cancer Res., *39*: 4975-4982, 1979.

145. Vandeputte, C., Guizon, I., Genestie-Denis, I., Vannier, B., and Lorenzon, G. A microtiter plate assay for total glutathione and glutathione disulfide contents in cultured/isolated cells: performance study of a new miniaturized protocol. Cell Biol.Toxicol., *10*: 415-421, 1994.

146. Collins, A., Jones, C., and Waldren, C. A survey of DNA repair incision activities after ultraviolet irradiation of a range of human, hamster, and hamster-human hybrid cell lines. J.Cell Sci., *56*: 423-440, 1982.

147. Chen, S. K., Tsai, M. H., Hwang, J. J., and Chan, W. P. Determination of 8-oxoguanine in individual cell nucleus of gamma- irradiated mammalian cells. Radiat.Res., *155*: 832-836, 2001.

148. Okayasu, R., Suetomi, K., Yu, Y., Silver, A., Bedford, J. S., Cox, R., and Ullrich, R. L. A deficiency in DNA repair and DNA-PKcs expression in the radiosensitive BALB/c mouse. Cancer Res., *60*: 4342-4345, 2000.

149. Boerrigter, M. E., Wei, J. Y., and Vijg, J. Induction and repair of benzo[a]pyrene-DNA adducts in C57BL/6 and BALB/c mice: association with aging and longevity. Mech.Ageing Dev., *82*: 31-50, 1995.

150. Hang, B., Singer, B., Margison, G. P., and Elder, R. H. Targeted deletion of alkylpurine-DNA-N-glycosylase in mice eliminates repair of 1,N6-ethenoadenine and hypoxanthine but not of 3,N4- ethenocytosine or 8-oxoguanine. Proc.Natl.Acad.Sci.U.S.A, *94*: 12869-12874, 1997.

151. De Flora, S., Rossi, G. A., and De Flora, A. Metabolic, desmutagenic and anticarcinogenic effects of N- acetylcysteine. Respiration, *50 Suppl 1*: 43-49, 1986.

152. Liu, S. X., Athar, M., Lippai, I., Waldren, C., and Hei, T. K. Induction of oxyradicals by arsenic: implication for mechanism of genotoxicity. Proc.Natl.Acad.Sci.U.S.A, *98*: 1643-1648, 2001.

153. Zhan, D. J., Heflich, R. H., and Fu, P. P. Molecular characterization of mutation and comparison of mutation profiles in the hprt gene of Chinese hamster ovary cells treated with benzo[a]pyrene trans-7,8-diol-anti-9,10-epoxide, 1-nitrobenzo[a]pyrene trans-7,8-diol-anti-9,10-epoxide, and 3-nitrobenzo[a]pyrene trans-7,8- diol-anti-9,10-epoxide. Environ.Mol.Mutagen., *27*: 19-29, 1996.

154. Steenken, S. Structure, acid/base properties and transformation reactions of purine radicals. Free Radic.Res.Commun., *6*: 117-120, 1989.

155. Malins, D. C. Johnson P. M. Wheeler T. M. Barker E. A. Polissar N. L. & Vinson M. A. Age-related radical-induced DNA damage is linked to prostate cancer. Cancer Res. 2001. Ref Type: In Press

156. Minowa, O., Arai, T., Hirano, M., Monden, Y., Nakai, S., Fukuda, M., Itoh, M., Takano, H., Hippou, Y., Aburatani, H., Masumura, K., Nohmi, T., Nishimura, S., and Noda, T. Mmh/Ogg1 gene inactivation results in accumulation of 8-hydroxyguanine in mice. Proc.Natl.Acad.Sci.U.S.A, *97*: 4156-4161, 2000.

157. Hazra, T. K., Izumi, T., Venkataraman, R., Kow, Y. W., Dizdaroglu, M., and Mitra, S. Characterization of a novel 8-oxoguanine-DNA glycosylase activity in Escherichia coli and identification of the enzyme as endonuclease VIII. J.Biol.Chem., *275*: 27762-27767, 2000.